Satellite & Aerial Coastal Water Quality Monitoring in the San Diego / Tijuana Region

By Jan Svejkovsky, Ph.D., Mark Hess

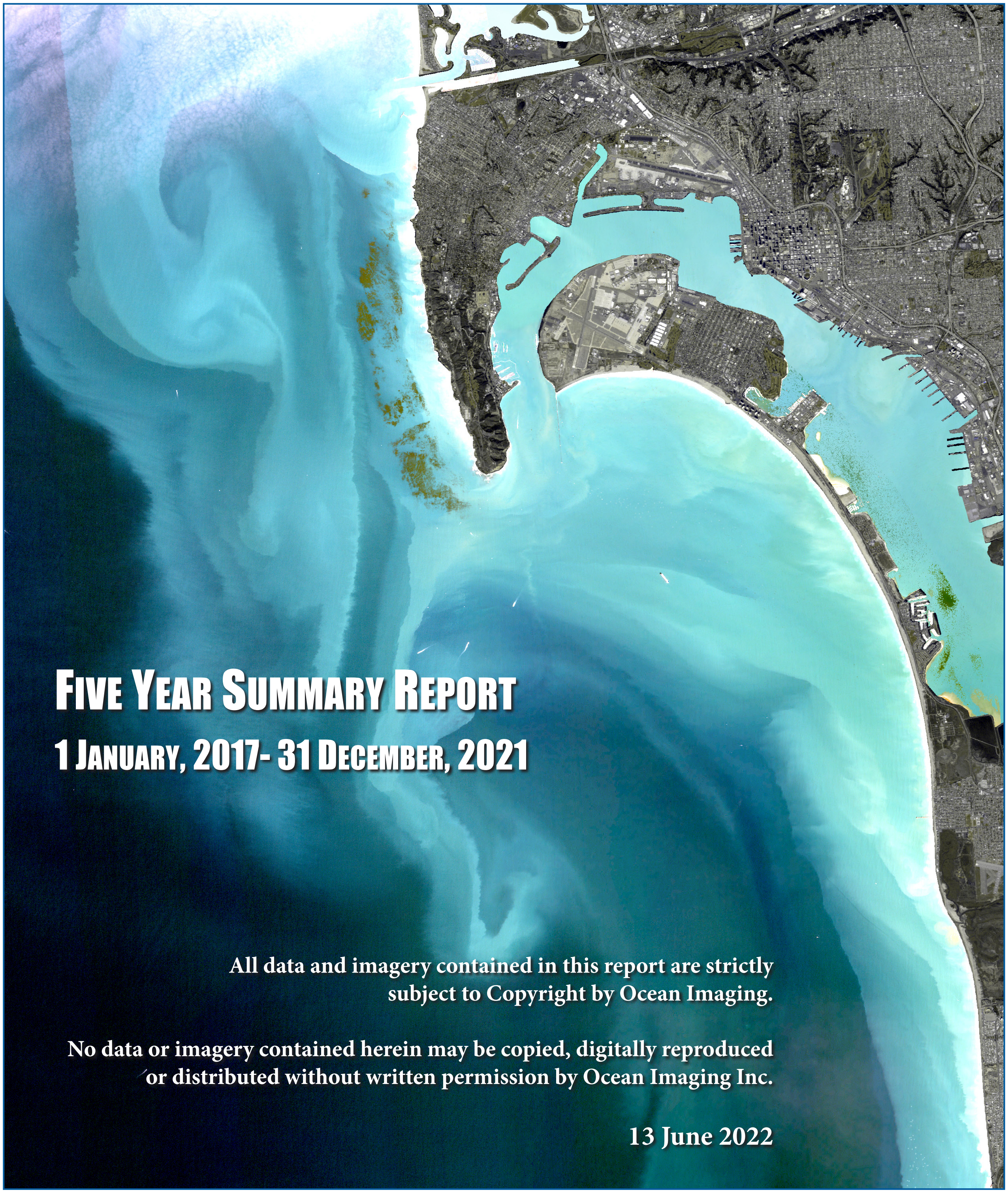

Five Year Summary Report

1 January, 2017- 31 December, 2021

13 June 2022

Ocean Imaging

13976 West Bowles Avenue, Suite 100, Littleton CO 80127 Phone: 303-948-5272 Fax: 303-948-2549 www.oceani.com

Table of Contents

EXECUTIVE SUMMARY

Following initial NASA-funded development in the 1990s and subsequent demonstration projects with the EPA and California State Water Resources Control Board, in October 2002 Ocean Imaging Corporation began providing regional ocean water quality monitoring for the City of San Diego and the International Boundary Waters Commission. The monitoring utilizes various aerial and satellite sensors in the visible, near-infrared and thermal infrared to detect patterns in the coastal ocean due to oceanographic variables as well as point and non-point terrestrial runoff, and anthropogenic sources such as the region's offshore sewage outfalls. These image data are utilized to spatially and temporally augment regular field sampling surveys, and to help interpret results from those surveys. In the early years of the project its focus was primarily on the detection and monitoring of the sewage outfall plumes and runoff from historically high contamination sources such as the Tijuana River and San Antonio de los Buenos Creek. The project's objectives later expanded to include the generation of multiple spatial data products on a larger, regional scale to provide information on oceanic variables affecting San Diego's coastal waters. The project's results include the determination of dispersal pattern trends of the South Bay Ocean Outfall plume when it reaches the ocean's surface layer, dispersal pattern trends of stormwater runoff from multiple shoreline point sources and their relation to beach contamination potential, as well as short term patterns and long-term trends of oceanic phenomena such as phytoplankton blooms and red tides, and growth cycles of the region's kelp beds. Some of the results have been published in peer-reviewed journals. This report provides a summary of the most important results and gives highlights of notable events in the last 5 years.

List of Abbreviations

ADCP	Acoustic doppler current profilers
AOI	Area of Interest
AVHRR	Advanced Very High Resolution Radiometer
CMML	City Marine Microbiology Laboratory
CORDC	Coastal Observing Research and Development Center
DMSC	Digital Multispectral Camera
EFF	Effluent
EPA	Environmental Protection Agency
ESA	European Space Agency
FC	Fresh Core (River plume components)
HAB	Harmful Algal bloom
HF Radar	High Frequency Radar-derived surface currents
HYCOM	Hybrid Coordinate Ocean Model
IBWC	International Boundary and Water Commission
INF	Influent
MGD	Millions of Gallons Per Day
mg/L	Milligrams per Liter
MODIS	Moderate Resolution Imaging Spectroradiometer
MSI	Multispectral Instrument
NASA	National Aeronautics and Space Administration
Near-IR	Near-Infrared
OC	Old Core (River plume components)
OI	Ocean Imaging Corporation
OLCI	Ocean and Land Color Instrument
ONI	Oceanic Niño Index
OP	Old Plume (River plume components)
PLOO	Point Loma Ocean Outfall
REST	Representational State Transfer
RTOMS	Real-time oceanographic mooring station
SAR	Synthetic Aperture Radar
SBIWTP	South Bay International Wastewater Treatment Plant
SBOO	South Bay Ocean Outfall
SCB	Southern California Bight
SDIA	San Diego International Airport (SDIA)
SDPUD	San Diego's Public Utilities Department
SDR	San Diego River
SDWQ	San Diego Water Quality
SLSTR	The Sea and Land Surface Temperature Radiometer
SPOT	Satellite Pour l'Observation de la Terre
SST	Sea Surface Temperature
SWRCB	State Water Resources Control Board
TIR	Thermal Infrared
TJR	Tijuana River
TM	Thematic Mapper
TSS	Total Suspended Solids
UV	Ultraviolet
VIIRS	Visible Infrared Imaging Radiometer Suite
WMS	Web Map Service

1. PROJECT BACKGROUND AND OBJECTIVES

Due to the economic benefits that accrue from access to ocean navigation, coastal fisheries, tourism and recreation, human settlements are often more concentrated in the coastal zone than elsewhere. Presently about 40% of the world's population lives within 100 kilometers of the coast (United Nations, 2017). The large population densities result in proportionately large volumes of municipal and industrial wastewater which, in large metropolitan areas, are most commonly disposed of through submarine wastewater outfalls. The practice of wastewater disposal into coastal environments in the U.S. has advanced tremendously over the past 50 years from discharging untreated or partly treated sewage effluent in shallow water close to shore to the discharge of highly treated effluent through deep ocean outfalls (Rogowski, Peter, et al, 2012). The actual efficiency of effluent treatment varies with outfall design, location, discharge depth and distance from shore, regional ocean current patterns, etc. A sub-efficient outfall can thus have significant negative consequences for both environmental impact and human health in the surrounding area. In the United States, municipal outfalls operate under permits issued by the Environmental Protection Agency (EPA). Often, permits allowing the discharge of effluent that has undergone only primary (large objects and some suspended sediment removed) or secondary (most organic matter removed) treatment require a regional water quality monitoring plan that includes regular sampling of biological, chemical and physical parameters around the outfall discharge site. This monitoring is typically done by field sampling performed at regular time intervals (e.g., monthly) at sampling locations comprising a predetermined sampling grid. In the case of the City of San Diego a total of 69 offshore water quality monitoring stations are sampled quarterly to assess coastal oceanographic conditions in the two outfall regions monitored. The City of San Diego Biennial reports summarize additional monitoring efforts such as the sampling of sediments and fish species (City of San Diego, 2020).

The position of the sampling grid usually includes the offshore outfall discharge location and the ocean area surrounding it to a sufficient distance as to be able to deduce the vertical and horizontal extents of the discharge plume through indicator measurements such as salinity, indicator bacteria, and the plume's dilution rate and hence mixing parameters as it expands from its discharge location. In some cases, additional sampling locations may be located outside the main grid at nearby ecologically important sites such as reefs or kelp beds. In most regions, the field-sampling strategy to monitor the near-term and long-term fate of the discharged wastewaters is compromised by several factors: First, both the number of sampling sites and the frequency of sampling is limited by the budget that is reasonably available for such work. Second, coastal regions where municipal wastewater outfalls are located tend to contain other point and non-point sources that discharge possible pollutants into ocean and estuarine waters, either continuously (e.g., rivers and streams) or episodically (e.g., storm drains). Plumes from these sources sometimes enter the outfall sampling grid areas, making it difficult to separate the outfall plume's true effects from other external influences.

Satellite remote sensing has been utilized in oceanography since the 1970s to detect and monitor oceanic processes. In recent decades satellite and aerial imaging have provided means to study coastal discharges such as river and stormwater runoff plumes using multispectral visible and thermal imagery (Ruddick et al. 1994, Ouillon et al. 1997, Walker et al. 2005, Nezlin et al. 2005, Warrick et al. 2007, Svejkovsky et al. 2010), and microwave-based synthetic aperture radar (SAR) for detection of surfactant films associated with natural processes (Svejkovsky and Shandley 2001) and plumes containing anthropogenic substances (Svejkovsky and Jones 2001, Gierach et al. 2016, Holt et al. 2017).

The unique advantage of such imaging is that if a particular process, event or discharge plume feature is detectable, the image data provide a synoptic view of it on a spatial scale and often at spatial resolution that is impossible to attain with ship-based field sampling. Because of this, such imagery also provides increased potential for accurately separating features from multiple discharge sources in the same area. Additionally, the revisit frequency of many satellite systems has the potential to provide data on a time frequency not economically possible with ship-based field sampling programs. On the other hand, satellite and aerial remote sensing instruments can sample only the surface or near-surface waters, thus not providing any three-dimensional information, or detection capabilities of phenomena not reaching the upper water column. Also, with the exception of SAR, imaging is blocked by clouds, so useful data acquisition cannot be relied upon during every satellite overpass. Imaging from aircraft is somewhat less compromised since imagery can be acquired by flying under the cloud layer when feasible.

The utilization of remote sensing specifically for the detection or monitoring of offshore wastewater outfall plumes has been significantly less common than for river and stormwater sources. With the exception of the Massachusetts Water Resources Authority who have utilized 1 km resolution satellite chlorophyll imagery since the mid 1990s as part of their Boston Harbor sewage outfall monitoring program (Werme and Hunt 2000, Hyde et al. 2007), other efforts tend to be short term studies or one-time technology demonstrations. In the early 1990s multispectral visible and thermal satellite imagery were used in studies linked to the installation of new deep-water outfalls in Sydney, Australia (Howden 1995). Axiak et al. (2000) utilized satellite SAR imagery to assess the spatial extent of coastal impact from the island of Malta's main wastewater outfall in the Mediterranean Sea. Keeler et al. (2005) utilized very high resolution (70 cm – 1 m) panchromatic satellite imagery to detect internal wave effects from a deep-water outfall in Hawaii, USA. Aerial multispectral and thermal imagery were used by Marmorino et al. (2010) to demonstrate the direct detection of a wastewater outfall in Florida, USA, and characterize its dilution patterns. More recently, multiple mid-resolution satellite instruments were used to monitor chlorophyll, sea surface temperature (SST) and surfactant distributions during two wastewater outfall diversion events in Southern California (Gierach et al. 2017, Trinh et al. 2017).

In the 1990s, Ocean Imaging Corporation (OI) received multiple research grants from NASA's Commercial Remote Sensing Program for the development and commercialization of novel remote sensing applications in the coastal zone. As part of these projects, OI developed methods to utilize various types of remotely sensed data for the detection and monitoring of stormwater runoff and wastewater discharges from offshore outfalls. The methodology was initially demonstrated with collaboration of the Orange County Sanitation District in California (Svejkovsky and Haydock 1998). The NASA-supported research led to a proof-of-concept demonstration project in the San Diego, California region co-funded by the EPA in 2000. Those results led, in 2002, to adding an operational remote sensing-based monitoring component to the San Diego region's established water quality monitoring program. The project continues as a joint effort between the Ocean Monitoring Program of the City of San Diego's Public Utilities Department (SDPUD). This report provides background information for the entire project, historical data and analyses as well as summarizes notable events from the period between 2017 through 2021.

2. STUDY AREA

2.1 Southern California and San Diego Regions

The San Diego coastal region lies within the Southern California Bight (SCB) – a broad ocean embayment created by an indentation of the coastline south of Pt. Conception, California. Much of the Bight coastline is heavily urbanized, with estimates of as much as 90% of original coastal wetlands having been lost to development (Schiff et al. 2000). The related damming of rivers and streams emptying into the wetlands has resulted in drastic reductions of natural freshwater inputs to the ocean, and with it the loss of sand transport that has accelerated beach erosion (Bird and Lewis 2015). As is shown in **Figure 1,** this project's present monitoring efforts strive to provide remote sensing data on two main regional scales: 1) SCB image products spanning the entire Southern California Bight at spatial resolutions of approximately 250 m – 1000 m; 2) "Core" image products focusing on coastal waters around the Point Loma Ocean Outfall (PLOO) and South Bay Ocean Outfall (SBOO) and approximately 15 km to their North and South at spatial resolutions of 30 m and finer.

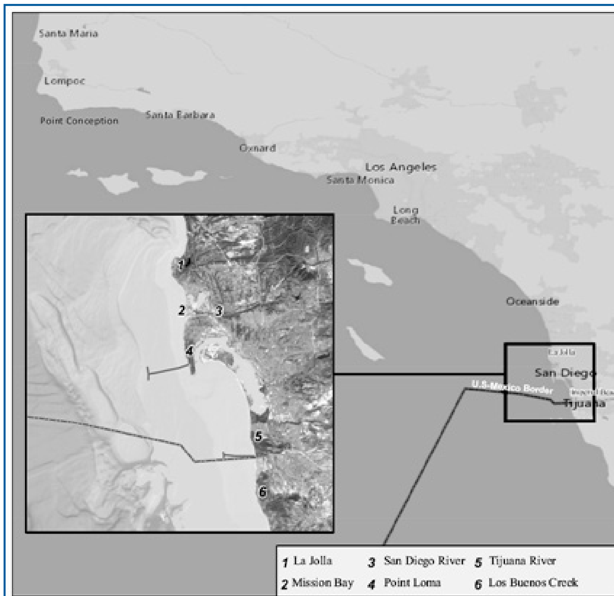

Figure 1. Coverage areas of satellite image products generated for San Diego's water quality monitoring program: 1) SCB products (large area); 2) "Core" area (inset); 2) "Core" area (inset).

The PLOO discharges wastewater treated by the Point Loma Wastewater Treatment Plant under a 301(h) modified treatment permit. The PLOO average discharge in 2018 and 2019 was roughly 141 MGD (million gallons per day). It extends 7.2 km offshore from Pt. Loma (see Figure 1 above). The end of the pipeline connects to a perforated "Y" diffuser section of two legs, each 762 meters long. Wastewater is discharged through diffuser ports ranging in depth from 93.3 m to 97.5 m. At present only the south leg of the diffuser section is operational in order to maintain sufficient water pressure. (City of San Diego, 2020).

The Tijuana River (TJR) watershed is approximately 4465 km^2 in size. It straddles the United States and Mexico border, with about 72% in Mexico and 28% in the United States. During the dry season (approximately April through September) none or only minimal flow tends to reach the TJR Estuary and no appreciable discharge thus enters the ocean. Following rain events, however, the TJR discharges excess runoff into the ocean in a highly turbid plume, readily discernible in satellite imagery. In addition to high suspended solids concentrations, the runoff waters have been repeatedly shown to contain high levels of toxic contaminants (Gersberg et al., 2004), bacteria, and hepatitis and enteroviruses (Gersberg et al., 2006). Public health hazards posed by the TJR discharge result in beach advisory postings or closures northward along the U.S. shoreline and lasting from several days to months.

The frequent shoreline contamination problems associated with stormwater runoff from the TJR prompted the U.S. to construct the SBIWTP, which began operation in January of 1999. Each day the plant processes approximately 26 MGD of sewage from Tijuana's sewer system to advanced primary level (full secondary level since November 2010) and discharges it into the Pacific Ocean through the SBOO (Figure 1 above). In addition to receiving wastewater from Tijuana's municipal sewer system, the plant is connected to the TJR directly through a diverter channel system above the TJR Estuary, which diverts up to 13 MGD of flow from the river into the plant for treatment. The diverter system thus delays somewhat the initial entry of runoff into the estuary and the ocean following a storm and lessens the total volume of effluent entering the ocean during the TJR active flow. The average SBOO discharge in 2018-2019 was approximately 28 MGD through a "Y" diffuser system approximately 5.6 km offshore at a depth of 27 meters. This included about 3 MGD of secondary and tertiary treated effluent from the SBWRP, and 25 MGD of secondary treated effluent from the SBIWTP (City of San Diego, 2020 and San Diego Regional Water Quality Control Board, 2020).

Although some studies have shown a possible slight decrease in the frequency of beach contamination after the SBOO began operation (as measured by fecal coliform and enterococci bacteria indicators), the shoreline contamination problem persists, primarily through continued discharge from the Tijuana River (Gersberg et al. 2008). This is particularly common during the rainy season when the SBIWTP reaches its full capacity and excess runoff is bypassed and allowed to flow out to sea (San Diego Regional Water Quality Control Board, 2020).

2.2 Climate and Oceanography

The climate of Southern California is of the Mediterranean type, with distinct dry (summer) and wet (winter) seasons. Aside from the outfall discharges, the majority of annual water and sediment loads entering the ocean from land sources are linked to winter storms (Inman and Jenkins 1999). The accumulation of pollutants on terrestrial surfaces occurs during the dry season, which then get swept into the ocean during the first few annual storms, resulting in a "First Flush Effect" that has been well documented with field measurements (Bertrand-Krajewski et al., 1998; Cristina and Sansalone, 2003; Tiefenthaler and Schiff, 2003) and even from space with satellite imagery (Svejkovsky and Jones, 2001). The "Core" study region around the PLOO and SBOO includes numerous sources of episodic stormwater runoff entering the coastal zone. The largest include the already-mentioned Tijuana River, the San Diego River (its dry season flow tends to be very low, less than 2 cubic meters per second), and the entrances to Mission and San Diego Bay. Stormwater runoff plumes flowing out of coastal lagoons and wetlands in San Diego's North County and Orange County further to the north are often also advected southward into the "Core" region after heavy rains. Additionally, a multitude of storm drains from city streets and other, non-point sources discharge seasonal runoff directly onto the shoreline.

The prevailing nearshore surface flow pattern along San Diego's coastline is southward, with a localized, headland-related upwelling zone south of Pt. Loma (Roughan et al. 2005). Plankton blooms and red tides (most common in the spring and summer months) periodically affect water clarity in the San Diego County region as well as the entire SCB. Occasional flow reversal episodes lasting up to several days occur throughout the year and advect nearshore waters from south of the US/Mexico border northward. One significant shoreline discharge source needs to be noted south of the US/Mexico border, as it is in relative proximity to US waters and the SBOO: San Antonio de los Buenos Creek located approximately 10 km south of the border (Figure 1 above) has no natural flow during the dry season, but receives a daily input of 20 – 30 MGD of minimally treated sewage effluent from the San Antonio de los Buenos Sewage Treatment Facility near Tijuana, Mexico. This volume can more than double during rain events. Treatment consists of passing part of the sewage influx through sedimentation and aeration ponds and, at least on some days, the addition of chlorine to the water. Due to capacity limitations, how¬ever, 6 MGD or more of untreated sewage can be diverted around the ponds and is left untreated. The untreated water is dis¬charged into the creek channel 1 km upstream from its mouth and flows into the surf zone over a rocky beach (Graf et al. 2005).

The variety of natural and anthropogenic discharge sources, coupled with a dynamic and varied oceanographic regime make San Diego's region-wide water quality monitoring quite challenging. Utilizing satellite and aerial remote sensing to augment traditional field sampling has provided additional capabilities to better spatially define the various effluent plumes and monitor their variability during both wet and dry season conditions.

3. METHODS AND TECHNOLOGY OVERVIEW

OI uses several remote sensing technologies to monitor San Diego's offshore outfalls and shoreline water quality. Their main principle is to reveal light reflectance and heat emission patterns that are characteristic of the different discharges, water masses, plankton blooms and suspended sediment loads. Most often this is due to specific substances contained in the effluent but absent in the surrounding water.

3.1 Imaging in the UV-Visible-Near Infrared Spectrum

This is the most common technique used with satellite and aerial images. Wavelengths (colors) within the range of the human eye are most often used but Ultraviolet (UV) wavelengths are useful for detecting fluorescence from petroleum compounds (oil, diesel, etc.) and near-IR wavelengths can be useful for correcting atmospheric interference from aerosols (e.g., smog and smoke). Near-IR wavelengths are also highly reflected from kelp seaweeds, so such data are very useful for delineating the region's kelp beds and monitor their extents through time.

The best detection capabilities are attained when several images in different wavelengths are acquired simultaneously. These "multispectral" data can be digitally processed to enhance features not readily visible in simple color photographs. For example, two such images can be ratioed, thus emphasizing the water features' differences in reflection of the two specific wavelengths. A multi-wavelength image set can also be analyzed with "multispectral classification algorithms" which separate different features or effluents based on the correlation relationships between the different color signals.

The depth to which the color sensors can penetrate depends on which wavelengths they see, their sensitivity and the general water clarity. In the San Diego region, green wavelengths tend to reach the deepest and, as elsewhere, UV and near-IR wavelengths penetrate the least. Generally, OI's satellite and aerial sensor data reveal patterns in the upper 15-40 feet.

3.2 Imaging in the Thermal Infrared Spectrum

Some satellite and aerial sensors image heat emanating from the ground and the ocean. They thus reveal patterns and features due to their differences in temperature. Since thermal infrared (TIR) wavelengths are strongly absorbed by water, the images reveal temperature patterns only on the water's surface. Such images can help detect runoff plumes when their temperatures differ from the surrounding ocean water. Runoff from shoreline sources tends to be warmer than the ocean water, although the reverse can be true during the winter. Plumes from offshore outfalls can sometimes also be detected with thermal imaging. Since the effluent contains mostly fresh water, it is less dense than the surrounding salt water and tends to rise towards the surface. How far it rises depends on outfall depth, ocean currents, and stratification conditions. If it makes it all the way, it is usually cooler than the surrounding sun-warmed surface water. A plume signature detectable in multispectral color imagery but not detectable in simultaneously collected TIR imagery indicates the rising plume has not reached the actual ocean surface and remains submerged.

3.3 Satellites and Sensors Utilized

In October 2002, the operational monitoring phase of the project was initiated. To date, this work utilizes 1100 m resolution Advanced Very High Resolution Radiometer (AVHRR)-derived imagery (available multiple times per day), 1000 m resolution chlorophyll and SST Moderate Resolution Imaging Spectroradiometer (MODIS)-derived imagery (available multiple times per day), 500 m resolution MODIS true color imagery (available near-daily), 750 m resolution Visible Infrared Imaging Radiometer Suite (VIIRS) chlorophyll and SST imagery (available multiple times per day), 300 m resolution Sentinel 3 color and thermal imagery (available daily), 30 m & 60 m Landsat 7 ETM+ , Landsat 8 OLI/TIRS and Landsat 9 OLI-2/TIRS color and thermal imagery (each available approximately every 16 days), 10 m resolution Sentinel 2 multispectral imagery (available 2-4 times per week), and 6 m resolution Satellite Pour l'Observation de la Terre (SPOT) 6 and SPOT 7 (available approximately every 4-5 days). Synthetic Aperture Radar (SAR) from the Sentinel 1A and 1B satellites (available every 3-6 days at a spatial resolution of 5m x 20 m) were added to the mix of remote sensing data in late 2021.

Until 2010, the project relied heavily on acquisition of multispectral color imagery with OI's DMSC-MKII aerial sensor and TIR imagery from a Jenoptik thermal imager integrated into the system (see details in the "Technology Overview" section). These aerial image sets were most often collected at 2 m resolution. The flights were done on a semi-regular schedule ranging from 1-2 times per month during the summer to once or more per week during the rainy season. The flights were also coordinated with the City of San Diego's regular offshore field sampling schedule so that the imagery was collected on the same day (usually within 2-3 hours) of the field data collection. Additional flights were done on an on-call basis immediately after major storms or other events such as sewage spills. In late 2010, OI negotiated a special data collection arrangement with Germany's RapidEye Corporation and this project began utilizing their multispectral imagery in lieu of most of the aerial Digital Multispectral Camera (DMSC) image acquisitions. The use of satellite as opposed to aerial data also enables a more regionally contiguous monitoring of events affecting the target areas. In late 2019 the RapidEye satellite constellation was decommissioned by the current operator Planet Labs. Subsequently, OI secured the regular acquisition of SPOT 6 and SPOT 7 satellite imagery covering the same geographical area beginning in 2020. **Table 1** lists the properties of the remote sensing image sources routinely used during the project.

The prime objectives of the project have expanded somewhat since its inception. Initially, emphasis was on utilizing the image data to discern and monitor surface and near-surface signatures from the SBOO and PLOO, separate them from other nearshore point and non-point runoff features, and monitor their locations, extents and potential impact on the shoreline. Prior to this project, the spatial extents of the plumes could only be estimated from a relatively sparse spatial grid of field samples, which made it very difficult to separate, for example, the SBOO near surface plume from the Tijuana River runoff plume. This ambiguity made it difficult, in turn, to objectively evaluate the potential contribution, if any, of the SBOO plume to beach contamination along the nearby shoreline. The satellite and aerial imagery helped directly establish the dispersal trajectories of the SBOO effluent during months when it reaches the near-surface layer and support the claim that it likely never reaches the surf zone.

Over the past five to ten years, the project's objectives have broadened from focusing primarily on the outfalls to also provide larger-scale, regional observations of the physical and biological patterns and processes affecting the San Diego County and Tijuana River discharge regions. It is this broader-view perspective that led to the creation of the

Table 1. Satellite sensors utilized in the project and their characteristics.

Sensor	Utilization Period	Resolution (m)	Utilized Wavelength Range
AVHRR	2003 - Present	1100	Channel 4: 10.30 – 11.39 um Channel 5: 11.50 – 12.50 um
MODIS	2003 - Present	250/500/1000	Band 1 (250 m): .620 – .670 um Band 2 (250 m): .841 – .876 um Band 3 (500 m): .459 – .479 um Band 4 (500 m): .545 – .565 um
Landsat TM/ETM+ 4-7	2013 - 2022	30 (visible - Near-IR) 60 (Thermal-IR)	Band 1: .450 - .520 um Band 2: .520 - .600 um Band 3: .630 - .690 um Band 4: .760 - .900 um Band 6: 10.40 - 12.50 um (TM5 Thermal not used due to noise)
Landsat 8 OLI-1, TIRS	2003 - Present	30 (visible - Near-IR) 100 (Thermal-IR)	Band 2: .452 - .512 um Band 3: .533 - .590 um Band 4: .636 - .673 um Band 5: .851 - .879 um Band 10: 10.60 - 11.19 um Band 11: 11.50 - 12.51 um
Landsat 9 OLI-2, TIRS	2022 - Present	30 (visible - Near-IR) 100 (Thermal-IR)	Band 2: .452 - .512 um Band 3: .533 - .590 um Band 4: .636 - .673 um Band 5: .851 - .879 um Band 10: 10.60 - 11.19 um Band 11: 11.50 - 12.51 um
Sentinel 2A/2B	2017 - Present	10 (visible - Near-IR) 60 (Vegetation Red Edge) 60 (UV, SWIR)	Band 1: .443 um Band 2: .490 um Band 3: .560 um Band 4: .665 um Band 5: .705 um Band 6: .740 um Band 7: .783 um Band 8: .842 um Band 8A: .865 um
Sentinel 3A/3B	2018 - Present	300 (all utilized bands)	Band Oa2: .412.5 um Band Oa3: .442.5 um Band Oa4: .490 um Band Oa5: .510 um Band Oa6: .560 um Band Oa7: .620 um Band Oa8: .665 um Band Oa10: .68125 um Band Oa11: .07875 um Band Oa17: .865 um
VIIRS	2019 - Present	750 (all utilized bands)	Band M1: 0.402 - 0.422 um Band M2: 0.436 - 0.454 um Band M3: 0.478 - 0.488 um Band M4: 0.545 - 0.565 um Band M5: 0.662 - 0.682 um Band M6: 0.739 - 0.754 um Band M7: 0.846 - 0.885 um Band M8: 1.23 - 1.25 um Band M9: 1.371 - 1.386 um Band M10: 1.58 - 1.64 um Band M11: 2.23 - 2.28 um Band M12: 3.61 - 3.79 um Band M13: 3.97 - 4.13 um Band M14: 8.4 - 8.7 um Band M15: 10.26 - 11.26 um Band M16: 11.54 - 12.49 um
SPOT 6/7	2019 - Present	6	Band 1: .450 - .745 um Band 2: .450 - .525 um Band 3: .530 - .590 um Band 4: .625 - .695 um Band 5: .760 - .890 um
Sentinel 1A/1B SAR	2021 - Present	5 x 20	C-band operating at a center frequency of 5.405 GHz

additional image products from additional sensors for the City.

In 2012, OI added additional broad-scale products to the datasets available to the City and project partners. These include two types of ocean current products: High Frequency Radar-derived surface currents (HF Radar) and Hybrid Coordinate Ocean Model (HYCOM) model-derived surface currents (http://hycom.org). The raw data for the HF Radar currents are retrieved from National HF Radar Network via the Scripps Coastal Observing Research and Development Center (CORDC) on an hourly basis and reformatted into ESRI-compatible shapefiles. The hourly products are averages of the previous 25 hours and generated at 1 km and 6 km spatial resolutions. Additional HYCOM model-based products include daily ocean salinity, mixed layer depth, and subsurface temperature at 50, 100, 150 and 200 meters. In 2016 these products were delivered in a Web Map Service (WMS) Representational State Transfer (REST) service format compatible with the City's now retired BioMap server. They are presently being generated and archived in preparation for delivery via a next generation WMS dashboard planned for the future. The existing high resolution (6-30 m) observation region extends from approximately La Jolla southward to Rosarita Beach, Mexico and out approximately 50 miles. The coarser-scale products (250-1000 m) such as chlorophyll, SST, ocean currents and HYCOM-derived products encompass the entire SCB.

3.4 Recent Data Enhancements

Beginning in 2017, OI also began processing and posting imagery from the Sentinel-2A satellite. Sentinel-2A is a satellite operated by the European Space Agency (ESA) and is the spaceborne platform for the Multispectral Instrument (MSI). The Sentinel 2 MSI samples 13 spectral bands: four bands at 10 meters, six bands at 20 meters and three bands at 60-meter spatial resolution. The green band focusing in the 560 nm wavelength is ideal for detecting turbidity plumes from the outfalls both at the surface and at depths down to 40 feet depending on ocean conditions. A second satellite carrying the MSI sensor, the Sentinel-2B (identical to 2A), was launched into orbit by the ESA and provided the first set of data from the MSI sensor as of March 17, 2017. In 2018, data from Sentinel 2B became a regular addition to the satellite imagery products posted to the OI San Diego Water Quality (SDWQ) web portal. On average the Sentinel 2A and 2B imagery processed to highlight anomalous turbidity signals emanating from the PLOO, SBOO, the discharge from the Tijuana River, as well as the Pt. Loma kelp bed are posted to the OI web portal within 24-36 hours of satellite data acquisition. In some cases, if the data are available to OI earlier, the image products are delivered as quickly as 12 hours after acquisition. During the 2017 to 2021 time period, the Sentinel 2A and 2B satellites provided the most temporarily comprehensive set of high-resolution satellite imagery. In total, 526 high resolution satellite images showing the offshore San Diego County region were acquired, processed, and delivered during that time span. Between 2012 and 2016 196 high resolution satellite images were used for the monitoring. This equates to a 168% increase in the high-resolution satellite data used to document the project area of interest (AOI) between 2017-2021 when compared to the previous five years. Of the 526 total images, 333 were from Sentinel 2A or 2B making up ~63% of the high-resolution satellite data used for analysis. On average, the addition of Sentinel 2 data effectively increased the number of high-resolution satellite observations of the San Diego region to ~105 per year, compared to the prior average of ~39/yr. 2021 showed the highest number of high-resolution datasets to date (135) used for the project.

In October 2018, OI incorporated imagery from Sentinel-3A into the program. Shortly thereafter, in December of 2018 imagery from Sentinel-3B was added. Just like Sentinel 2, Sentinel-3A and Sentinel-3B are earth observation satellites developed by the

ESA for the Copernicus Program. Sentinel-3A was launched on February 16, 2016, and Sentinel-3B followed on April 25, 2018. The 3A and 3B satellites are identical and deliver products in near-real time. The satellites include 4 different remote sensing instruments. The Ocean and Land Colour Instrument (OLCI) covers 21 spectral bands (400–1020 nm) with a swath width of 1270 km and a spatial resolution of 300 m. The Sea and Land Surface Temperature Radiometer (SLSTR) covers 9 spectral bands (550–12000 nm), using a dual-view scan with swath widths of 1420 km (nadir) and 750 km (backwards), at a spatial resolution of 500 m for visible and near-infrared, and 1 km for TIR channels. The Sentinel 3 mission's main objectives are to measure sea surface topography along with the measurement of ocean/land surface temperature and ocean/land surface color. One of the satellites' secondary missions is to monitor sea-water quality and marine pollution. The instrument on these satellites designed for these purposes is the OLCI. Ocean Imaging creates daily products dependent on cloud cover for the entire San Diego/Tijuana region using the OLCI instrument. Between the 3A and 3B satellites this results in better than daily coverage with 3A and 3B data occasionally both being available on the same day. True color, near infrared, products are posted bi-monthly along with the similar resolution MODIS products. Other possible, future products derived from the Sentinel 3 sensors being considered as additions to the monitoring data set include chlorophyll, sea surface temperature, total suspended matter (TSM), as well as cyanobacteria monitoring. Sentinel 3 carries the only satellite sensor package with the necessary spectral bands, spatial resolution, and coverage for near real-time detection of cyanobacteria. The results of these products may also be compared to the field sampling data in order to assess accuracy. **Figure 2** shows a time series of the offshore San Diego region using Sentinel 3 data between 11/24/20 and 12/04/20. During this period, a plankton bloom developed west of Pt. Loma and Coronado and forms a cyclonic eddy off the coast. The plankton bloom then dissipates but forms again towards the middle of December. This unique time series highlights the usefulness of how daily Sentinel 3 data at 300-meter resolution can provide informative temporal documentation of the oceanographic and biological conditions in the region. An animated version of this figure better illustrating the dynamics of the changing conditions through 12/30/20 can be found on the Ocean Imaging-San Diego Water Quality website at: https://oceani.com/SDWQ/2020-S3-Time-Series.gif.

As stated above, the RapidEye satellite data were discontinued as of late 2019 and replaced by data from the SPOT 6 and SPOT 7 satellites in January of 2020. SPOT 6 and SPOT 7 are identical in design and function. They both image in spectral bands similar to the RapidEye satellites at a slightly better ground sampling distance of six meters for the multispectral data. The dynamic range of these sensors is 12-bits per pixel. OI uses the blue, green, red, and near-infrared bands from these sensors. We have found that the SPOT data have a high signal to noise ratio and therefore produce a high-quality product for detecting wastewater surface manifestations and delineating the river run-off plumes. Because of the ability of these sensors to image from off-nadir viewing angles it is also possible to obtain imagery close together in time. **Figure 3** shows a set of SPOT and Sentinel 2 images from 03/01/21, 03/04/21, 03/05/21 and 03/06/21 highlighting the ability to obtain high-resolution imagery from multiple satellites on successive days. Note the relatively small TJR discharge moving offshore to the west on the 03/01 which develops into a large, turbid plume, first continuing its push to the northwest towards Pt. Loma then dying down and dissipating within a 24-hour period. 25-hour averaged HF Radar ocean currents from these days derived within one to two hours of the satellite data acquisition are overlaid on the imagery corroborate the shift in current direction seen in the imagery.

In 2021, there were 21 occurrences when either Sentinel 2A or 2B data were acquired within minutes

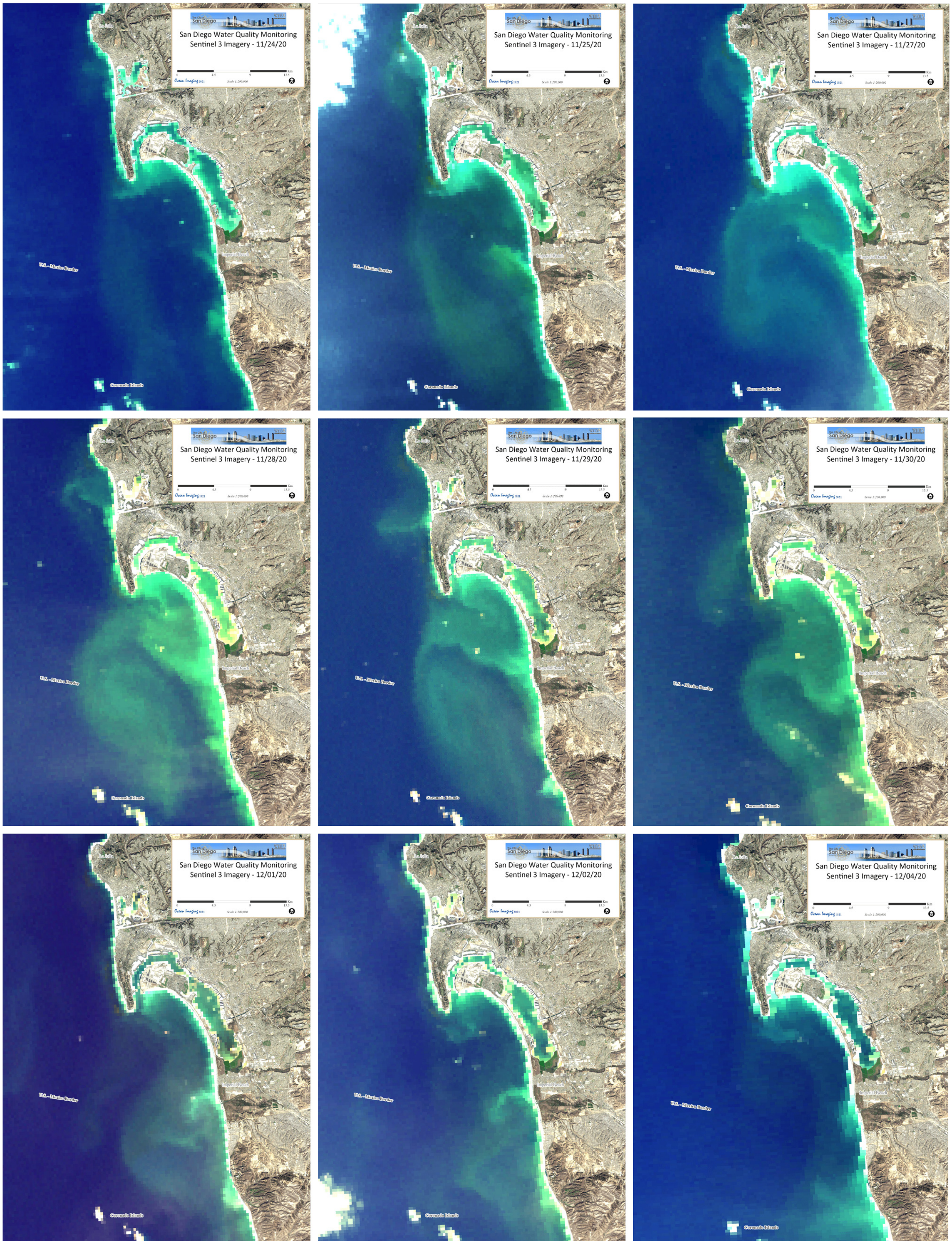

Figure 2. Sentinel 3 RGB Time series showing the development and dissipation of a phytoplankton bloom and large eddy west of San Diego. For a more complete time series presented as an animation visit: https://oceani.com/SDWQ/2020-S3-Time-Series.gif.

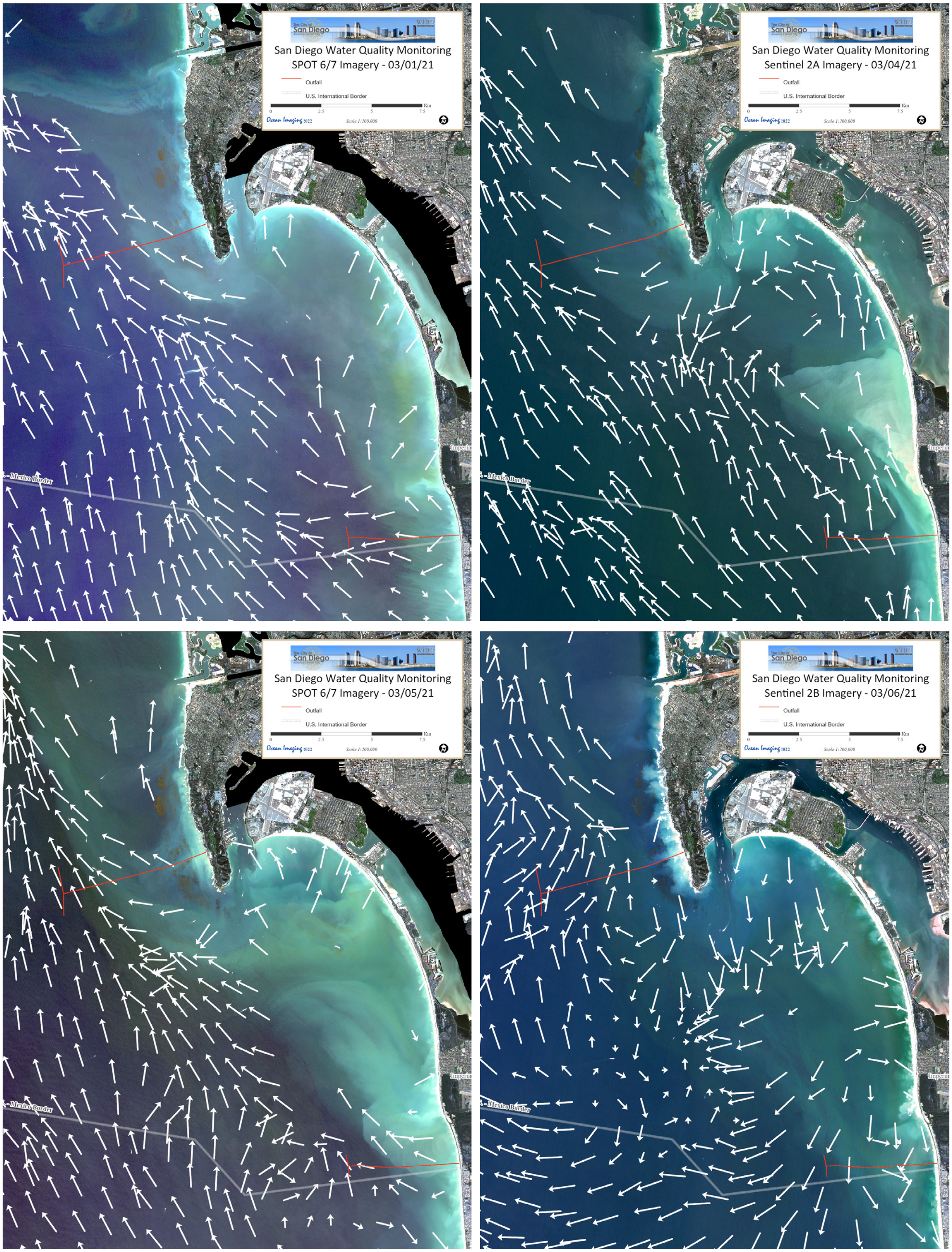

Figure 3. SPOT and Sentinel 2 imagery of the SBOO region between 03/01/21 and 03/06/21. Both satellite systems show the development and expansion of a large TJR discharge plume fist moving to the west, then northwest and finally dissipating over the 5-day period. 25-hour averaged HF Radar currents from the same day and time are overlaid on the image data.

to hours of either SPOT, Landsat TM7 or Landsat 8 OLI/TIRS data providing a near time-coincident validation of features (or lack thereof) observed in the imagery. There was one day on which all three satellite/sensors acquired data of the San Diego offshore region within hours of each other. **Figure 4** provides an example of the SBOO surface turbidity expression observed 28 minutes apart by SPOT 7 and the Landsat 8 satellite sensors on 01/04/21. The surface turbidity plume extending to the south from the SBOO is one of the largest/strongest observed that year. The Landsat thermal imagery reveals that the turbid water coming from the wye is cooler than the surrounding water. A relatively large turbidity plume emanating from the TJR and moving to the south is also readily apparent in the imagery.

3.5 Data dissemination and analysis

The satellite data are made available to the SDPUD and other project constituents through a dedicated, password-protected web site. Although it is possible to process most of the used data in near-real-time, earlier in the project it was decided that the emphasis of this project is not on providing real-time monitoring support and the extra costs associated with the rapid data turn-around are not warranted. Most satellite data is thus processed and posted within 1-2 days after acquisition. As noted above however, OI has in a number of cases made imagery available to the SDPUD in near-real time (within 12-24 hours) via email when observations appeared to be highly significant to the management of beach closures or other sudden/anomalous events.

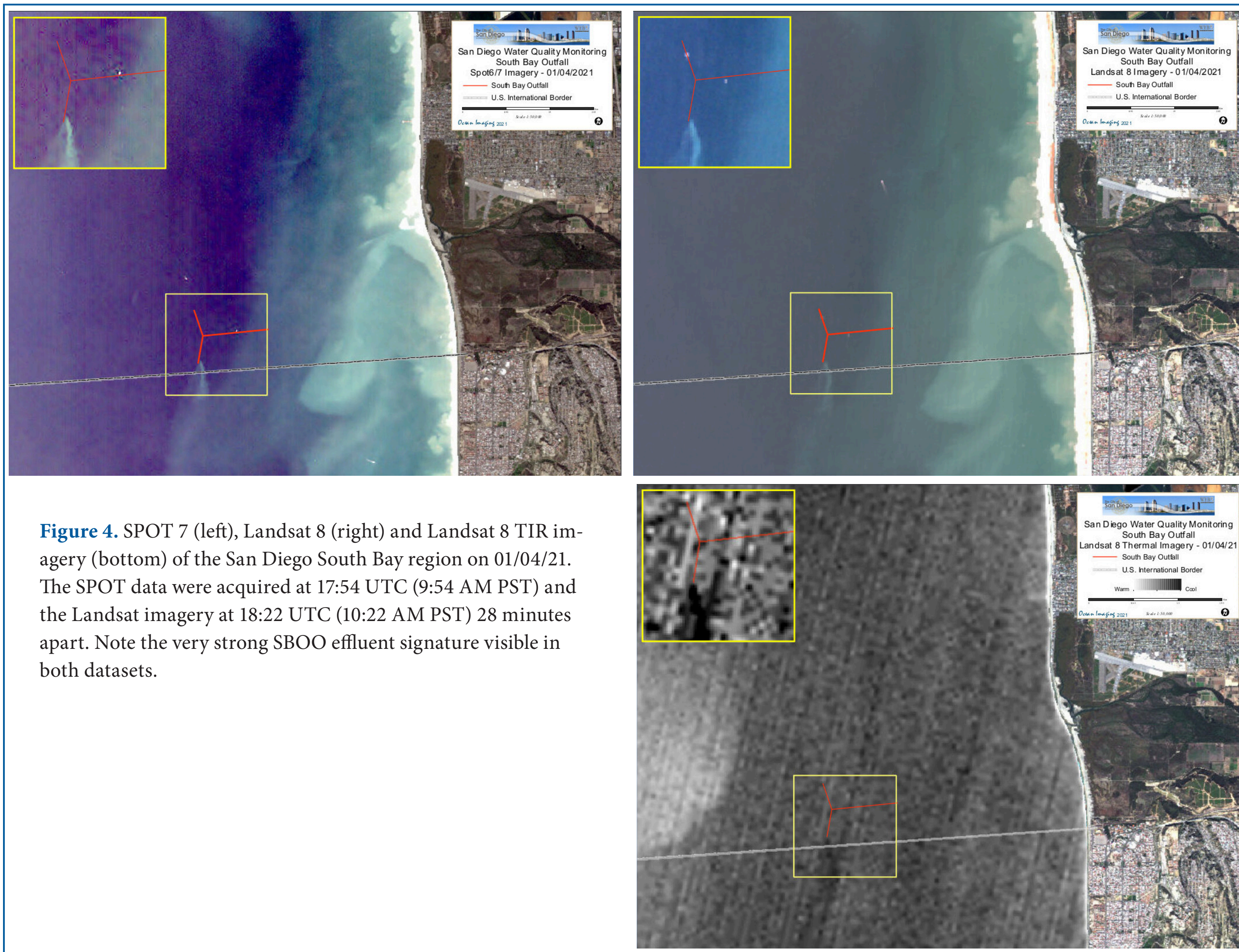

Figure 4. SPOT 7 (left), Landsat 8 (right) and Landsat 8 TIR imagery (bottom) of the San Diego South Bay region on 01/04/21. The SPOT data were acquired at 17:54 UTC (9:54 AM PST) and the Landsat imagery at 18:22 UTC (10:22 AM PST) 28 minutes apart. Note the very strong SBOO effluent signature visible in both datasets.

3.6 Field Sampling Data

A total of 19 shoreline stations, ranging from Mission Beach to northern Baja (across the US/Mexico border), are sampled weekly, by City of San Diego staff, to monitor the levels of three types of fecal indicator bacteria (i.e., total coliform, fecal coliform, and Enterococcus bacteria) in recreational waters (**Figure 5**). An additional 15 nearshore (kelp) stations are also sampled weekly to monitor Fecal Indicator Bacteria (FIB) and a range of water quality parameters (i.e., temperature, salinity, dissolved oxygen, pH, transmissivity, Chlorophyl-a, CDOM). Furthermore, 69 offshore stations are sampled quarterly to monitor both water quality conditions and one or more types of FIB. These stations are located from 9 to 55-m depth in the SBOO region, and 9 to 98-m depth in the PLOO region.

The City Marine Microbiology Laboratory (CMML) follows guidelines issued by the U.S. Environmental Protection Agency (USEPA) Water Quality Office, State Water Resources Control Board (SWRCB) including the 2019 Ocean Plan, the California Department of Public Health (CDPH),

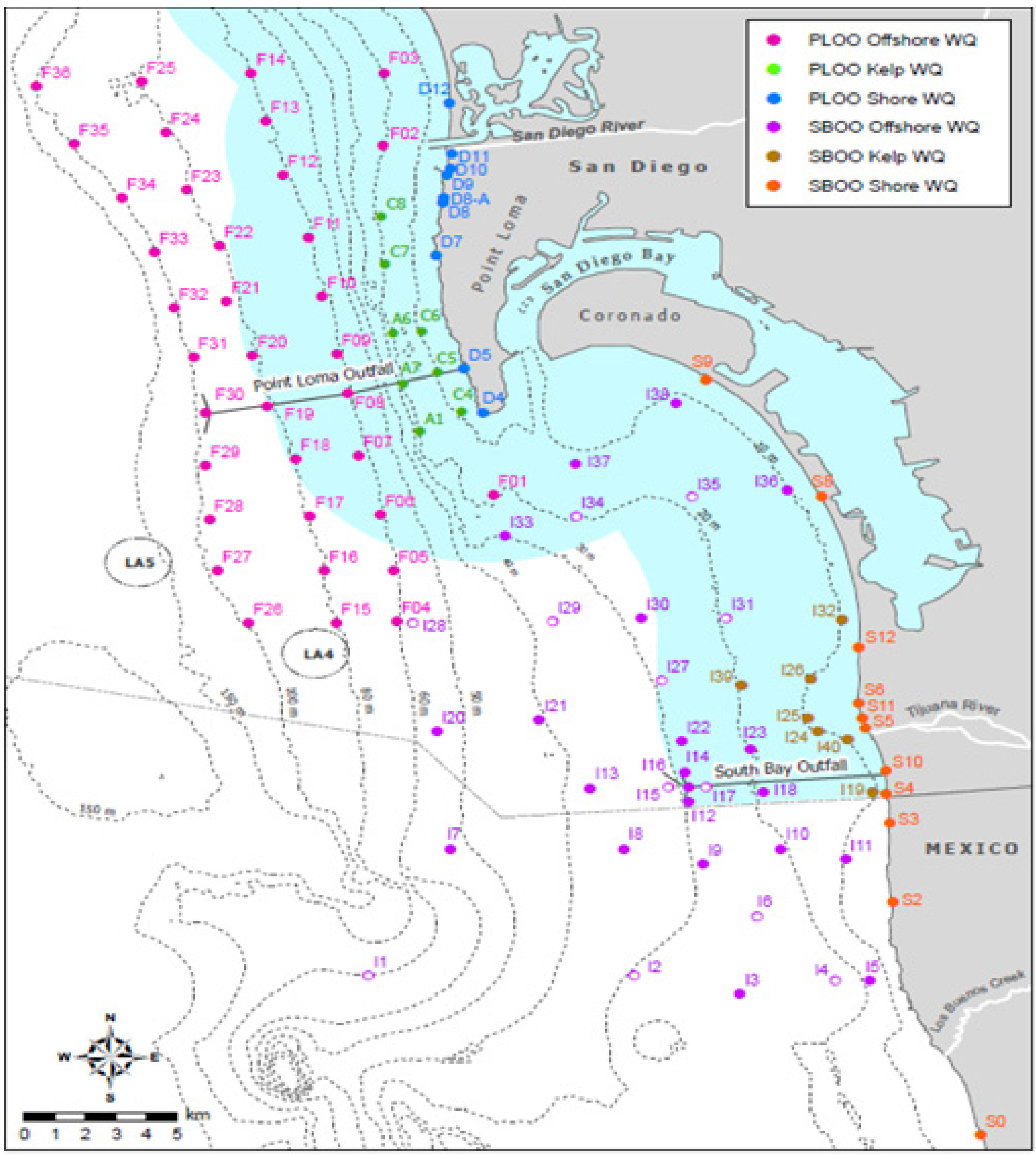

Figure 5. Outfall location and corresponding shoreline and offshore field sampling stations for SBOO and PLOO

and Environmental Laboratory Accreditation Program (ELAP) with respect to sampling and analytical procedures (Bordner et al. 1978, APHA 2012, CDPH 2000, USEPA 2009). All bacterial analyses were initiated within eight hours of sample collection and conformed to standard membrane filtration techniques, for which the laboratory is certified (ELAP Field of Testing 126). FIB densities were determined and validated in accordance with USEPA and APHA guidelines as follows. [APHA] American Public Health Association. (2012). Standard Methods for the Examination of Water and Wastewater, 22nd edition. American Public Health Association, American Water Works Association, and Water Environment Federation.

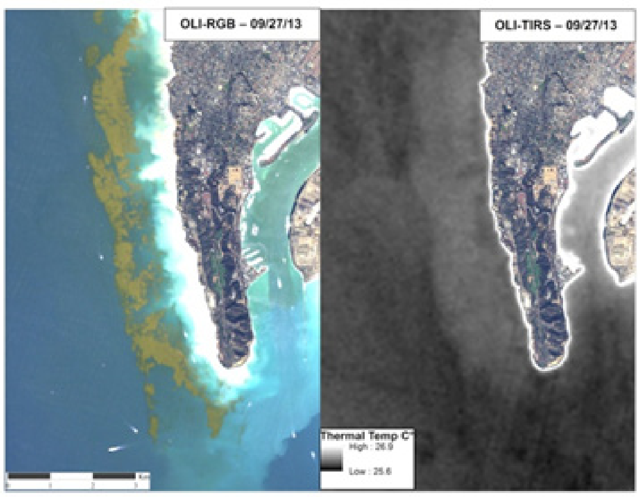

Figure 6. Satellite image of the Pt. Loma region showing the kelp bed (yellow) and corresponding thermal boundary patterns.

4. HISTORICAL RESULTS

4.1 The Point Loma Ocean Outfall

The PLOO represents a major contrast to the SBOO both in greater distance from shore (7.2 vs. 5.5 km) and primarily in depth of discharge (@95 vs. 27 m). Also, its daily discharge volume is nearly five times greater. During the 21 years of this project no satellite or aerial image was ever collected with a verifiable surface turbidity or thermal signature of the PLOO's effluent plume. Regular field sampling results also support the notion that the plume rarely, if ever, reaches the surface layer in concentrated or detectable form. This is likely due not only to the outfall's great depth but also to its location near the break in the mainland shelf. The shelf drops precipitously immediately offshore from the diffuser, and a significant portion of the discharged effluent is believed to be carried off into deep water by swift currents. Remote sensing work in the PLOO region has primarily concentrated on monitoring shoreline phenomena such as discharges from the San Diego River and Mission Bay to the north that affect water quality along Pt. Loma, and mesoscale phenomena such as plankton blooms and runoff events from the north and south that get swept over the PLOO location and thus affect offshore sampling results. High resolution imaging also provides a comprehensive means to monitor changes in the Pt. Loma kelp bed — one of the largest in California — which the PLOO bisects.

The PLOO transects three primary areas along its 7.2 km underwater length: 1) shallow waters with rocky and sandy bottom between the shoreline and the Pt. Loma kelp bed; 2) The kelp bed itself; 3) a bottom slope and deeper waters west of the kelp. Multispectral and thermal imagery acquired for this project shows that the offshore location of the PLOO wye often places it outside a relatively stable alongshore upper-column water mass boundary that is detectable in the imagery and tends to represent a current shear zone as well (as revealed in HF-Radar data). During the warmer months, surface waters between the shore and the kelp bed, and sometimes within the kelp bed itself tend to be warmer by a degree Celsius or more than the waters immediately west of the kelp bed. As is exemplified in **Figure 6**, a region 2-4 km wide with noticeably cooler SSTs often rounds the outside of the bed. We believe the cooler SST band represents upwelling associated with the drop-off in bottom topography outside the kelp bed. Since upwelled water could provide a mechanism to bring the submerged PLOO effluent to the surface and closer to shore, we have paid particular attention in analyzing the thermal and turbidity/color patterns in that zone relative to time-coincident monthly and (more recently) quarterly field sampling done by the CMML. We have never identified a thermal or color anomaly similar to those from the SBOO, that was separate from larger scale patterns outside the region. Correspondingly, while some offshore sampling stations (e.g., F08/A17) occasionally show elevated bacteria counts at 60 m (rarely up to 25 m) and deeper, the elevated counts generally do not extend to shallower depths monitored by the remote imaging. (City of San Diego, 2020) An area of cool SSTs is also commonly seen in the region's thermal imagery just south of Pt. Loma, which we believe corresponds to locally driven upwelling modeled and field-validated by others (e.g., Roughan et al. 2005).

As is the case with much of the San Diego coastline, the most commonly occurring near-shore current regime along Pt. Loma is southward. Under such conditions, nearshore waters from San Diego's North County are swept southward, deflected offshore somewhat by the La Jolla peninsula, and thus often cover the area over the PLOO wye. During the rainy season those waters contain highly turbid runoff from North County's several lagoons, sweeping it over the offshore PLOO area along with (after heavy storms) turbid discharge from the San Diego River and Mission Bay (**Figure 7A**). Since the North County nearshore waters also tend to give rise to intense red tide (dinoflagellate) blooms during various times of year, the plankton-laden streams also tend to be advected over the PLOO wye area (**Figure 7B**). The area within and inside the Pt. Loma kelp bed tends to be more often affected by direct shore runoff, and discharges from the San Diego River and Mission Bay during the southward current regime. Unlike the TJR plume which contains heavy suspended sediment loads and very high indicator bacteria concentrations, the San Diego River and Mission Bay

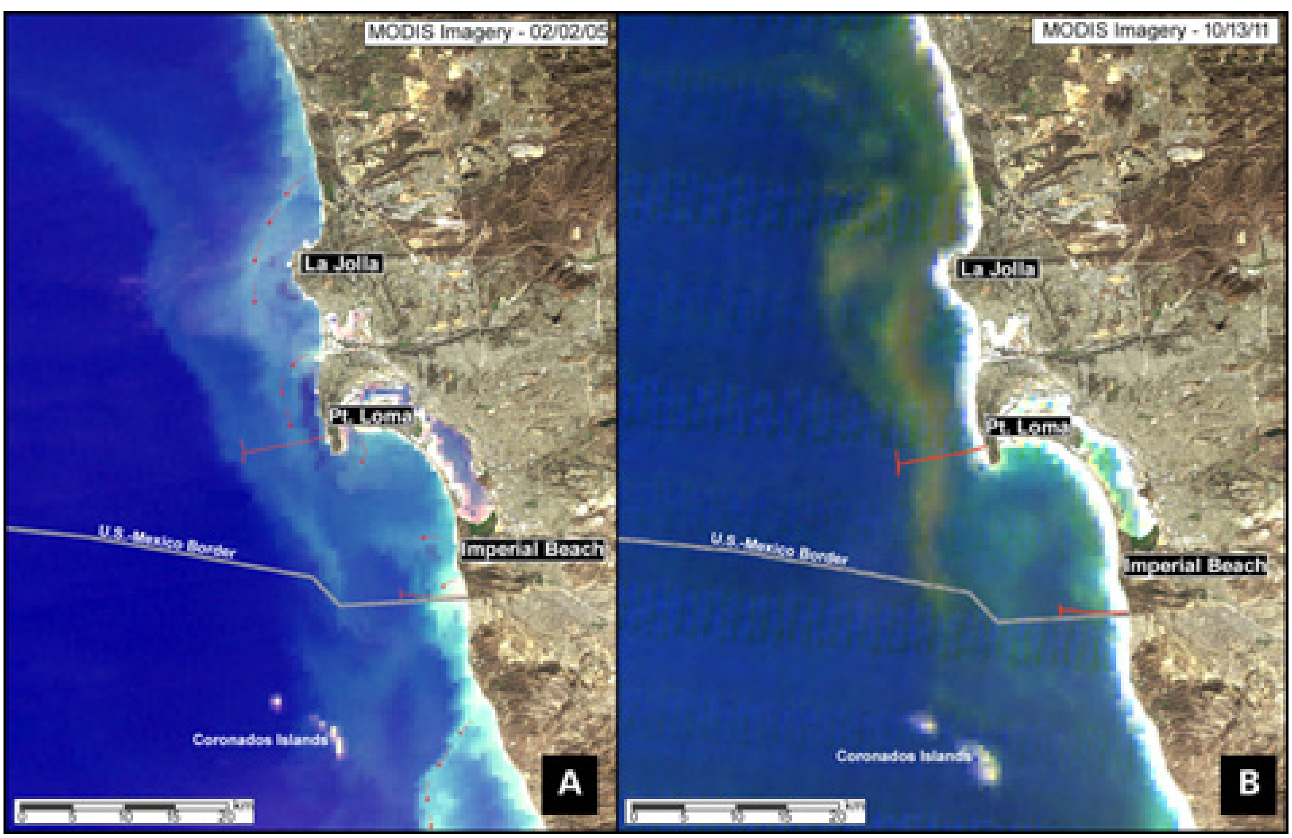

Figure 7. MODIS satellite imagery of the San Diego region showing (A) stormwater runoff from the north advecting over the PLOO region and (B) a north-originated dinoflagellate "red tide" bloom being advected over the region.

plumes tend to more commonly have only sub-exceedance bacteria levels. As was described above for the SBOO region, occasional northward flow regime episodes also affect the waters along Pt. Loma. Both tidal and storm runoff plumes from the San Diego River and Mission Bay are deflected northwestward under such conditions, and runoff outflow from San Diego Bay tends to round Pt. Loma and affect the southern section of the kelp bed, as well as the area between the kelp bed and the PLOO wye (**Figure 8**).

4.2 The South Bay Ocean Outfall

The wastewater plume emitted from the SBOO generally remains well below the surface between approximately late March and November due to vertical stratification of the water column. Seasonal breakdown of the vertical stratification results in the plume's rise closer to the surface or to actually reach the surface between approximately late November and late March, when it can sometimes be detected in near-surface field samples at sampling stations over the outfall wye. Prior to this project, regular field sampling at a preset station grid around the outfall (Figure 5 above) provided the only means to estimate its plume's trajectory and whether it had reached the surface. Since the SBOO wye is located relatively close to the TJR mouth, it was often difficult or impossible to positively separate plumes from the two sources with the field samples, especially during the rain seasons when the TJR plume was large and both plumes expanded in the ocean surface layer. This situation led to contentions by some that the SBOO effluent reaches the shoreline and is thus directly responsible for some beach contamination events. Remote sensing observations early in this project established that the two plumes are detectable in imagery with Landsat TM resolutions or better (≤30 m). The plumes are almost always spatially separated, allowing their identification and separation directly from their location. The rare exceptions occur immediately after extreme storm events when the TJR runoff plume can

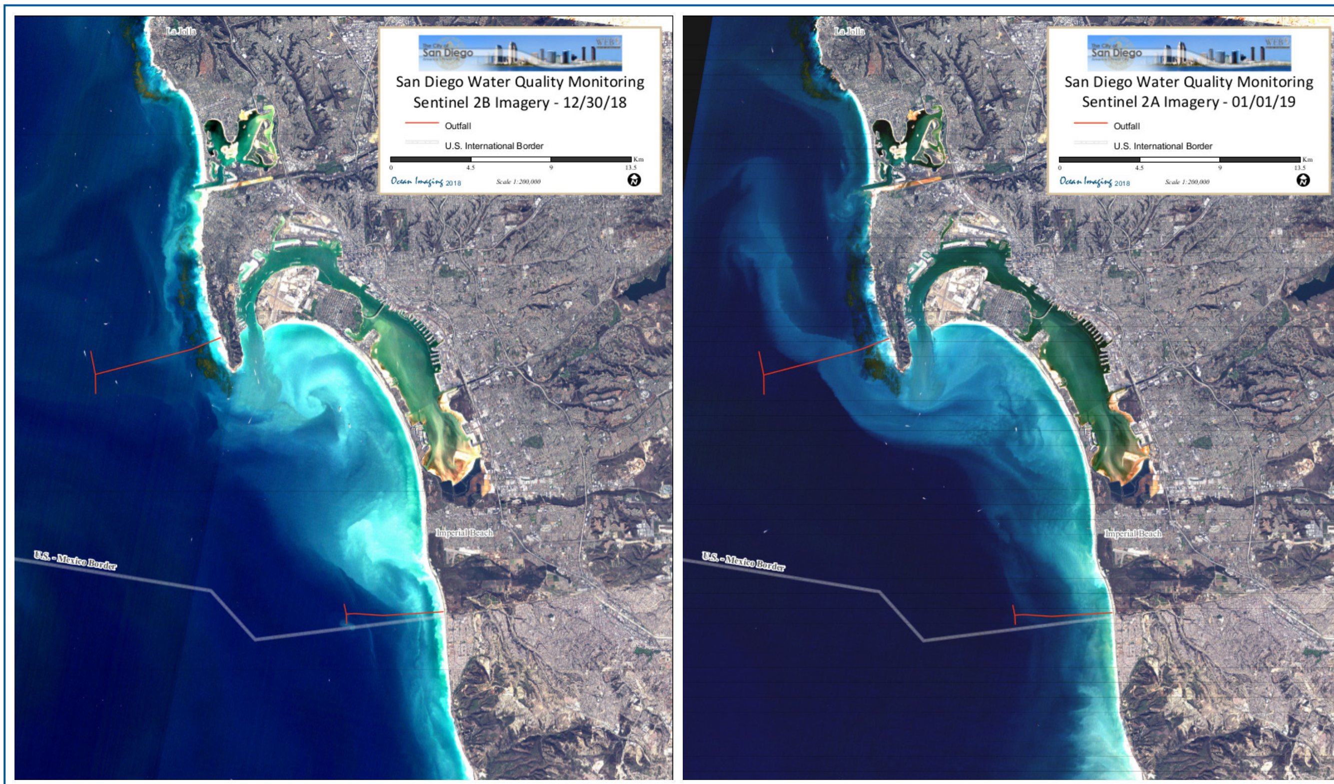

Figure 8 – Sentinel 2 satellite imagery showing parts of the TJR plume being advected up and around the west side of Pt. Loma and up during a 12/30/2018 – 01/01/2019 northward current regime episode. The PLOO and SBOO are shown in red.

extend far offshore and overrun the SBOO wye region. Upon breaking the surface, the SBOO plume was also found to exhibit an identifiable thermal signature, distinctly cooler than the surrounding water (see Figures 4 above and 11 below).

Internally, the SBOO plume tends to exhibit a relatively homogenous spectral signature which decreases in intensity with distance from the wye, as the discharge progressively mixes into the surrounding ocean. Within the first few years of this project the characteristic SBOO plume extents and trajectories (when it reached the surface layer) were established through repeated imaging. The most common near-surface current pattern in the SBOO wye region is southward (Roughan et al. 2005). Under such circumstances, the plume tends to be directed from the wye toward the south-south-east (**Figure 9A**) or more directly southward (**Figure 9B**). The plume tends to have a sharply defined triangular shape, expanding with distance from the wye and decreasing in intensity for up to several kilometers, as its effluent dilutes through mixing into the surrounding water column. Except for station I9, the field sampling grid has no established stations in that area, and so the plume tends to remain mostly undetected in field data under southward current field conditions except for, occasionally, station I12 over the wye.

The SBOO outfall is also affected by periodic northward current episodes. These events usually last from less than 24 hours to 2-3 days. In such conditions, observations of the outfall plume show it to be most often advected northwestward (**Figure 10A**) and on rare occasions to the north or northeast, as is exemplified in **Figure 10B**. Acoustic doppler current profilers (ADCPs) near the SBOO indicate that the currents often alternate between a north northwest and southeast direction (City of San Diego 2020). During northward current episodes the high-resolution satellite observations have shown it to be detectable up to several kilometers from the outfall wye, often curving northwestward. We believe the reason for the westward motion component corresponds to the general offshore veering of the region's flow pattern as waters from the south become deflected by the shallower bottom topography of the TJR's alluvial fan (as seen in the protrusion of the bathymetric contour lines shown in Figure 5 above). More immediate mixing appears to occur along the plume's edges during northward flow, since they tend to be considerably less sharp than in the southward flowing patterns. During the northward flow conditions,

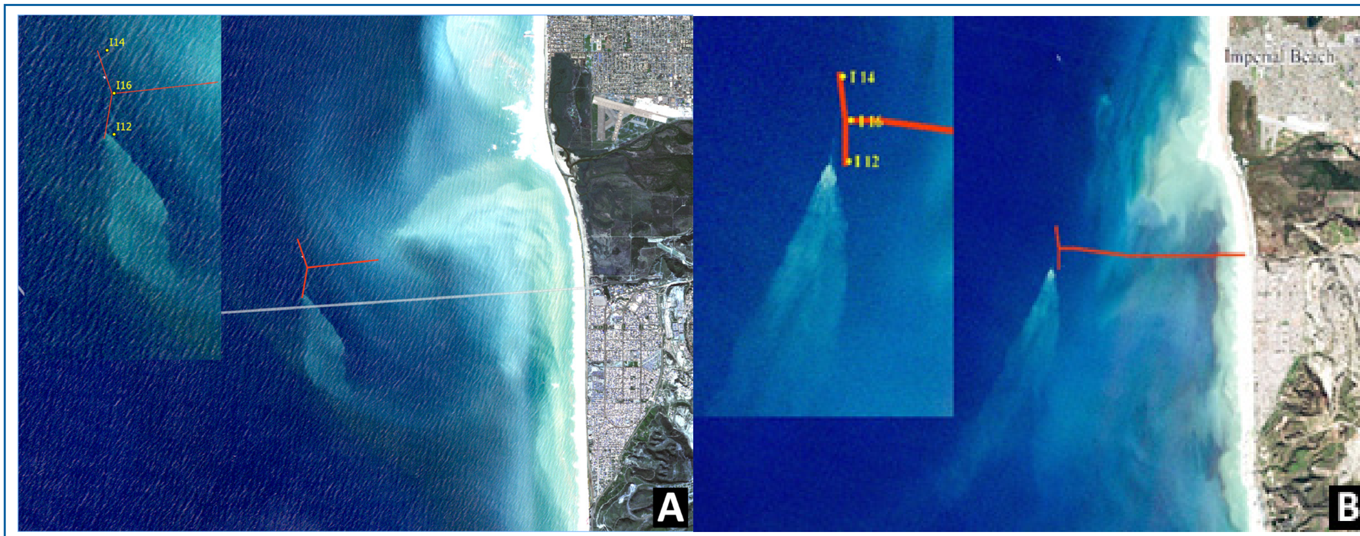

Figure 9. Typical SBOO plume dispersal patterns during southward current conditions on 02/03/2020 imaged with the Sentinel 2B (left), and on 01/04/2012 imaged with RapidEye satellite (right). Multi-depth field samples were taken at the three wye stations on the same day of the RapidEye image (01/04/2012) but showed no elevated bacteria values.

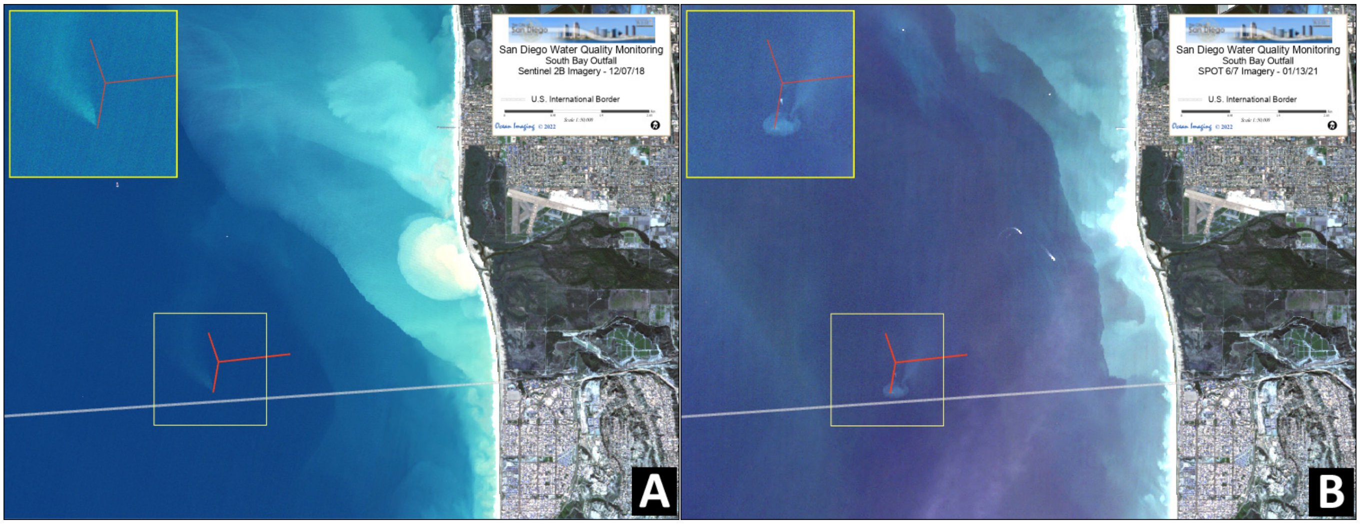

Figure 10. Unusual SBOO plume dispersal patterns during northward current conditions on 12/07/18 imaged with the Sentinel 2B (left), and a rare situation when the SBOO plume was pushed to the northeast on 01/13/2021 imaged with SPOT 6 (right).

evidence of the effluent's near-surface manifestation is also sometimes seen in time coincident field samples at stations I-12 and I-16 and/or I-14 to the north.

Under low to mild current conditions the higher resolution satellite and aerial images can sometimes discern separate plume components emanating from the different active diffuser groups along the SBOO wye. Examples are shown in **Figure 11**. The uneven intensity of some of them initially caused a concern to the outfall's designer – Parsons Corporation – when first such images were made available in 2003-2004. Parsons conducted an underwater video survey of the wye and found all risers operating normally. The effluent intensity pattern has remained the same since then throughout the project, providing rather novel information on the continuing functioning of the diffuser groups.

Since this project's inception, the collected imagery showed that under both current regimes (but especially the southward regime) the outfall plume tends to commonly have very sharp side boundaries. In relatively strong surface current conditions the apex of the plume is also often displaced 50 m or more from the actual wye location (indicating a diagonal vertical travel path due to the currents) but it tends to retain the sharp edge boundaries. This characteristic was found to have important ramifications on the interpretation of field samples collected around the outfall: Because the sampling site grid is fixed, near-time-coincident field sampling and aerial image data have shown cases where the plume clearly existed on the surface but, due to its particular orientation that day and its very sharp delineation at the wye, was entirely missed by the field sampling. On 1/4/2012, for example, the sharply defined plume was detectable in RapidEye satellite imagery for more than 4 km southward from its source (Figure 9B above). It did not breach any of the field sampling locations over the wye, however, where time-coincident samples showed no indicator bacteria between the surface and 27 m. An alternate situation is illustrated in **Figure 12** which shows an aerial image overlaid with the actual sampling vessel track during sampling at stations I12 and I16 over the outfall wye on 1/6/2004. The multi-depth samples were acquired while the vessel drifted (Global Positioning System ticks spaced closely together). The data show the vessel passed in and out of the "Wye Riser" plume while sampling at I16 and drifted out of the "S28-S85 Riser" plume at I12 during sampling. This resulted in an uneven vertical sampling profile, with plume indications at some depths but not others, potentially confusing interpretation without the imagery.

The SBOO area is also subject on occasion to practically no current flow. This is reflected in the imagery by the surfacing plume components being located directly over the wye, indicating direct vertical effluent rise. During such no-current conditions we have occasionally observed the outfall's effluent to create circular standing wave patterns around the wye. The plume then tends to spread in a more concentric pattern over the wye area – and thus also in the shoreward direction. The project's extensive image data base since 2003 shows it is only under such circumstances that portions of the surfacing SBOO plume reach any appreciable distance shoreward from the wye location. Generally, this extent is detectable with the multispectral and thermal sensors 1000 – 1500 meters eastward or northeastward.

Since this project's aerial and satellite image-based monitoring of the SBOO outfall began, we have observed the plume to disperse in the four patterns discussed above. We have also witnessed the plume's

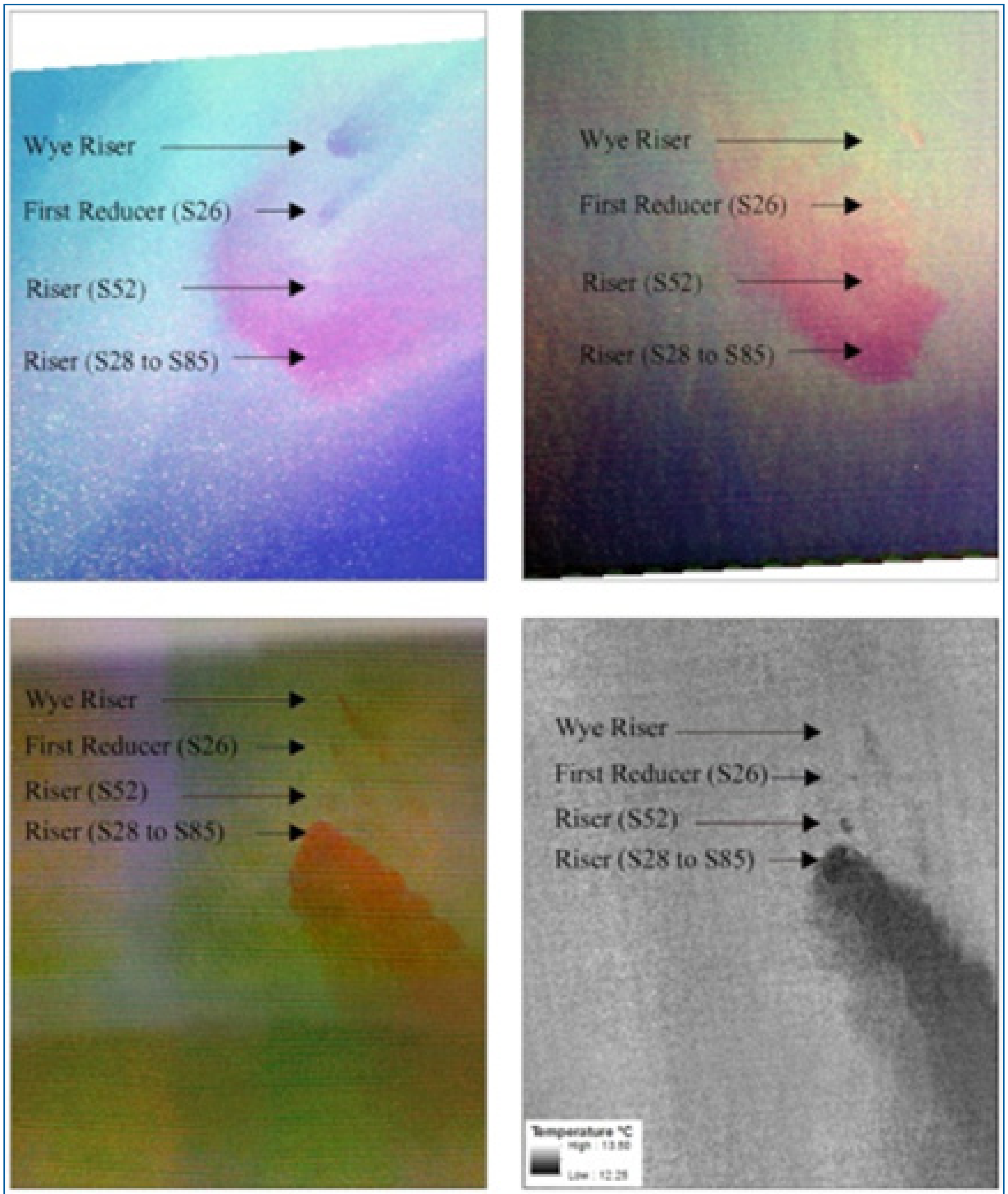

Figure 11. Examples of SBOO plume sub-components imaged during weak current conditions by the DMSC aerial sensor: (A) 2/6/2003, (B) 12/9/2003, (C) 12/14/2005, (D) 12/14/2005 (thermal).

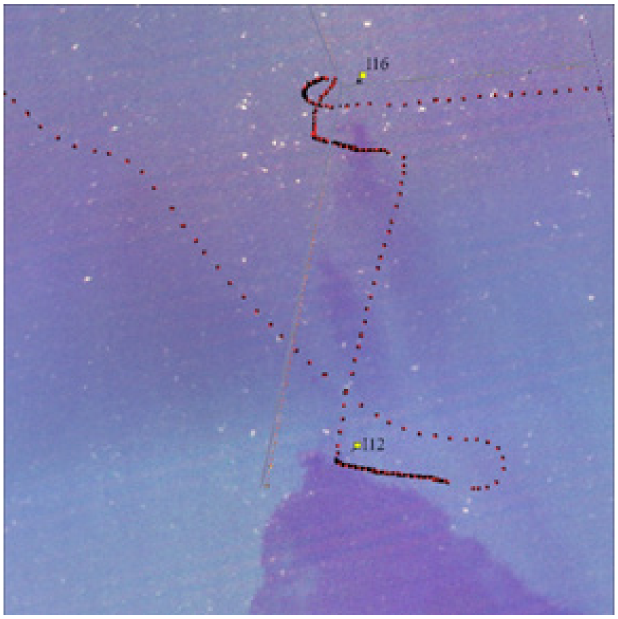

Figure 12. Time coincident DMSC imagery of the SBOO plume on 1/6/2004 and track of field sampling vessel during vertical sampling at stations I12 and I16. Each tick represents 10 seconds duration.

trajectory to be directly westward (offshore) on a few, rare occasions when offshore-directed Santa Ana winds caused a relatively anomalous strong offshore forcing of the surface waters. We have, however, never observed the SBOO plume trajectory to be directed east or shoreward past approximately 1500 m. It must be noted, however, that all of this project's SBOO plume trajectory observations reflect the plume's behavior during vertically unstratified conditions when it reaches the upper ocean layer. These observations cannot thus be extended to the summer months when the plume is undetectable with multispectral visible and thermal imaging. It must also be noted that detection of the surface or near-surface plume depends on sufficient thermal or turbidity contrast between the effluent and the surrounding waters. Hence it must be assumed that certain physical and biological components of the plume continue past the distance at which it becomes undetectable with OI's aerial and satellite imaging, albeit at an ever-increasingly diluted concentration.

Table 2 shows the number of high-resolution satellite images acquired and processed per year between 2012-2021 along with the number of instances when the SBOO effluent was observed in the remote sensing data at the ocean's surface. Over the past 10 years the number of high-resolution data sets acquired to monitor the region has increased by 400%. As noted above, there are often days when the SBOO plume is visible by more than one satellite. To account for duplicate datasets showing the SBOO plume on the same day, the number of days the SBOO region was imaged along with the number of SBOO observation days are listed in the table. The percent of SBOO observations per number of image days is shown, adjusting for the increasing number of satellite datasets used over the years. Rarely has the SBOO plume been observed at the surface prior to November or after April. This is most likely due to the seasonal water column stratification timing discussed above. It also coincides with California's rainy season. Therefore, the table also lists the observation data by the November to April, rain/vertical mixing season (lack of water column stratification). 2013 (and the 2012-2013 season) and 2016 (and the 2015-2016 season) stand out as the years during which the fewest and most SBOO surface plumes were seen in in the imagery respectively. All other years/seasons show the percentage of observations within one standard deviation of the mean.

Figure 13 shows monthly averages of Influent (INF) and effluent (EFF) volume and TSS for the SBIWTP since 2003. While the effluent volumes and intake TSS concentrations did not change appreciably through time (aside from a spike in the EFF Flow during 2020), there were two notable reductions and one spike in the exiting effluent's TSS concentrations. The first occurred through 2006-2007 when the TSS loads were reduced from approximately 90 mg/L to approximately 60 mg/L, and the second reduction was in November 2010 when the SBIWTP switched to full secondary treatment. Starting in 2012 the exiting TSS loads have been consistently below 20 mg/L. In the latter part of 2020 into the early months of 2021 there was an appreciable increase in the EFF flow rate as well as extreme spikes in EFF TSS concentrations with the monthly EFF flow average peaking during the month of September and the average monthly EFF TSS levels peaking in November of 2020. Daily TSS numbers reached as high as 512 mg/L on 01/31/2021 (**Figure 14**). These dramatic increases have been attributed to excessive flows (>25 MGD) into the SBIWTP from the Mexican wastewater system that were not attributed to rains (Morgan Rogers, personal communication).

The plume's reflectance signature in the multispectral visible and near-IR imagery is dominated by reflectance spectrum characteristics of its suspended sediment. Hence a reduction in the sediment concentration should be expected to affect the detectability of the plume. However, analysis of the size and intensity of the plume patterns as well as the number of SBOO plume observations in the satellite data relative to the TSS reductions as seen between 2017 and 2021 does not show a direct correlation. In fact, some of the largest plume signatures have been imaged after the 2010 secondary treatment switch, such as 01/19/2019 when the EFF TSS amounts were recorded at 12.0 mg/L and on 04/11/20 when the EFF TSS level was only 7.4 mg/L. The median EFF TSS load between 2017 and 2021 was 10.4 mg/L. The median on days when the SBOO surface plume as observed in the remote sensing data was 11.6 mg/L. These plumes were identifiable more than 4.1 km and 5.6 km away from SBOO wye respectively (**Figure 15**). Other plume signatures imaged during 2013 through 2021 when TSS loads were approximately 16 mg/L or less show that such TSS amounts are sufficient for adequate distinction of the effluent from surrounding waters if the plume remains concentrated.

Table 2. SBOO Surface Observations in the High-Resolution Satellite Imagery

Year	Number of High-Res Images Processed and Reviewed	Number of Days Imaged	Number of SBOO Surface Observations	Number of Days SBOO Observed on Surface	Percent of SBOO Observations per Days Imaged
2012	26	25	6	6	24.0%
2013	32	31	1	1	3.2%
2014	50	46	10	9	19.6%
2015	46	44	12	12	27.3%
2016	42	42	13	13	31.0%
2017	60	54	10	8	14.8%
2018	82	75	19	15	20.0%
2019	122	109	19	17	15.6%
2020	133	111	34	27	24.3%
2021	134	112	19	16	14.3%
Season					
2012-2013	21	19	1	1	5.3%
2013-2014	33	31	6	5	16.1%
2014-2015	31	29	11	10	34.5%
2015-2016	35	34	16	16	47.1%
2016-2017	36	34	6	6	17.6%
2017-2018	56	49	17	13	26.5%
2018-2019	64	56	20	16	28.6%
2019-2020	76	68	22	20	29.4%
2020-2021	105	85	36	27	31.8%

Season = November through April. 2012-2021 mean observation ratio = 19.4% annually and 26.3% seasonally. 2012-2021 observation ratio standard deviation = 7.9% annually and 12.1% seasonally.

However, during those years, numerous instances also occurred when, on a given day, the plume was detectable with both the multispectral visible and thermal sensors but became detectable only with thermal imaging a day or two later. The existence of a thermal plume signature proves the effluent reached the ocean surface, but its simultaneous lack of a color signature implies it reached the surface in a significantly diluted state. Additionally, there are alternate situations during which a relatively clear (low TSS) plume is detected via remote sensing because the effluent breaks through surrounding turbid water caused by either an offshore extension of the TJR discharge or heavy plankton blooms over the SBOO wye. Therefore, our data thus suggest that on days with significant subsurface currents and/or vertical mixing the effluent is sufficiently dilute as it travels up through the water column and/or the EFF TSS levels are lower than ~12.0 mg/L, the effluent can still be detectable by the sensors utilized in this project. Also, analysis of the size and intensity of the plume patterns relative to the

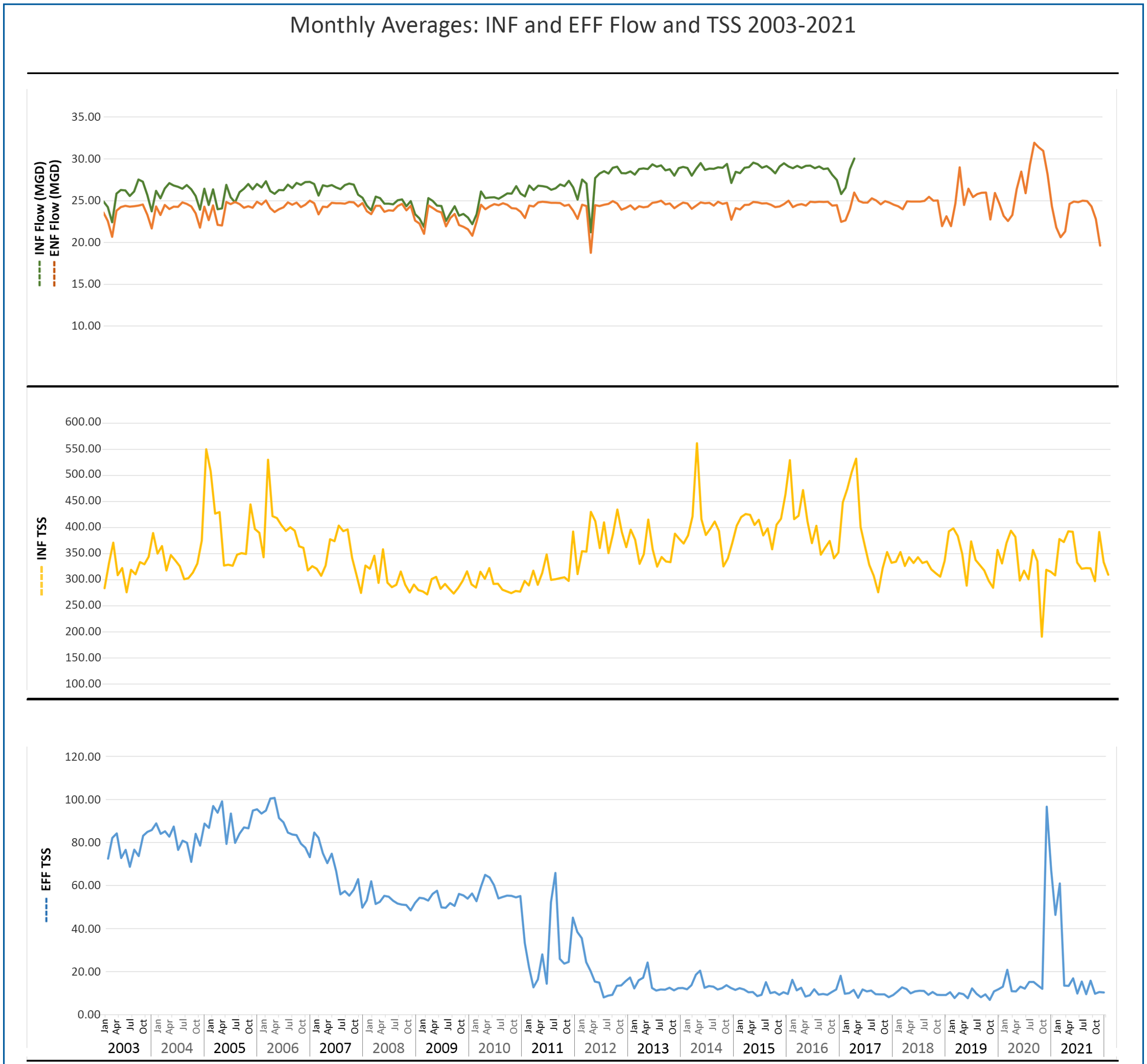

Figure 13. Influent (INF) and effluent (EFF) volume and total suspended solids (TSS) concentrations for wastewater processed through the SBIWTP and released into the ocean through the SBOO.

TSS reductions does not show a direct correlation. Furthermore, no significant correlation was found, between color-based detection of the SBOO plume and high frequency radar-derived surface currents or nearby shore station wind measurements. Similarly, no correlation was found between plume detection and imaging time within the tidal cycle.

4.3 The Tijuana River and San Antonio de los Buenos Creek

Since its inception in 2003, this project has provided an extensive image data set of the TJR runoff plume under various oceanic and atmospheric conditions. This data set was utilized by Svejkovsky et al. (2010), to study the TJR plume's extents and resulting effects on shoreline contamination. Unlike the

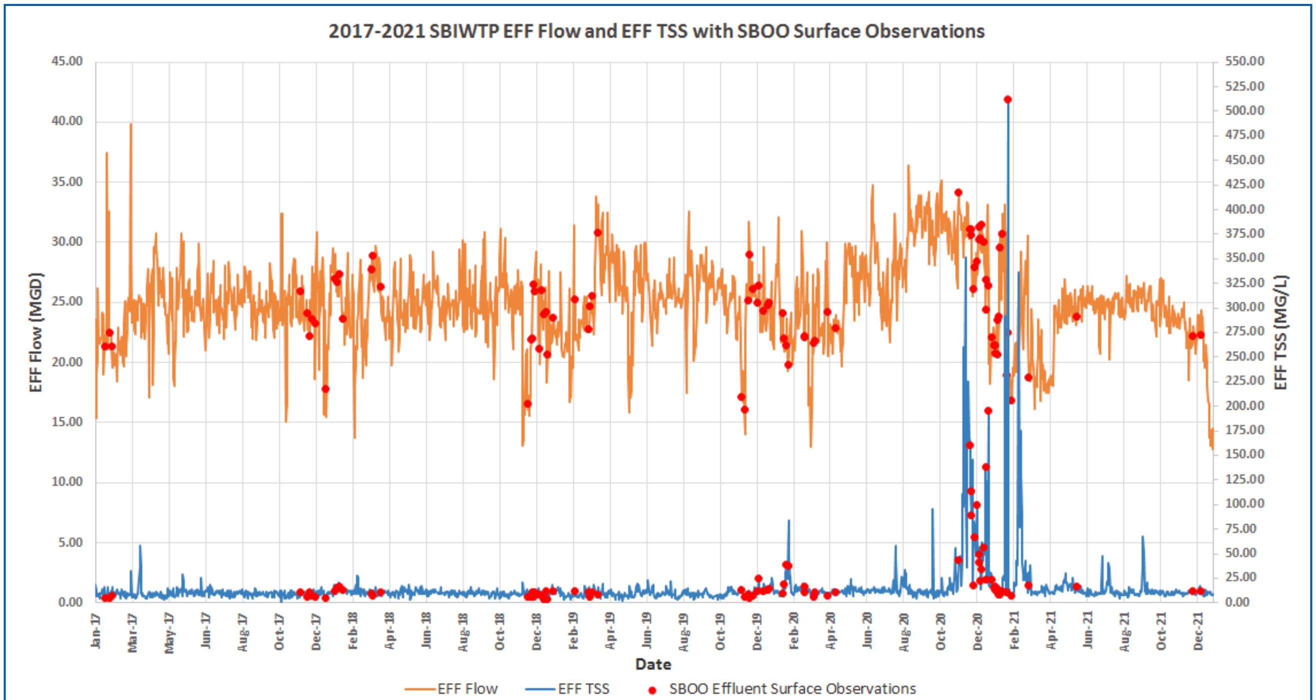

Figure 14. Daily EFF Flow volume EFF TSS concentrations for wastewater processed through the SBIWTP and released into the ocean through the SBOO from 2017 through 2021.

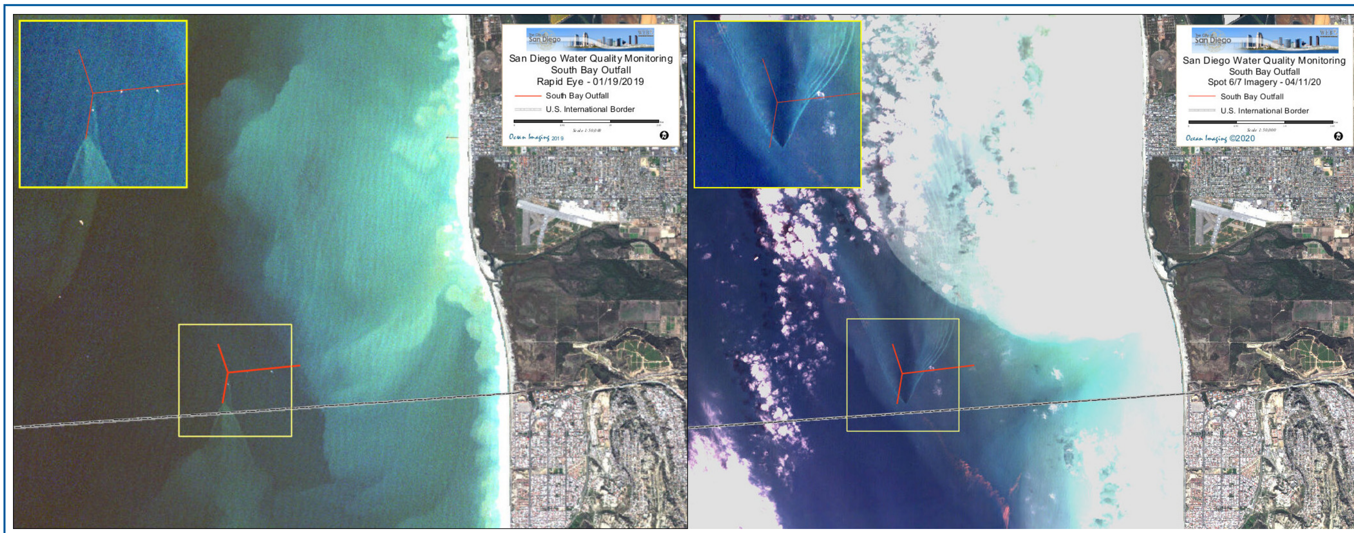

Figure 15. Examples of large SBOO effluent plumes at the oceans' surface observed in a RapidEye image acquired on 01/19/19 and a SPOT image from 04/11/20 when the measured EFF TSS levels were relatively low (12.0 mg/L and 7.4 mg/L respectively).

SBOO plumes spectrally homogenous reflectance signature, the investigators found the TJR plume to consist of 3 spectrally distinct components which they believe are related to different discharge ages within the plume. The Svejkovsky et al. (2010) study found that wave direction was the prime variable affecting the along-shore distribution of the TJR plume's core components (**Figure 16**).

Following heavy rains, the satellite and aerial imagery has shown the TJR plume to extend up to tens of kilometers offshore. When this occurs during a northward current regime, portions of the TJR's highly contaminated plume are advected northward and can reach Pt. Loma, potentially affecting water quality within the PLOO's field sampling grid more than 16 km to the Northwest. This was first noticed in October 2004 when satellite imagery acquired during a prolonged northward current episode and following intense rain events showed the TJR plume to reach the southern end of Pt. Loma. The image data indicated a possible explanation for anomalously high indicator bacteria concentrations in field samples taken in the area during the same time. This event is not common but has occurred several times in the 18 years since it was first observed. More recent examples are shown in Figures 3 and 8 above.

This project's monitoring of the San Antonio de los Buenos Creek discharge plume in Mexico revealed that the plume rarely reaches the U.S. border in concentrations sufficient for detection in the imagery. Its usual trajectory is southward. We have observed it to spread a considerable distance, as far south as past Rosarito Beach, Mexico. During northward flow events, its northward trajectory due to currents and south swell tends to be diminished by the coastal geography (the shore angles northwestward immediately north of the Creek mouth) and its usual size vs. the distance needed to reach the U.S. border in detectable concentrations. US-collected shoreline sampling has shown relatively regular elevated bacteria concentrations at stations south of and on the US/Mexico border, but these could have been caused by other localized point and non-point sources. OI has not collected any imagery directly linking such measurements to a detectable San Antonio de los Buenos plume crossing the border in the surf or immediate coastal zone, although the lack of such imagery does not preclude that possibility. Imagery showing the plume crossing the border shows most of it to travel in a northwestward (i.e., offshore) trajectory, and mixing with the TJR discharge once across the border.

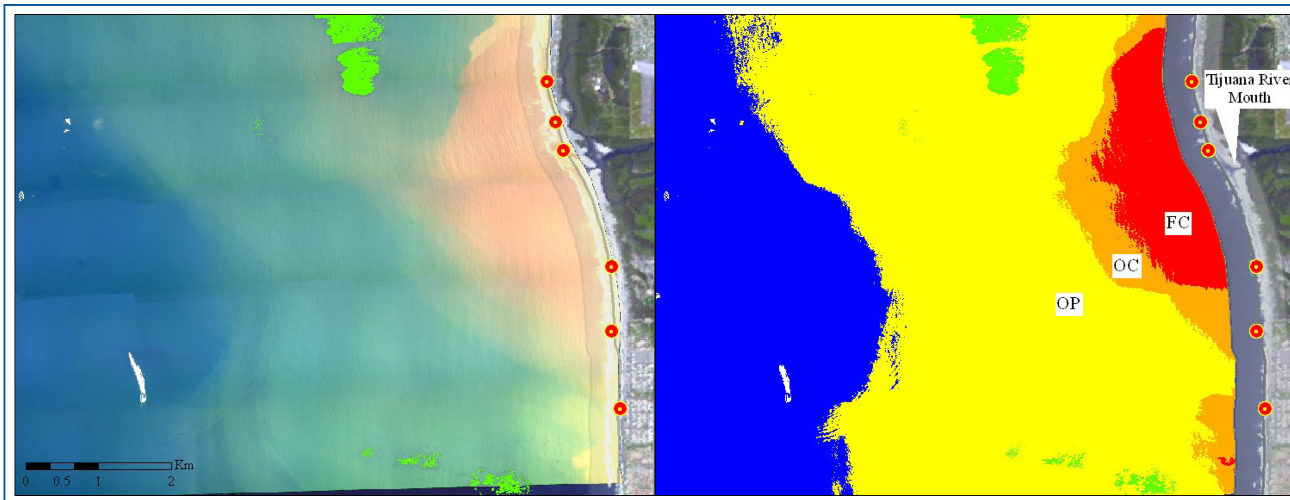

Figure 16. Example of the Tijuana River stormwater runoff plume as it appears in DMSC aerial multispectral color data (left) and after classification for various plume components with distinguishing spectral reflectance characteristics: "Fresh Core" (FC), "Old Core" (OC), and "Old Plume" (OP). Kelp is shown in green, and the locations of shoreline bacteriological sampling stations are also shown.

5. NOTABLE CONDITIONS AND EVENTS 2017 – 2021

5.1 Overall Atmospheric and Oceanographic Trends

San Diego's nearshore water quality gets affected by a combination of factors during the dry and wet seasons. In the absence of rain from late spring to fall, stormwater runoff is nonexistent, San Diego River (SDR) discharge is minimal (and generally uncontaminated), and discharges from North County's lagoons, Mission Bay and the TJR are primarily the result of tidal flushing. In the absence of rare events such as sewage spills or channel dredging of closed lagoon mouths, events affecting the nearshore waters are primarily of oceanic origin such as phytoplankton blooms and harmful algal blooms (HABs) - red tides included. Diatoms (primarily *Pseudo-nitzschia* spp) and dinoflagellates are largely responsible for the local HABs and red tides when they occur (Southern California Coastal Water Research Project, 2019). During the rainy season the most prominent factors are stormwater runoff from point and non-point sources along the shore, and sediment resuspension caused by strong winds and large waves in the surf zone. As is discussed below, our observations show that the sizes and extents (and hence also beach contamination potential) of the stormwater plumes is not simply related to the total amount of rainfall, but also to the intensity (i.e., amount within a time interval) with which it fell.

In the last five years (2017-2021) San Diego was subject to only moderately variable oceanographic conditions when compared to the past 10 years (2012-2021) in its entirety, but there were significant year-to-year differences in atmospheric and precipitation conditions. This includes a few extremes in high (2019) and low (2018) rainfall both annually and seasonally, heavy phytoplankton and red tide blooms, weak to moderate El Niño and La Niña conditions as well as a summer marine heat wave in 2019 commonly referred to as "The Blob 2.0" (Amaya, Dillon J., et al., 2020). Many of these episodes led to events and processes observed in the satellite and aerial imagery acquired for this project. The following is a summary of notable events through the latest 5-year period. Although the scope of this report is 2017-2021, we use conditions over the past 10 years as a "baseline" for comparison.

5.1.1 Ocean Temperature Conditions

Aside from the reoccurrence of a marine heat wave, termed the Blob 2.0, centered off central California and Oregon during the summer of 2019, the northeast Pacific and in particular the Southern California Bight region did not experience dramatic fluctuations in ocean temperature outside of climatic norms. The direct effect, if any, of the Blob 2.0 on regional conditions is not yet known (Amaya, Dillon J., et al., 2020). Figure 17 shows the average monthly temperatures recorded at the Scripps Institution of Oceanography pier between 2012 and 2021 along with the years experiencing either El Niño or La Niña conditions according to the Oceanic Niño Index (ONI). Note the average Scripps pier temperature for 2017-2021 differed by only 0.1 °C from the 2012-2021 average. The only El Niño period between 2017-2021 was during the late summer of 2018 through the late spring of 2019 and it was only considered a weak event. The fall to spring months of 2017 to 2019 and much of the latter part of 2020 through 2021 experienced weak to moderate La Niña conditions. The 2018-2019 El Niño event can be seen in a summer peak in the 2018 Scripps pier temperatures as can the 2020-2021 La Niña episode. These warmer and cooler periods are also apparent in the 2019 and 2021 NOAA sea surface temperature anomaly analyses (**Figure 18**). **Figure 19** shows a VIIRS-generated SST image from one of the warmest SST days in 2018 (left) and a MODIS SST image from the same day in 2021 (right). The satellite image data help illustrate the ~4.6°C difference between the warmest year on average (2018) and the coolest (2021) during the five-year period of this report – especially in the San Diego region.

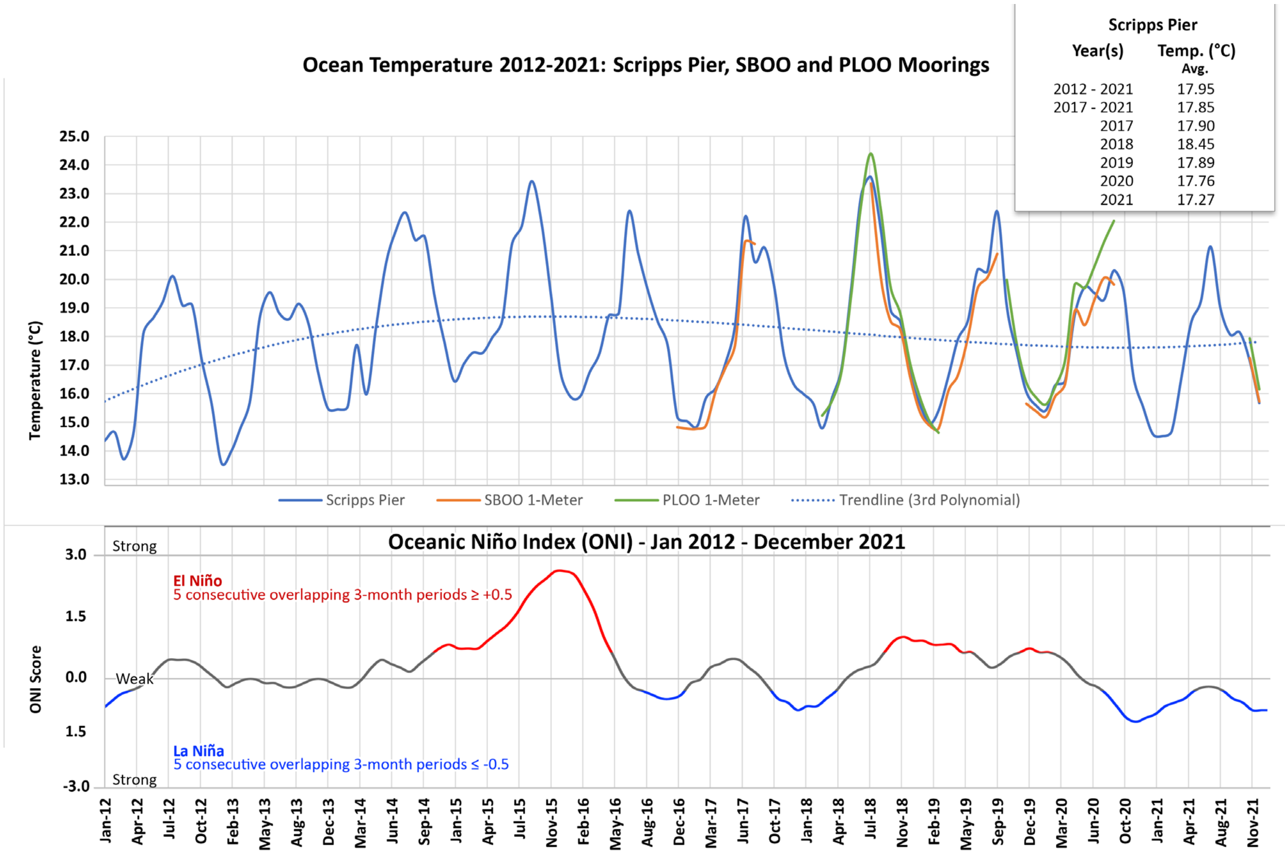

Figure 17. Average monthly ocean temperature from 2012 through 2021 as recorded at the Scripps Pier automated shore station, the PLOO real-time oceanographic mooring station (RTOMS) (1 meter depth) and the SBOO RTOMS (1 meter depth). Below the temperature data is a plot of the El Niño Southern Oscillation (ENSO) cycle for the same time period as represented by the Oceanic Niño Index (ONI). PLOO and SBOO data being in 2016 and are incomplete due to periods when the RTOMS were either inoperable or out of the water. Additional information on the City's RTOMS can be found in the City of San Diego 2018-2019 biannual report (City of San Diego, 2020).

5.1.2 Ocean Chlorophyll and Plankton Levels

Ocean chlorophyll levels generally followed seasonal norms over the past five years with levels indicative of phytoplankton blooms peaking in the spring to early summer months. A few exceptions in the San Diego region were a brief, but somewhat unusual, large phytoplankton bloom in September of 2018, frequent plankton blooms through September in 2019 and the extreme phytoplankton and red tide events which occurred during the months of April and May of 2020. **Figure 20** shows the chlorophyll levels measured at a depth of one meter at the SBOO and PLOO RTOMS from 2017 to 2021. Data gaps exist due to sensor issues or the moorings being out of the water (Stephanie Jaeger, personal communication). When the RTOMS data were available, however, the satellite data correspond well to the SBOO and PLOO measurements. **Figure 21** provides examples when the satellite data corresponded with the RTOMS data while providing a more synoptic view of the conditions recorded at the single stations. Additional details on the regional water clarity and quality for each year are provided in subsequent sections.

5.1.3 Regional Precipitation

As noted above the 5-year period between 2017-2021 experienced significant interannual rainfall totals both in terms of the amount of precipitation over a season or year as well as the intensity and duration of rainfall events. Table 3 shows the 2017-2021 monthly cumulative precipitation as recorded at the San Diego International Airport (SDIA) and

TJR Estuary stations (NOAA National Climactic Data Center). The average precipitation recorded at the SDIA over the past five years (8.34 in./yr.) was much the same as the past 10 years (8.13 in./yr.). The average at the TJR Estuary station between 2017-2021 (9.19 in./yr.) was 26% higher than the past 10 years (7.61 in./yr.). 2018 and 2019 were the outliers with 2018 having the lowest annual total of 4.99

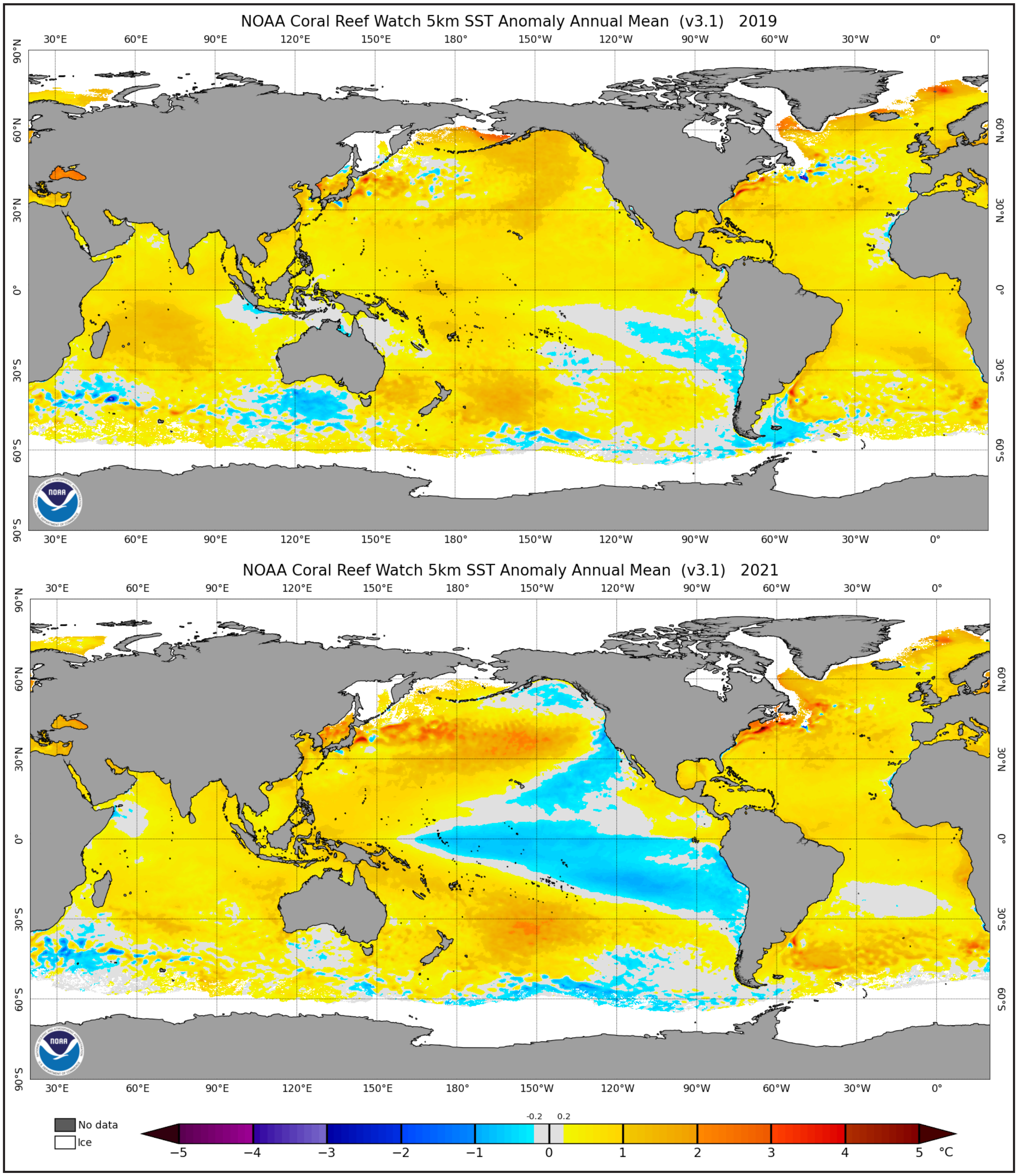

Figure 18. NOAA annual mean sea surface temperature anomaly analyses for the years 2019 (weak El Niño) and 2021 (weak La Niña).

inches recorded at SDIA and 2019 having the highest total rainfall of 15.52 inches. When approached seasonally with the period between November and April considered as the rainy season in California (although a recent study by Luković et al., 2021 suggests that the season should now be considered to start in December), the 2017-2018 season proved to be the lowest over the past 10 years (2.81 inches at SDIA) and the 2019-2020 season the highest (13.44 inches at SDIA) compared to the 10-year seasonal average of 6.89 inches. The data from the TJR Estuary were similar with the 2019-2020 rainy

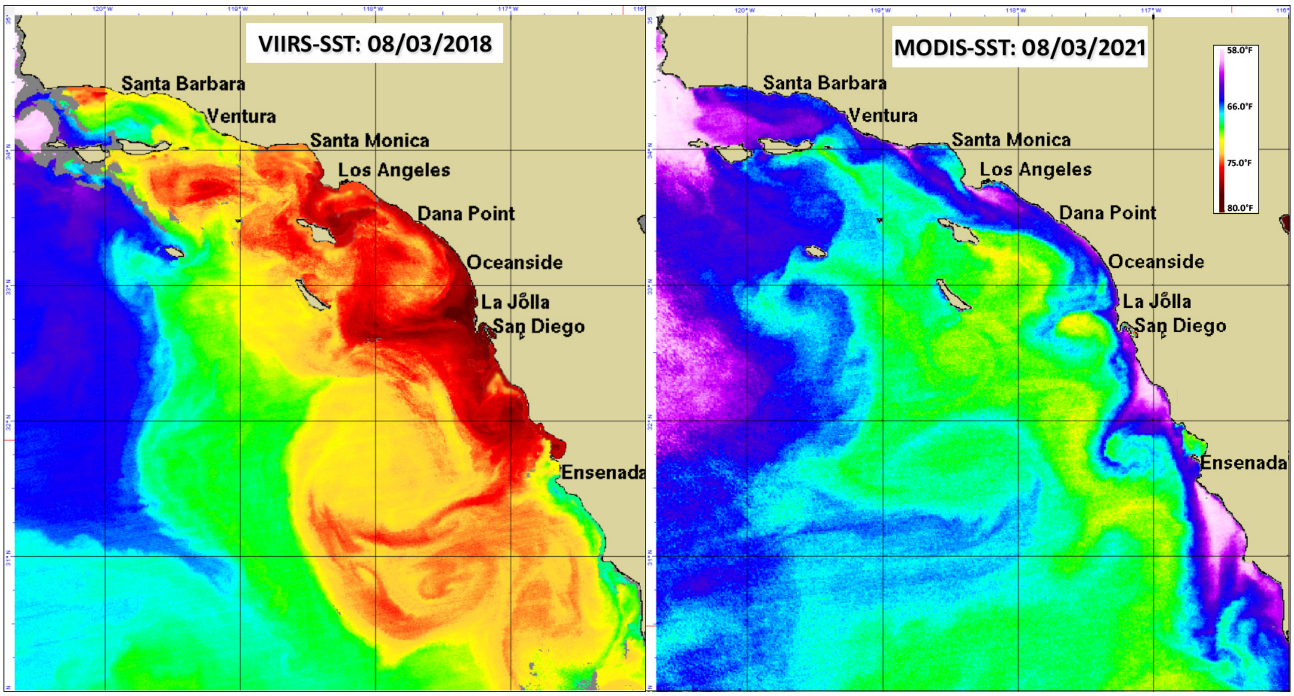

Figure 19. VIIRS SST image from 08/03/2018, one of the warmest SST days in 2018 (left) and a MODIS SST image from the same date in 2021 (right).

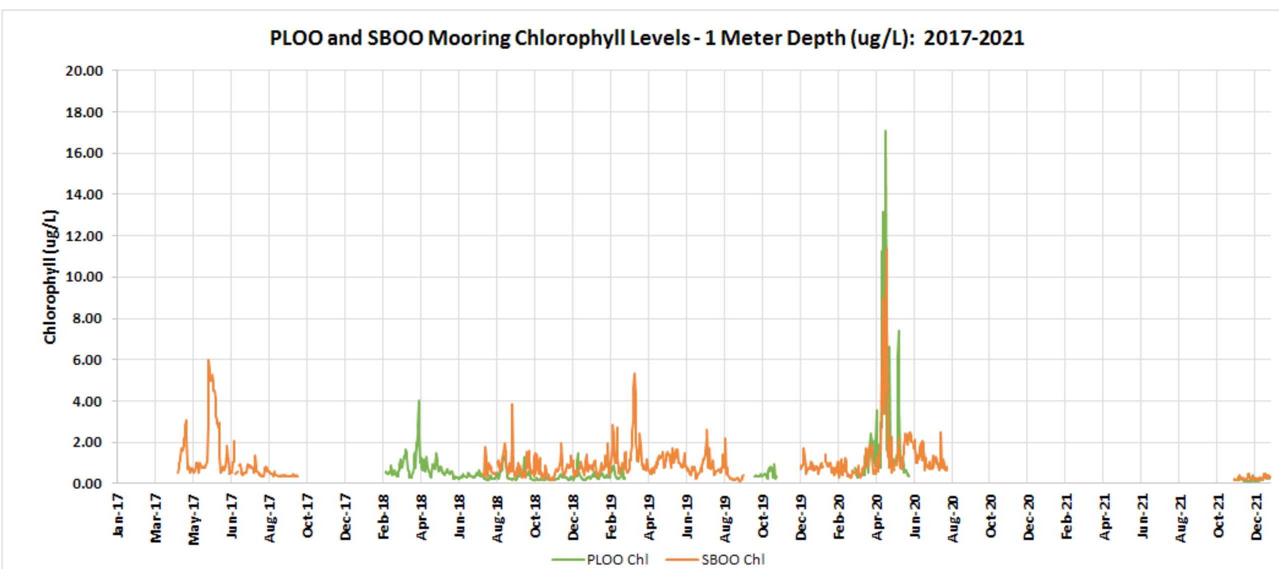

Figure 20. Average daily chlorophyll levels measured at the PLOO and SBOO moorings at the one-meter depth level between 2017 and 2021. Records flagged as "bad" or "suspect" were removed from the dataset. Gaps in the data record were either due to the moorings being out of the water or inoperable sensors. Note the spike the chlorophyll levels during the unusually strong red tide events in the spring of 2020.

season experiencing the most rain (16.04 inches), the 2017-2018 season the second lowest amount (2.71 inches), and the 2012-2013 season showing the lowest precipitation with a total of 1.63 inches. As discussed above rainfall has not been shown to have a direct effect on the surfacing of the SBOO effluent plume, however it does correlate well with the number of high volume TJR discharge events as well as the relative size of the plume entering the ocean as observed in the satellite data. All but one of the high-resolution satellite images acquired and processed for this project between 2017-2021 showed a significant TJR plume within 0-2 days of a rain event totaling 0.1 inches or more. A significant plume being defined as a clearly visible "Fresh Core" or "Old Core" plume (Svejkovsky, 2010) extending from the shoreline. There were many instances, however, when a relatively large TJR plume was visible in the image data during a period of no precipitation. These situations were likely the result of excess cross-boundary flow into the TJR Estuary caused by pump station failures, collection system overflows and/or debris obstructing the inlets (San Diego Regional Water Quality Control Board, 2020). These events and subsequent observations are discussed in more detail in the following sections.

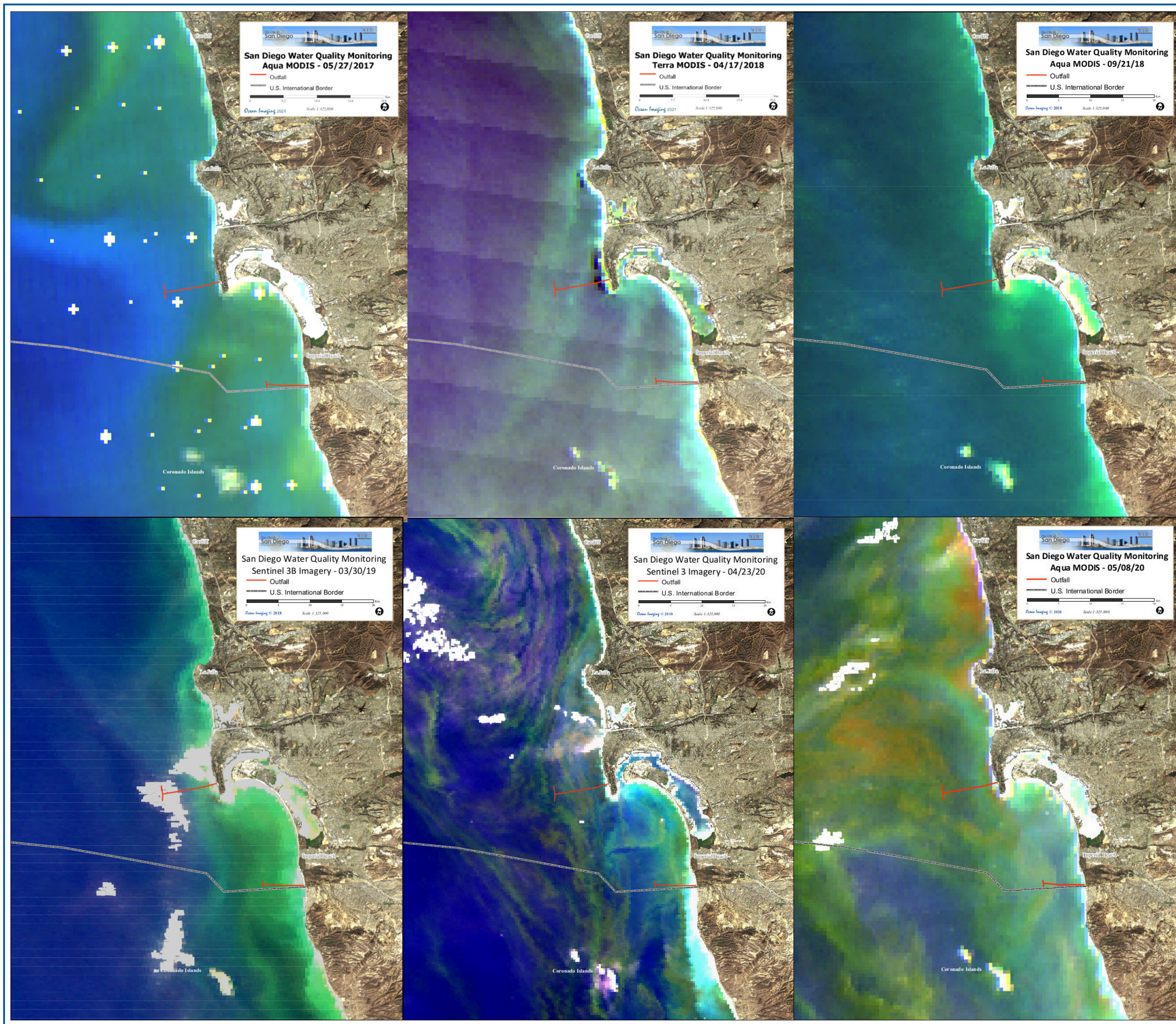

Figure 21. Representative Sentinel 3 and MODIS images showing plankton blooms during peaks seen in the chlorophyll measurements shown in Figure 20.

5.2 Conditions in 2017

The conditions in 2017 off the San Diego coast could perhaps be considered the most "average" when compared to the past ten years in the sense that the oceanic conditions were close to normal, and both annual and seasonal precipitation numbers did not deviate widely from the 10-year means. As seen in **Table 3**, 2017 had the lowest percentage of SBOO surface plume observations per imaged day compared to the 2017-2021 period. From a seasonal perspective the 2016-2017 season showed the fewest number of SBOO detections since 2013-2014. The few satellite detections of the SBOO surfacing were in January and then no plumes were seen in the data until December when vertical

Table 3. Sand Diego and Tijuana Estuary precipitation totals 2012-2021

San Diego International Airport Cumulative Monthly Precipitation in Inches

	2012	2013	2014	2015	2016	2017	2018	2019	2020	2021
January	0.40	0.70	0.01	0.42	3.21	2.99	1.77	2.42	0.48	1.80
February	1.19	0.63	1.00	0.28	0.05	1.58	0.35	4.04	0.38	0.10
March	0.97	1.22	1.28	0.93	0.76	0.08	0.65	1.23	2.15	1.48
April	0.88	0.01	0.54	0.02	0.55	0.01	0.02	0.10	3.68	0.07
May	0.02	0.26	--	2.39	0.44	0.87	0.09	0.86	0.02	0.07
June	--	--	--	0.04	--	0.02	--	0.01	0.14	0.01
July	--	0.05	--	1.71	--	--	--	--	--	--
August	--	--	0.08	0.01	--	--	0.02	--	--	0.23
September	--	--	--	1.24	0.32	0.06	--	0.11	--	0.50
October	0.70	0.25	--	0.43	0.07	--	0.57	--	0.12	1.01
November	0.28	1.48	0.37	1.54	0.61	0.02	0.69	2.72	0.14	--
December	2.19	0.46	4.50	0.88	4.22	--	0.83	4.03	0.60	2.58
Annual Total	**6.63**	**5.06**	**7.78**	**9.89**	**10.23**	**5.63**	**4.99**	**15.52**	**7.71**	**7.85**

Tijuana Estuary Cumulative Monthly Precipitation in Inches

	2012	2013	2014	2015	2016	2017	2018	2019	2020	2021
January	0.70	0.05	0.08	0.32	2.40	3.61	0.82	1.80	0.61	2.21
February	0.86	--	1.35	0.13	0.02	4.06	0.47	3.62	0.51	0.06
March	1.21	1.43	0.55	1.01	1.28	0.04	1.17	1.33	2.59	1.12
April	0.82	0.11	0.35	0.07	1.91	0.01	0.10	0.33	5.52	0.04
May	--	0.36	--	1.13	0.97	1.07	0.08	0.50	0.02	0.01
June	--	--	0.12	--	--	--	--	0.02	0.21	0.06
July	--	0.01	0.33	0.39	--	0.01	0.01	--	--	0.00
August	--	--	0.04	--	--	0.02	--	--	--	0.02
September	0.02	0.01	--	0.48	0.49	0.03	--	--	--	0.00
October	0.50	0.41	--	0.21	--	--	0.13	--	0.04	0.91
November	--	0.25	0.29	0.61	0.34	0.06	0.82	2.99	0.08	0.02
December	0.04	0.50	3.09	0.61	4.32	0.09	3.16	3.82	0.60	1.18
Annual Total	**4.15**	**3.13**	**6.20**	**4.94**	**11.73**	**8.99**	**6.76**	**14.41**	**10.18**	**5.63**

water column stratification likely weakened again. Offshore plankton blooms started earlier than usual. High levels of chlorophyll throughout the entire Southern California Bight developed as early as January and lasted through the end of March. As can be seen in the MODIS image archive locally high concentrations persisted into mid-July with intense blooms developing off the northern San Diego coast and TJR area and spinning off into plankton-rich eddies to the west. The vast January to March blooms can partially be attributed to heavy, region-wide rainfall events beginning in January introducing nutrients from coastal runoff into the ocean system. Nearshore blooms occurring after March were primarily fueled by coastal upwelling.

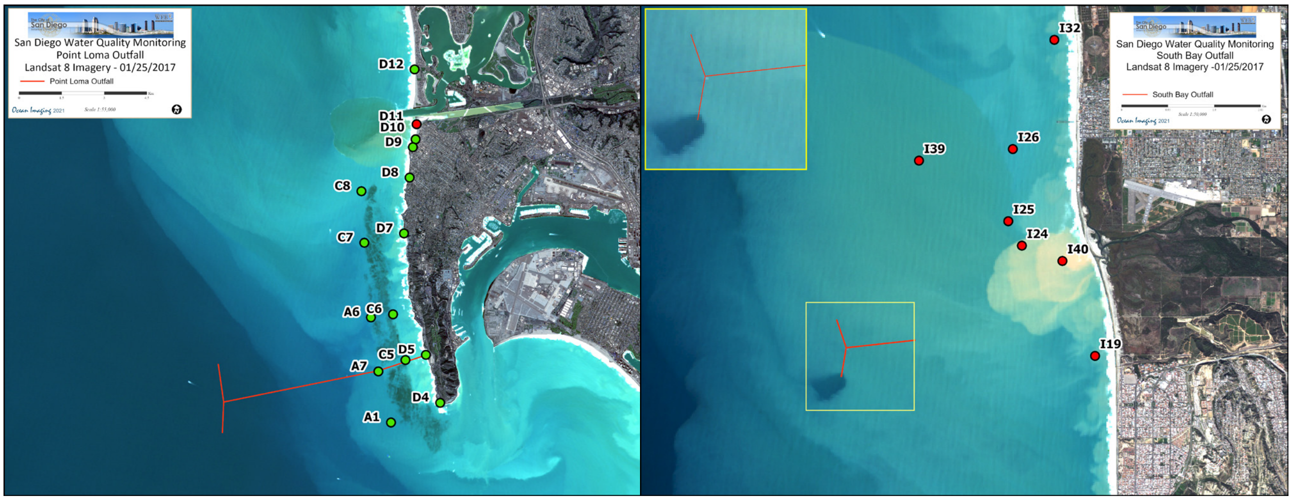

Station	Depth (M)	Entero	Fecal	Total
D11	NA	3400e	1000e	>=8600

Station	Depth (M)	Entero	Fecal	Total
I19	2	580	440	4000
	6	540	300e	3800e
	11	800	440	5600
I24	2	820	3400e	>16000
	6	480	220e	1400e
	11	50	200e	2000e
I25	2	260e	220e	1200e
	6	220e	220e	1300
	9	400e	76	800
I26	2	60	48	400e
	6	220e	50	700
	9	240e	60	960
I32	2	40	14e	200e
	6	110	36e	580
	9	220e	66	540
I39	2	1600e	1200e	>16000
	12	80	26e	160e
	18	160e	6e	320e
I40	2	4400	4400	>16000
	6	760	320e	2000e
	9	2200e	1300e	7800

Figure 22A. 2017 high resolution satellite image examples from the Landsat 8 sensors with the near-surface bacterial sampling data overlaid from the same day or within two days of image acquisition. Continued in Figure 22B.

Even though the 2017 total annual rainfall (7.87 inches - averaged between the SDIA and TJR Estuary stations) was very close to the 10-year mean (8.13 inches), a few strong, multi-day storms in January and February brought over 3.6 and 4.0 inches of rain to the TJ Estuary. This resulted in heavy TJR discharge and subsequent high bacteria counts at the SBOO stations. **Figures 22A & B** show examples of satellite data with the near-surface bacterial sampling data overlaid from the same day or within two days of image acquisition. The TJR plume can be seen extending for several kilometers offshore driven by the heavy and persistent rains. Aside from a few days in May, these rainy periods

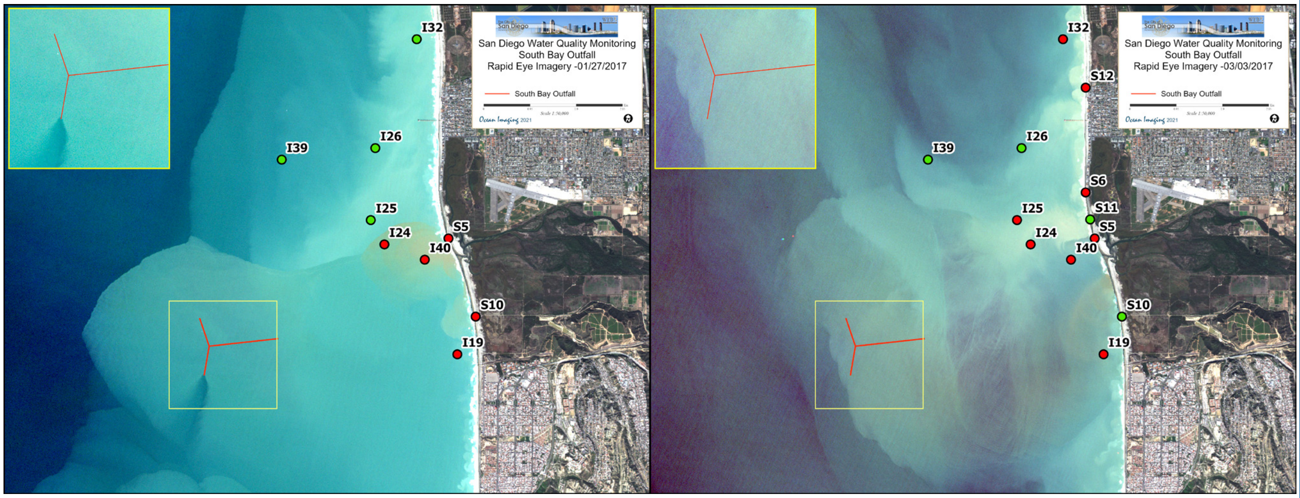

Station	Depth (M)	Entero	Fecal	Total
I19	2	10e	<2	34e
	6	6e	<2	14e
	11	160e	8e	180e
I24	2	140e	400	1100
	6	280e	700	3000e
	11	120	52	100e
I40	2	140e	180e	1800e
	6	700	660	5400
	9	180e	80e	300e
S5	NA	>12000	>12000	>16000
S10	2	3000e	NS	NS

Station	Depth (M)	Entero	Fecal	Total
I19	2	80e	150e	1900e
	6	150e	64	800
	11	540	120e	1900e
I24	2	40e	120	780
	6	840	150e	1800e
	11	140e	320e	2600e
I25	2	150e	52	620
	6	680	60e	2000e
	9	140e	180e	1600e
I32	2	12e	<2	4e
	6	110	44	840
	9	520	140e	1100
I40	2	82	92	360e
	6	68	38e	440
	9	260e	140e	1400
S5	NA	420	NS	NS
S6	NA	920	NS	NS
S12	NA	460	NS	NS

Figure 22B. 2017 high resolution satellite image examples from the RapidEye sensors with the near-surface bacterial sampling data overlaid from the same day or within two days of image acquisition. These images were acquired following multi-day storms bringing heavy rainfall resulting in heavy TJR runoff. Stations showing FIB measurements exceeding the single sample maximum as defined by the California Ocean Plan are shown as red dots (Total coliform density will not exceed 10,000 per 100 mL; or Fecal coliform density will not exceed 400 per 100 mL; or Total coliform density will not exceed 1,000 per 100 mL when the ratio of fecal/total coliform exceeds 0.1; or enterococcus density will not exceed 104 per 100 mL). Green dots identify stations at which the FIB levels were in compliance. The tables below each image show the measurement values by depth for each station with elevated bacteria levels.

were the only significant precipitation events for the year. This is evidenced by the mostly turbidity-free image data from April through the end of November and infrequent observations of significant TJR discharge. All other conditions exhibiting a lack of water clarity were related to the summer plankton blooms discussed previously. The 21 shoreline closures in San Diego County during 2017 was the second lowest in the 2017-2021 period. This is also likely related to the dry post-March conditions.

5.3 Conditions in 2018

2018 was a transitionary year in regard to the El Niño Southern Oscillation (ENSO) index. A mild La Niña phase was in place from September of 2017 through May of 2018. This shifted to an El Niño which lasted from August of 2018 to July of 2019. Typically, Southern California will experience less precipitation during a La Niña and more during an El Niño phase (NOAA Climate Prediction Center, 2012). Two predominant effects of the the La Niña and El Niño conditions were an overall decrease in precipitation and an increase in summer to fall ocean temperatures when compared to the past 10 years. While January of 2018 brought a decent amount of rainfall to the San Diego region, the county experienced very little additional precipitation until late November-early December, but even the totals for those months were below average. The SDIA gauge recorded the lowest annual rainfall in 2018 compared to 2012-2021 and while the TJR Estuary totals were above the 10-year average, it was only because of significant rain recorded at that station during the month of December. These conditions were likely related to the switching of the ENSO pattern during the summer. The average annual ocean temperature recorded at the Scripps Pier was 0.5°C warmer in 2018 than that of the past ten years. The average water temperatures during the month of August recorded at the Scripps Pier, the PLOO RTOMS (1 meter depth) and the SBOO RTOMS (1 meter depth) were near 24°C which were the highest temperatures recorded between 2012 and 2021. The warm ocean temperatures are well documented in

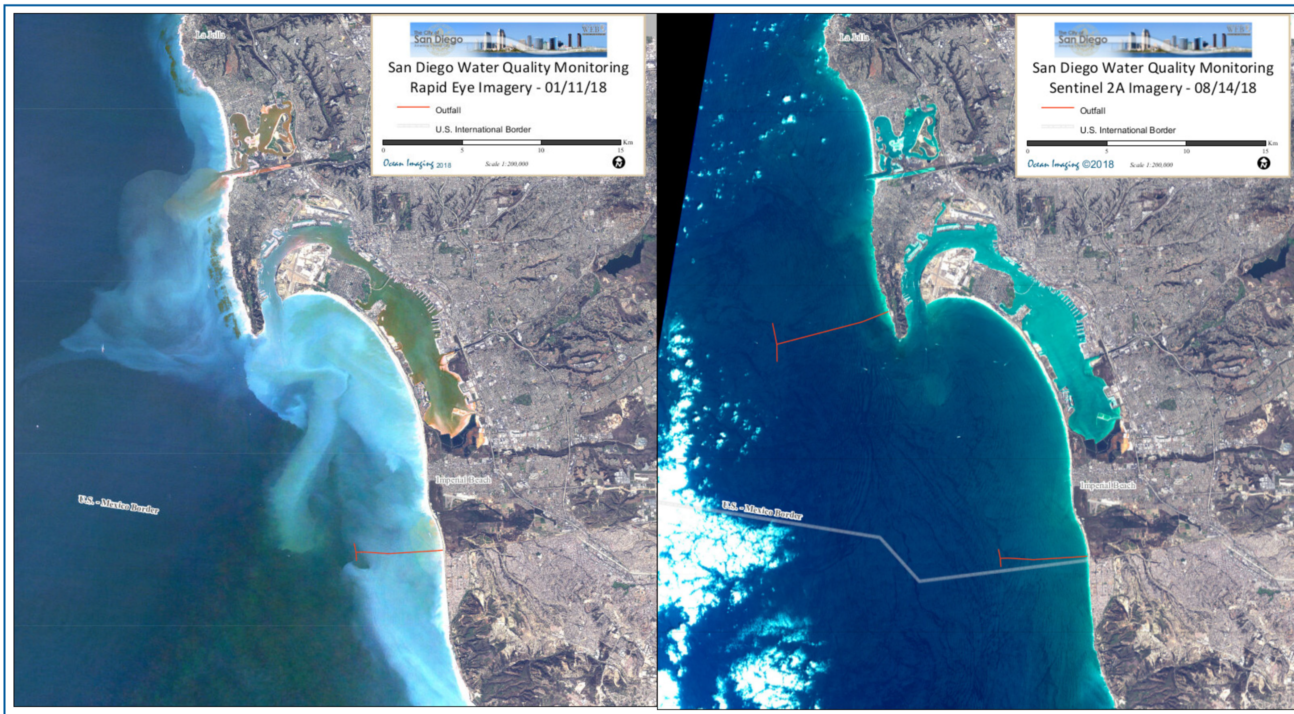

Figure 23. RapidEye image from 01/11/18 (left) one day after a significant rain event in which the strong San Deigo River discharge is evident. In contrast the Sentinel 2A image from 08/14/18 exhibits the clear water conditions resulting from a near rain-free summer.

the satellite data archive. A comparative example of the high August SSTs is shown in Figure 19 above. One result of the low annual rainfall in 2018 was that there were only 12 significant TJR discharge events seen in the satellite data over the entire year. One very heavy coastal turbidity event was seen in the RapidEye imagery acquired on 01/11/18 following 0.81 inches of rain measured at the TJR Estuary station between 01/08/18-01/10/18. The aftereffect was seen in the San Diego River discharge as well. Given that only 0.15 inches of rain had fallen since September of 2017 prior to that rain event, it was a good example of the "first flush effect" described in section 2.2 above. **Figure 23** highlights the RapidEye image from 01/11/18 in contrast to a Sentinel 2A image from 08/14/18 exhibiting the clear water conditions along the coast after only 0.02 inches of rain the entire summer. Between April and October of 2018 most other conditions affecting water clarity and quality were likely due to either wave action and/or phytoplankton blooms. Chlorophyll levels indicative of phytoplankton blooms in the Southern California Bight followed seasonal upwelling and California Current cycles, however higher chlorophyll/plankton levels persisted along the San Diego County coast for a greater portion of the year. Rainfall events in November and December and a reportedly large sewage spill into the TJR on 12/10/18 contributed to the increase in coastal turbidity and decreased water quality during those months.

5.4 Conditions in 2019

Heavy and persistent rainfall was the defining characteristic in 2019 related to offshore water quality. According to SDIA station records, in 2019 San Diego showed the highest cumulative annual precipitation total from the past 10 years (15.52 inches). This is almost double the average rainfall from that period and the 17th highest rainfall total recorded in San Diego since 1850. The largest total of 27.59 inches recorded in 1884. The average annual precipitation between 1850 and 2019 was 9.86 inches (NWS, San Diego). The TJR Estuary station reported a lower cumulative precipitation total in 2019 than San Diego station of 14.41 inches but was still higher than any of the TJR totals from past 10 years (Table 3). The monthly precipitation totals recorded for 2019 did follow expected seasonal patterns with the months of January, November and December recoding high amounts of precipitation and June through October following the typical dry season patterns. February, March and November, however, were atypical months, recording unusually high rainfall totals. The rains during January, February, November and December were not only intense at times (high amount within a short time interval), but persistent. Between the SDIA and TJR Estuary stations during the months of January and February there was measurable precipitation recorded on 30 out of the 59 days with eight of those days recording 0.5 inches of rain or more on a single day. As stated above, the sizes and extents (and hence the beach contamination potential) of the associated stormwater plumes correlate not only with rainfall amounts, but also the intensity with which it fell. As a result, the discharge from the TJR was abnormally strong throughout the month of February. **Figure 24** presents a satellite image time series during the month of February highlighting six days when the Tijuana River plume reached beyond its normal offshore extent. There were 27 significant TJR discharge events documented in the satellite data in 2019, more than twice that of the year prior and the most observed between 2017-2021.

In 2019 the county of San Diego issued 166 posted shoreline and/or rain advisories and 32 beach/shoreline closures. This is twice as many closures when compared to 2018 and the highest number of closures during the 5-year period summarized in this report. The longest contiguous 2019 closure lasting 164 days between January 1 and June 14 was in Border Field State Park along the south end of the Tijuana Slough Shoreline (California State Water Quality Control Board). This closure was an extension from 2018 and so in reality lasted 197 days.

As is typical for the region, almost all the closures were in the area between the Tijuana River mouth and Avenida Del Sol at the south end of North Island. With the exception of those during the June through September summer months, almost all of the closures can be attributed to a rain event prior to and/or during the closure period. All except two were associated with Tijuana River discharge. The satellite imagery available on the web portal on or around the closure dates and rainfall events visually correlate with the closure information. Imagery during those time periods show high turbidity and suspended solid levels along the coastline in the closed region as well as persistent, higher than normal TJR runoff, sometimes being carried north by the ocean currents. **Figure 25** provides an example of the Tijuana River plume extending north corresponding with shoreline closures during the same time period.

The coast of San Diego County, as well as a large percentage of the California Bight, experienced moderate to high chlorophyll levels for most of the year indictive of frequent and persistent phytoplankton blooms throughout 2019. Only for short periods of time in March and May did

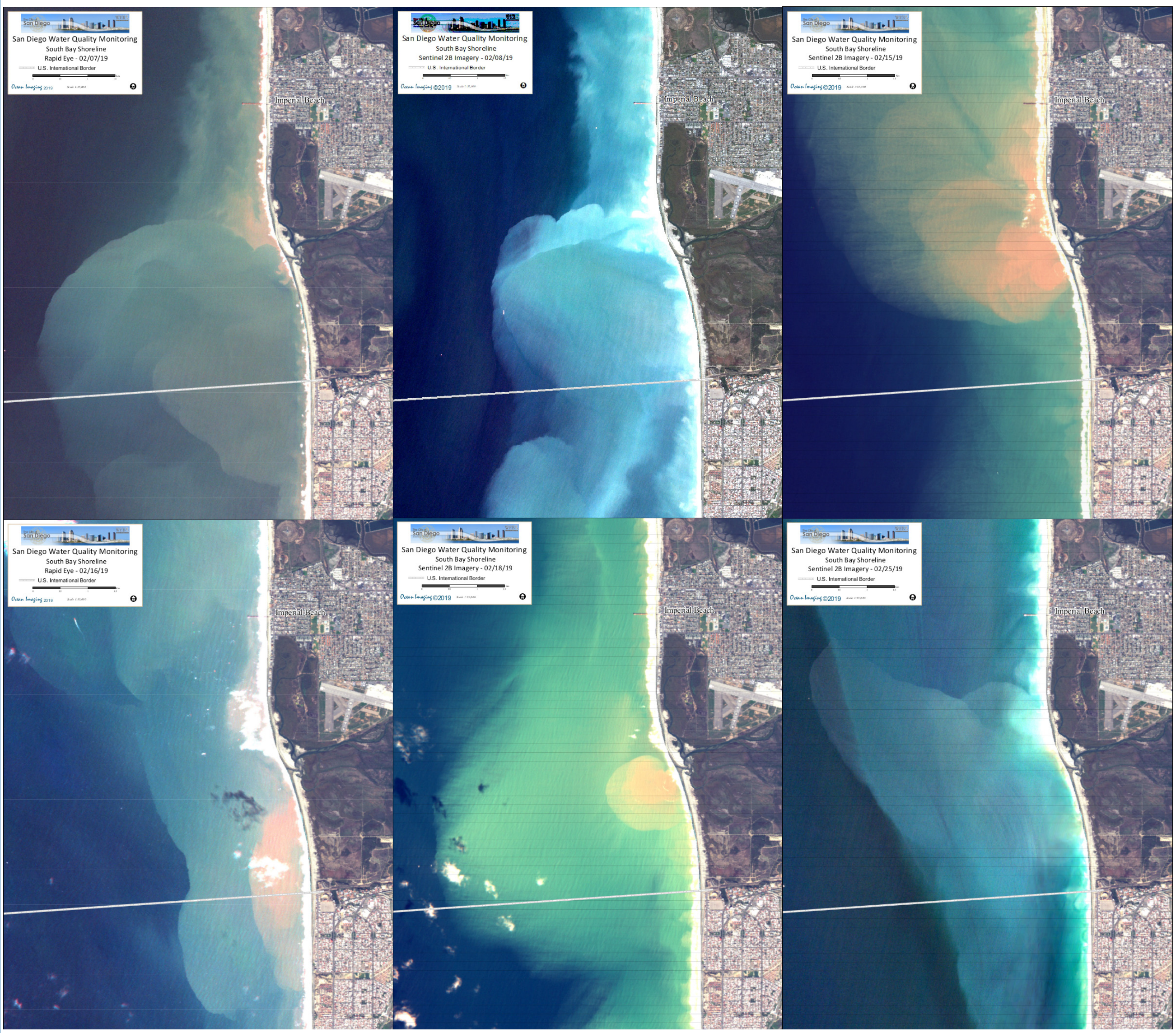

Figure 24. High resolution satellite time series between 02/07/19 and 02/25/19 showing strong TJR discharge events following a period of heavy precipitation.

the satellite data show relatively low levels of chlorophyll/phytoplankton or turbidity along the San Diego coastal region. The first half of 2019 was classified as being in a weak to moderate El Niño phase, however when averaged over the entire year, the ocean temperatures as recorded at the Scripps Pier, PLOO and SBOO RTOMS were actually 0.06 °C lower than the average of the past

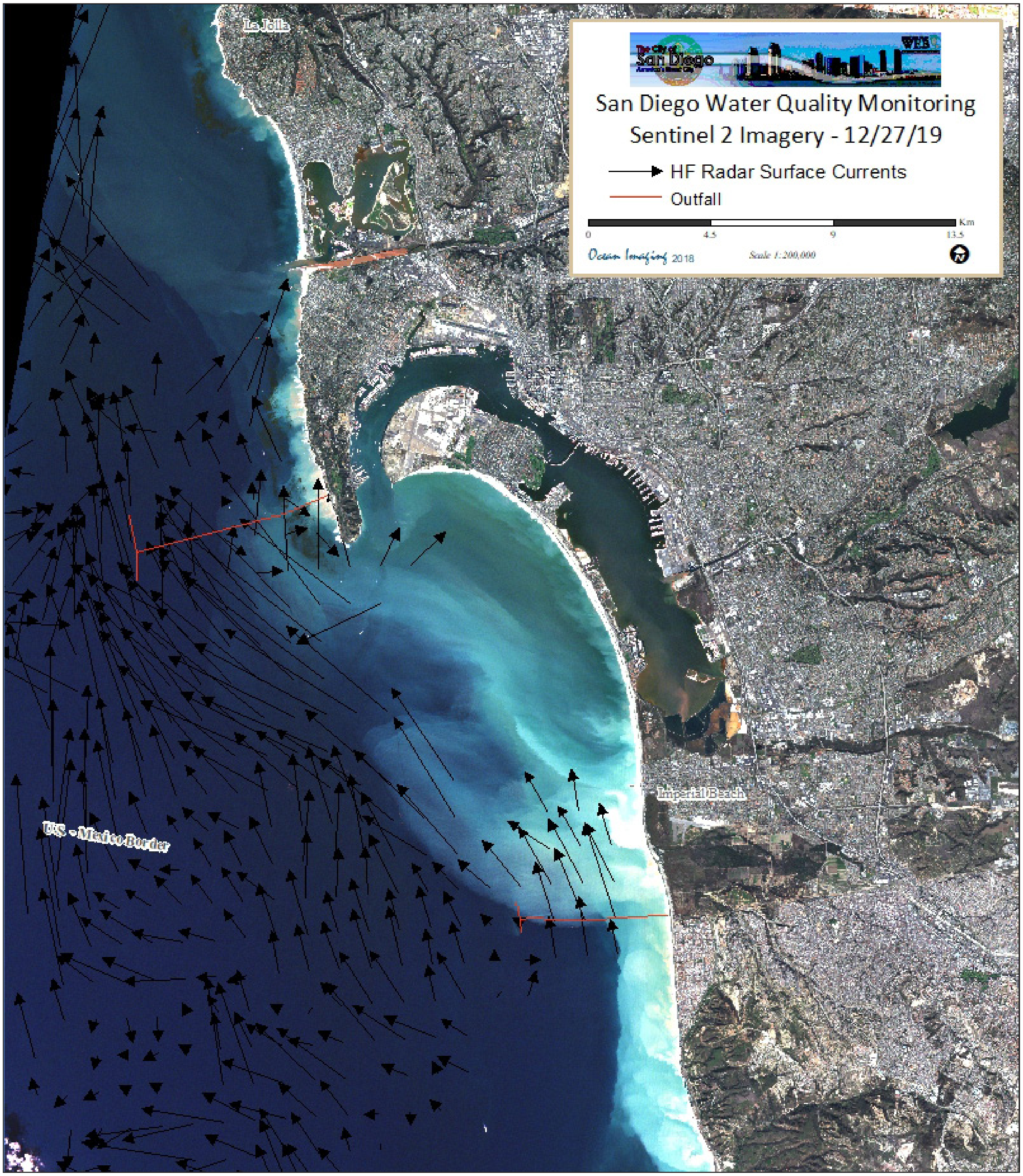

Figure 25. Sentinel 2 image with HF radar-derived surface currents showing the TJR plume extending north during a time of shoreline closures along San Diego.

10 years. The percentage of SBOO plume surface observations per days imaged from satellite was only 15.6% which is under the 10-year mean.

5.5 Conditions in 2020

2020 was marked by strong spring plankton blooms and red tide events. Besides the expected higher levels resulting from the California Current moving down past Point Conception, overall, the Southern California Bight experienced lower levels of chlorophyll during the months of January through early March. After mid-March the levels significantly increased region wide. A strong push of the California Current to the southeast along with coastal upwelling from May through December kept the chlorophyll in the bight high throughout the summer months and into winter. The coastal San Diego region showed normal to high coastal upwelling leading to phytoplankton blooms with the exception of months of March through May when large dense plankton blooms and red tide conditions existed for most of that three-month period from the border up past Oceanside. The blooms were unusually intense and were visible in all types of satellite data including observations in the relatively coarse resolution MODIS imagery. **Figure 26** provides a set of images from the Sentinel2 and SPOT satellites during April and May highlighting the anomalous conditions. The insets show the VIIRS- and MODIS-derived chlorophyll imagery on the same day or within one day of the high-resolution data. While red tides reflect strongly in the red wavelengths of the spectrum, they also reflect highly in the bands used to detect and quantify chlorophyll. In the MODIS and VIIRS imagery, the plankton blooms were so intense that chlorophyll levels surpassed normal cutoff values used to represent the data. Therefore, if examined closely the enhanced MODIS and VIIRs imagery for the months of April and May appear to show colors typically reserved for highly turbid water (as opposed to high chlorophyll). In these cases, the data are actually showing the unusually large and concentrated blooms.

The average ocean temperatures for 2020 recorded at the Scripps Pier, PLOO and SBOO RTOMS were about 0.2 °C below the 10-year mean, however a La Niña began to take hold in July of that year and lasted through June of 2021. This resulted in even lower overall water temperatures from fall into the following year.

Precipitation for the year was close to average at the SDIA station (7.71 inches for the year) and above average at the TJR Estuary station (10.18 inches). However, the majority of the rain fell in March and April while the rest of the year remained very dry. One extreme event was between 04/06/20 and 04/10/20 when a total of almost 5.4 inches were recorded at the TJR Estuary station during that five-day period. This unusually intense episode likely led to an influx of nutrients into the ocean system, sustaining and possibly exacerbating the strong plankton blooms and red tides documented in the satellite imagery during April and May. The number of significant TJR offshore plumes, SBOO effluent surfacings and beach closures were not necessarily high during this time period. The percentage of 2020 SBOO plume surface observations per days imaged was 24.3% which was above the 10-year mean, yet only two of those were in April and not necessarily linked to any storm event. The period of November 2020 through April of 2021 did show the second highest percentage of SBOO detections per image day at 31.8% but was more likely related to excessive flows (>25 MGD) into the SBIWTP from the Mexican wastewater system due to collection system overflows and pump failures later in 2020. These transboundary events were not solely responsible for the high effluent observations, but when they happened during the season when the ocean water column stratification weakened, the combination of factors probably resulted in the relatively frequent SBOO surface detections in the imagery. One such occurrence was on 12/11/20 shown in **Figure 27**. The Sentinel 2 data were acquired only a minute after the SPOT data. Both

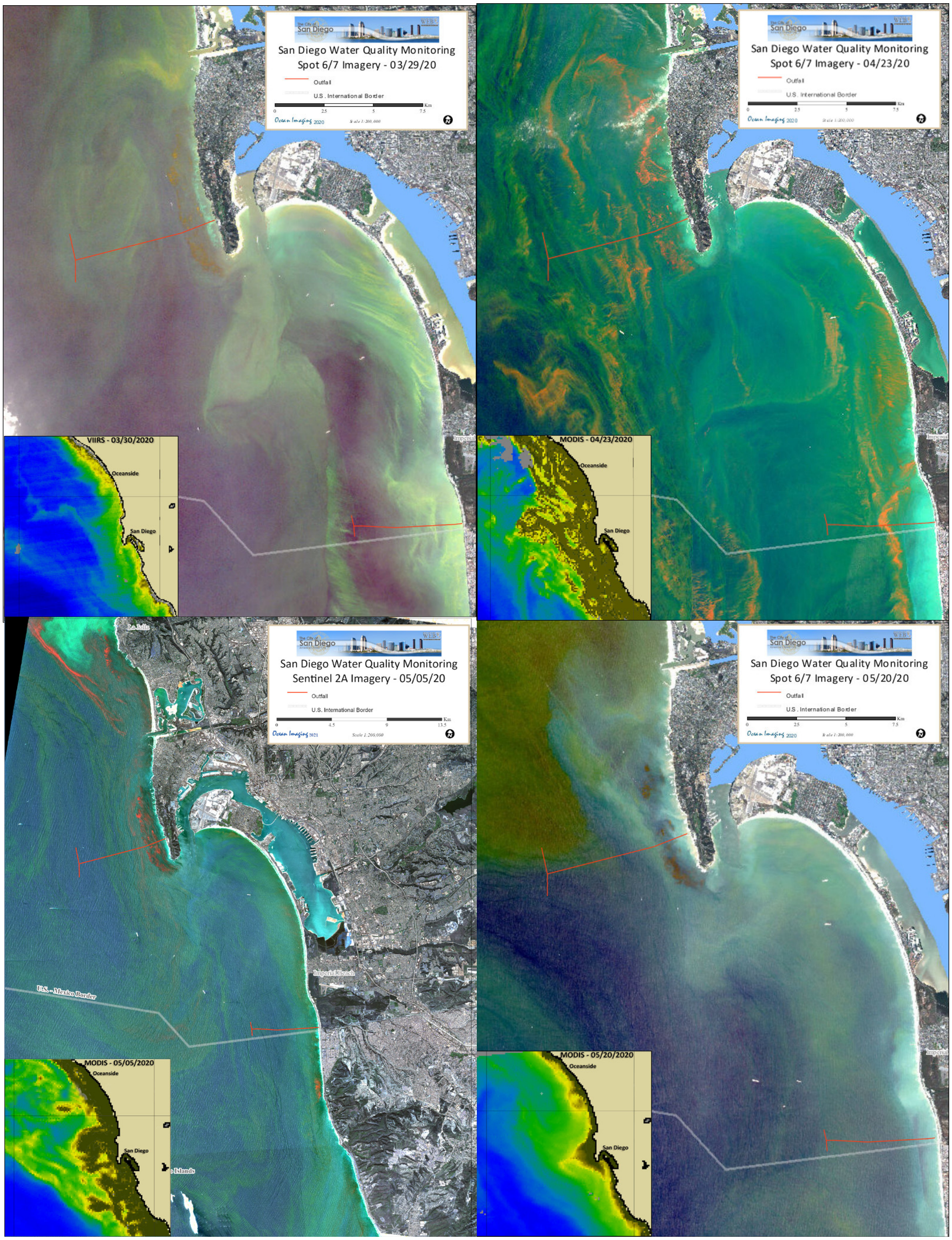

Figure 26. Plankton blooms visible in the SPOT and Sentinel 2 imagery on 03/29/20 (Red-Green-Blue), 04/23/20 (Red- Green-Near Infrared), 05/05/20 (Red-Green-Near Infrared) and 05/20/20 (Red-Green-Blue). Note the strong, probably coccolithophore bloom west of La Jolla in the 05/05/20 image as well as the intense reflectance in the Near-Infrared (NIR) channels (orange-red) in the imagery acquired on 04/23/20 and 05/05/20. The strong NIR signal illustrates the high levels of algae/phytoplankton in the blooms. Insets show MODIS- and VIIRS-derived chlorophyll imagery. Brown areas are where pixel value exceeded the 29.0 mg/L maximum typically used to represent the highest level of chlorophyll.

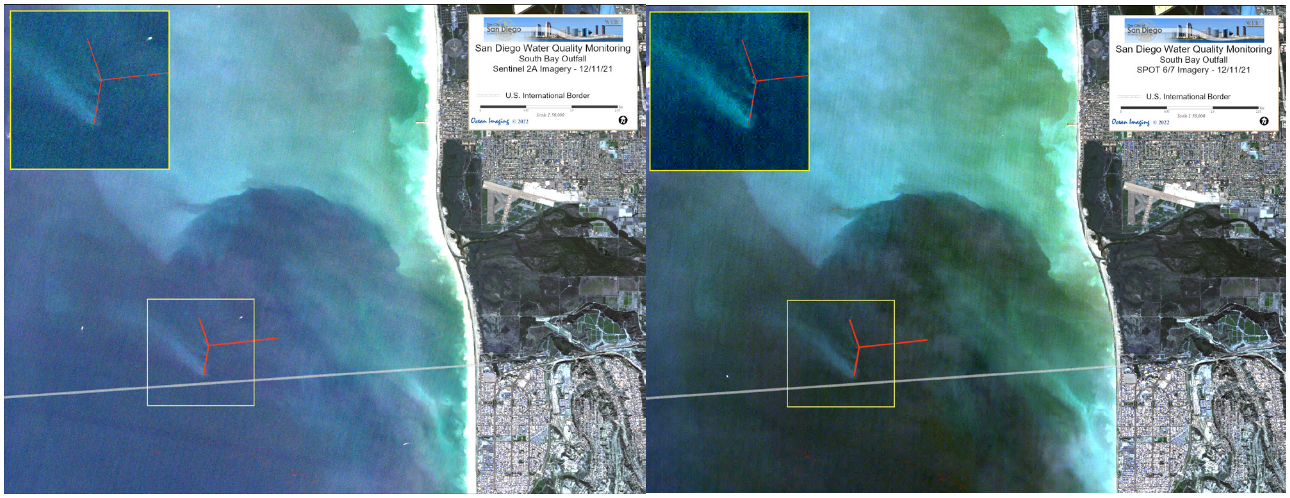

Figure 27. Sentinel 2A and SPOT imagery acquired within one minute of each other on 12/11/20 exhibiting a strong SBOO effluent plume.

images clearly depict the strong SBOO effluent plume emanating from at least three of the wye's risers. There was no storm or rainfall in the region prior to the date of these images. The most recent rainfall before these observations was on 11/09/20.

5.6 Conditions in 2021

While this report is a 5-year summary, it also serves as the 2021 annual report. Therefore, a more detailed discussion of 2021 follows.

5.6.1 Atmospheric and Ocean Conditions in 2021

Annual recorded precipitation for this year was close to the 10-year average for the region. The SDIA measured 7.85 inches and the TJR Estuary 5.63 inches, both a little lower than average (8.13 and 5.63 inches respectively – Table 3 above). The monthly rainfall followed normal patterns seasonally, with the winter and spring months matching the expected rainy season and the summer months being dry. Only 0.13 inches of rain were recorded at the TJR Estuary station from April through September. **Figure 28** shows cumulative daily precipitation in the estuary. The table to the side of the plot gives the dates for which there was measurable precipitation at that station.

The primary period of consistent and/or heavy precipitation occurred between mid-January and Mid-March. The vast majority (17 out of 22) of significant TJR discharge events seen in the remotely sensed data occurred from 01/04/21 to 03/05/21. **Figure 29** provides a dramatic example of the coastal turbidity and a large TJR plume following a long period of rain between 01/22/21 to 01/29/21.

River flow rates as shown in **Figure 30**, which plots the daily San Diego River flow rates in cubic feet per second (cfs) measured by the United States Geological Survey (USGS) Fashion Valley, gauge correspond with the rainfall data. Monthly precipitation totals at the San Diego International Airport station are displayed to the right of the plot. The flow rate of ~630 cfs on 01/29/21 correlates well the heavy coastal turbidity in the 01/30/21 Sentinel image in Figure 29.

In 2021 the county of San Diego issued 113 posted shoreline and/or rain advisories and 44 beach/shoreline closures. This is fewer postings, yet more closures compared to the previous year (151 and 28 respectively). The longest continuous 2021 closure lasting 142 days between January 1st and May 23rd was in Border Field State Park along the south end of the Tijuana Slough shoreline. This closure was an extension from 2020 and so in reality lasted 147

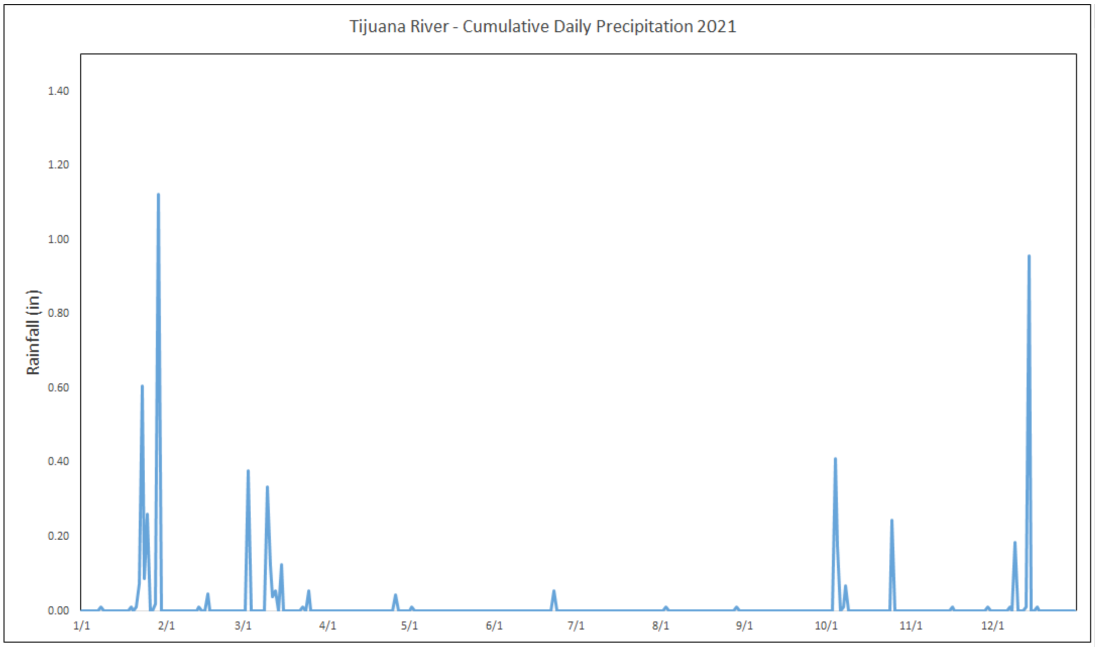

Date	CumPrcp (in)
01/08/21	0.01
01/19/21	0.01
01/21/21	0.01
01/22/21	0.07
01/23/21	0.61
01/24/21	0.09
01/25/21	0.26
01/28/21	0.02
01/29/21	1.12
02/13/21	0.01
02/16/21	0.05
03/03/21	0.38
03/10/21	0.33
03/11/21	0.12
03/12/21	0.04
03/13/21	0.06
03/15/21	0.13
03/23/21	0.01
03/25/21	0.06
04/26/21	0.04
05/02/21	0.01
06/23/21	0.06
08/03/21	0.01
08/29/21	0.01
10/04/21	0.41
10/05/21	0.17
10/07/21	0.01
10/08/21	0.07
10/25/21	0.24
11/16/21	0.01
11/29/21	0.01
12/07/21	0.01
12/09/21	0.19
12/13/21	0.01
12/14/21	0.96
12/17/21	0.01

Figure 28. Daily accumulated rainfall in the Tijuana Estuary

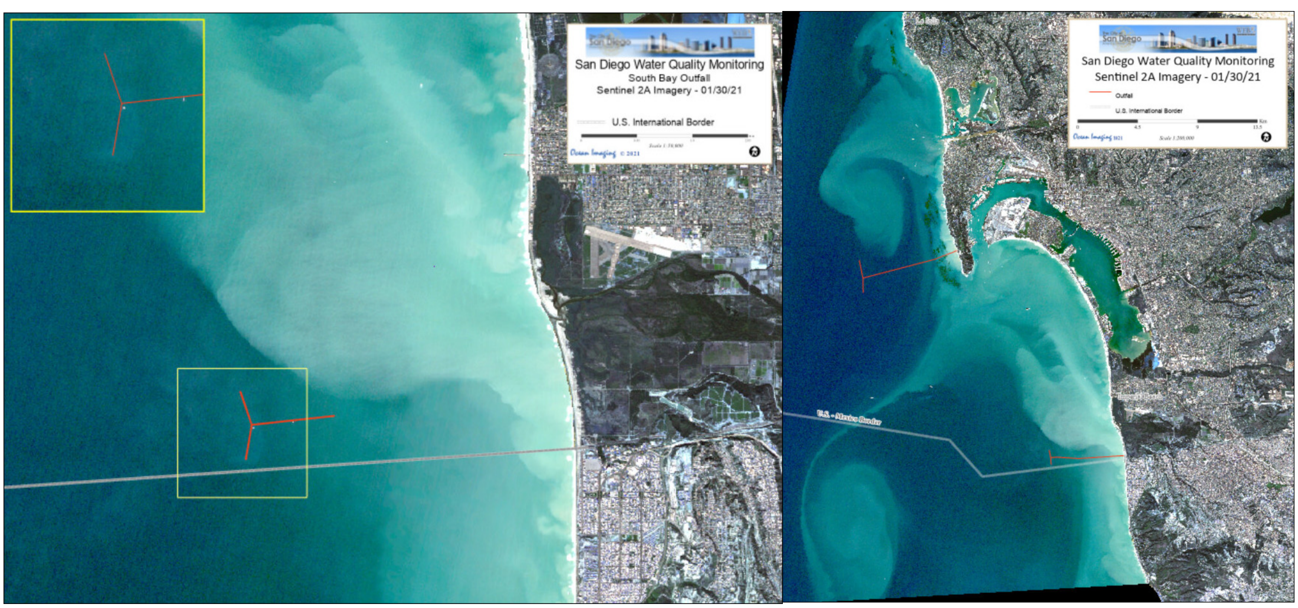

Figure 29. Sentinel 2A imagery from 01/30/21 showing heavy coastal turbidity resulting from heavy rains occurring during the previous seven days. The image on the left shows an expanded view of the TJR plume moving offshore and to the north.

days. As is typical for the region, all but one of the closures were in the area between the Tijuana River mouth and Avenida Del Sol at the south end of North Island and the result of contamination from the TJR runoff. The one exception was the beach to the west of Centennial Park which was closed due to a nearby sewage spill. In previous years most of the closures could be attributed to a rain event prior to and/or during the closure period. However, this was not necessarily the case in 2021 (**Table 4**). Many of the closures were likely the result of excess flow into the TJR Estuary caused by pump station failures and overflows in the TJR basin (San Diego Regional Water Quality Control Board, 2021, 2022 and Morgan Rogers, personal communication). Table 4 also shows the date of the high-resolution satellite data in the project's archive acquired closest in time to the start date of the closure and/or rain advisory.

2021 experienced consistently high chlorophyll/plankton levels throughout the year in the SCB and especially in the waters offshore of San Diego. **Figure 31** provides representative MODIS-derived chlorophyll images for each month of 2021. As is seen in the image data, the months of March, April and May experienced high chlorophyll levels along the Southern California coast with areas along the shoreline from Oceanside down past Pt. Loma often experiencing concentrations above 20 µg/L during the month of March. The California Current's south-eastward push relaxed a bit in July, August and September allowing for clearer water between Oceanside and the islands, however the coastal waters in the San Diego region remained chlorophyll rich through December. Despite the dry spring and summer, there were several days during this period exhibiting exceptionally strong phytoplankton blooms. June and August displayed significant phytoplankton blooms in the image archive with dramatic plankton-rich eddies spinning off the coast and moving offshore.

The City of San Diego CTD sampling results correlated well with what was observed in the satellite data. Some of the highest chlorophyll levels recorded via CTD (as high as 27.3 µg/L) occurred between March and May during the series of ubiquitous phytoplankton blooms. **Figure 32** offers examples of the CTD fluorometry data in correlation with the

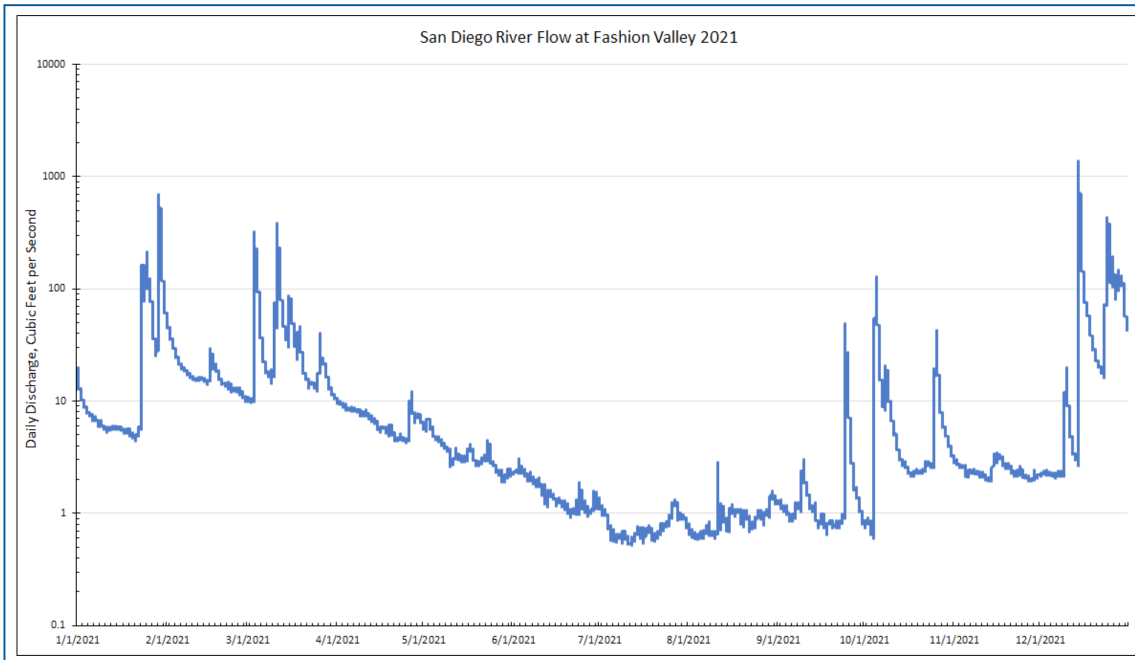

San Diego Intl. Airport Rainfall 2021	
Jan	1.80
Feb	0.10
Mar	1.48
Apr	0.07
May	0.07
Jun	0.01
Jul	--
Aug	0.23
Sep	0.50
Oct	1.01
Nov	--
Dec	2.58

Figure 30. Daily San Diego River flow rates in cubic feet per second measured by the USGS Fashion Valley gauge. Monthly precipitation totals at the San Diego International Airport station are displayed to the right of the plot.

Table 4. 2021 County of San Diego shoreline closures and advisories (courtesy of the County of San Diego Department of Environmental Health).

Station Description	Beach Name	Station Name	Type	Cause	Source	Start Date	End Date	Duration (days)	Nearest Rain Date	Time From Rain Event	Satellite Image Data
Border Fence N side	Border Field State Park	IB-010	Closure	TJR Associated	Sewage/Grease	1/1/2021	5/23/2021	142	1/8/2021	7	1/8/2021, 1/9/2021
All_SanDiego_County_Beaches	All_SanDiego_County	All_SanDiego_County_Beaches	Rain			1/23/2021	2/2/2021	10	1/23/2021	0	1/30/2021
All_SanDiego_County_Beaches	All_SanDiego_County	All_SanDiego_County_Beaches	Rain			1/23/2021	2/2/2021	10	1/23/2021	0	1/30/2021
All_SanDiego_County_Beaches	All_SanDiego_County	All_SanDiego_County_Beaches	Rain			1/23/2021	2/2/2021	10	1/23/2021	0	1/30/2021
All_SanDiego_County_Beaches	All_SanDiego_County	All_SanDiego_County_Beaches	Rain			1/23/2021	2/2/2021	10	1/23/2021	0	1/30/2021
All_SanDiego_County_Beaches	All_SanDiego_County	All_SanDiego_County_Beaches	Rain			1/23/2021	2/2/2021	10	1/23/2021	0	1/30/2021
All_SanDiego_County_Beaches	All_SanDiego_County	All_SanDiego_County_Beaches	Rain			1/23/2021	2/2/2021	10	1/23/2021	0	1/30/2021
Silver Strand N end (ocean)	Silver Strand State Beach	IB-070	Closure	TJR Associated	Sewage/Grease	1/29/2021	2/2/2021	4	1/29/2021	0	01/27/2021,01/28.2021, 01/30/2021
End of Seacoast Dr	Imperial Beach municipal beach, other	IB-050	Closure	TJR Associated	Sewage/Grease	1/29/2021	2/4/2021	6	1/29/2021	0	1/30/2021
End of Seacoast Dr	Imperial Beach municipal beach, other	IB-050	Closure	TJR Associated	Sewage/Grease	2/6/2021	2/7/2021	1	1/29/2021	-8	2/5/2022
Silver Strand N end (ocean)	Silver Strand State Beach	IB-070	Closure	TJR Associated	Sewage/Grease	2/10/2021	2/12/2021	2	1/29/2021	-12	2/11/2021
End of Seacoast Dr	Imperial Beach municipal beach, other	IB-050	Closure	TJR Associated	Sewage/Grease	2/10/2021	2/14/2021	4	1/29/2021	-12	02/11/2021, 02/12/2021, 02/14/2021
End of Seacoast Dr	Imperial Beach municipal beach, other	IB-050	Closure	TJR Associated	Sewage/Grease	2/25/2021	2/26/2021	1	2/16/2021	-9	2/25/2022
Silver Strand N end (ocean)	Silver Strand State Beach	IB-070	Closure	TJR Associated	Sewage/Grease	3/4/2021	3/19/2021	15	3/3/2021	-1	03/01/2021, 03/04/2021
End of Seacoast Dr	Imperial Beach municipal beach, other	IB-050	Closure	TJR Associated	Sewage/Grease	3/4/2021	3/19/2021	15	3/3/2021	-1	3/4/2021
End of Seacoast Dr	Imperial Beach municipal beach, other	IB-050	Closure	TJR Associated	Sewage/Grease	3/25/2021	3/27/2021	2	3/25/2021	0	3/26/2022
End of Seacoast Dr	Imperial Beach municipal beach, other	IB-050	Closure	TJR Associated	Sewage/Grease	3/30/2021	4/9/2021	10	3/25/2021	-5	3/31/2021
Avd. del Sol	Coronado City beaches	IB-080	Closure	TJR Associated	Sewage/Grease	4/3/2021	4/4/2021	1	3/25/2021	-9	4/3/2021
Silver Strand N end (ocean)	Silver Strand State Beach	IB-070	Closure	TJR Associated	Sewage/Grease	4/3/2021	4/5/2021	2	3/25/2021	-9	4/3/2021
End of Seacoast Dr	Imperial Beach municipal beach, other	IB-050	Closure	TJR Associated	Sewage/Grease	4/14/2021	4/15/2021	1	3/25/2021	-20	4/15/2022
End of Seacoast Dr	Imperial Beach municipal beach, other	IB-050	Closure	TJR Associated	Sewage/Grease	4/16/2021	4/18/2021	2	3/25/2021	-22	4/17/2021
Border Fence N side	Border Field State Park	IB-010	Closure	TJR Associated	Sewage/Grease	5/29/2021	5/30/2021	1	5/2/2021	-27	5/28/2021
Border Fence N side	Border Field State Park	IB-010	Closure	TJR Associated	Sewage/Grease	6/5/2021	6/11/2021	6	5/2/2021	-34	6/5/2021
Border Fence N side	Border Field State Park	IB-010	Closure	TJR Associated	Sewage/Grease	6/13/2021	6/22/2021	9	5/2/2021	-42	6/12/2021
Border Fence N side	Border Field State Park	IB-010	Closure	TJR Associated	Sewage/Grease	6/24/2021	7/1/2021	7	6/23/2021	-1	6/24/2021
Centennial Park, Beach To The West	Coronado north beach	EH-063	Closure	Sewage Spill	Unknown	6/30/2021	7/2/2021	2	6/23/2021	-7	6/26/2021
Border Fence N side	Border Field State Park	IB-010	Closure	TJR Associated	Sewage/Grease	7/15/2021	7/17/2021	2	6/23/2021	-22	7/16/2022
End of Seacoast Dr	Imperial Beach municipal beach, other	IB-050	Closure	TJR Associated	Sewage/Grease	7/15/2021	7/16/2021	1	6/23/2021	-22	7/16/2022
Border Fence N side	Border Field State Park	IB-010	Closure	TJR Associated	Sewage/Grease	7/25/2021	7/30/2021	5	6/23/2021	-32	07/22/2021, 07/29/2021
Border Fence N side	Border Field State Park	IB-010	Closure	TJR Associated	Sewage/Grease	8/8/2021	8/10/2021	2	8/3/2021	-5	8/8/2021
End of Seacoast Dr	Imperial Beach municipal beach, other	IB-050	Closure	TJR Associated	Sewage/Grease	8/9/2021	8/10/2021	1	8/3/2021	-6	8/11/2022
Border Fence N side	Border Field State Park	IB-010	Closure	TJR Associated	Sewage/Grease	8/20/2021	8/24/2021	4	8/3/2021	-17	08/23/2021, 08/24/2021
End of Seacoast Dr	Imperial Beach municipal beach, other	IB-050	Closure	Bacterial Standards Violation	Sewage/Grease	8/22/2021	8/24/2021	2	8/3/2021	-19	08/23/2021, 08/24/2021
Border Fence N side	Border Field State Park	IB-010	Closure	Bacterial Standards Violation	Sewage/Grease	9/2/2021	9/5/2021	3	8/29/2021	-4	9/2/2021
End of Seacoast Dr	Imperial Beach municipal beach, other	IB-050	Closure	TJR Associated	Sewage/Grease	9/2/2021	9/5/2021	3	8/29/2021	-4	09/02/2021, 09/05/2021
Border Fence N side	Border Field State Park	IB-010	Closure	Bacterial Standards Violation	Sewage/Grease	9/7/2021	9/11/2021	4	8/29/2021	-9	9/7/2021
Border Fence N side	Border Field State Park	IB-010	Closure	Bacterial Standards Violation	Sewage/Grease	9/15/2021	9/22/2021	7	8/29/2021	-17	09/14/2021, 09/15/2021
End of Seacoast Dr	Imperial Beach municipal beach, other	IB-050	Closure	Bacterial Standards Violation	Sewage/Grease	9/16/2021	9/19/2021	3	8/29/2021	-18	9/17/2021
Border Fence N side	Border Field State Park	IB-010	Closure	Bacterial Standards Violation	Sewage/Grease	9/28/2021	10/3/2021	5	8/29/2021	-30	09/29, 09/30
Border Fence N side	Border Field State Park	IB-010	Closure	TJR Associated	Sewage/Grease	10/5/2021	10/15/2021	10	10/5/2021	0	10/5/2021
End of Seacoast Dr	Imperial Beach municipal beach, other	IB-050	Closure	TJR Associated	Sewage/Grease	10/6/2021	10/11/2021	5	10/5/2021	-1	10/10/2021, 10/12/2021
Silver Strand N end (ocean)	Silver Strand State Beach	IB-070	Closure	TJR Associated	Sewage/Grease	10/9/2021	10/11/2021	2	10/8/2021	-1	10/12/2021
Border Fence N side	Border Field State Park	IB-010	Closure	TJR Associated	Sewage/Grease	10/26/2021	11/12/2021	17	10/25/2021	-1	10/26/2021
Border Fence N side	Border Field State Park	IB-010	Closure	TJR Associated	Sewage/Grease	12/3/2021	12/5/2021	2	11/29/2021	-4	11/28/2021
Border Fence N side	Border Field State Park	IB-010	Closure	TJR Associated	Sewage/Grease	12/8/2021	12/31/2021	23	12/7/2021	-1	11/28/2021
All_SanDiego_County_Beaches	All_SanDiego_County	All_SanDiego_County_Beaches	Rain			12/9/2021	12/12/2021	3	12/9/2021	0	12/11/2022
All_SanDiego_County_Beaches	All_SanDiego_County	All_SanDiego_County_Beaches	Rain			12/14/2021	12/18/2021	4	12/9/2021	-5	12/15/2021
End of Seacoast Dr	Imperial Beach municipal beach, other	IB-050	Closure	TJR Associated	Sewage/Grease	12/14/2021	12/18/2021	4	12/14/2021	0	12/15/2021, 12/16/2021
Silver Strand N end (ocean)	Silver Strand State Beach	IB-070	Closure	TJR Associated	Sewage/Grease	12/15/2021	12/18/2021	3	12/14/2021	-1	12/16/2022
End of Seacoast Dr	Imperial Beach municipal beach, other	IB-050	Closure	TJR Associated	Sewage/Grease	12/21/2021	12/31/2021	10	12/17/2021	-4	12/24/2022
All_SanDiego_County_Beaches	All_SanDiego_County	All_SanDiego_County_Beaches	Rain			12/24/2021	12/31/2021	7	12/17/2021	-7	
Silver Strand N end (ocean)	Silver Strand State Beach	IB-070	Closure	TJR Associated	Sewage/Grease	12/28/2021	12/31/2021	3	12/17/2021	-11	12/24/2022
Avd. del Sol	Coronado City beaches	IB-080	Closure	TJR Associated	Sewage/Grease	12/30/2021	12/31/2021	1	12/17/2021	-13	12/24/2022

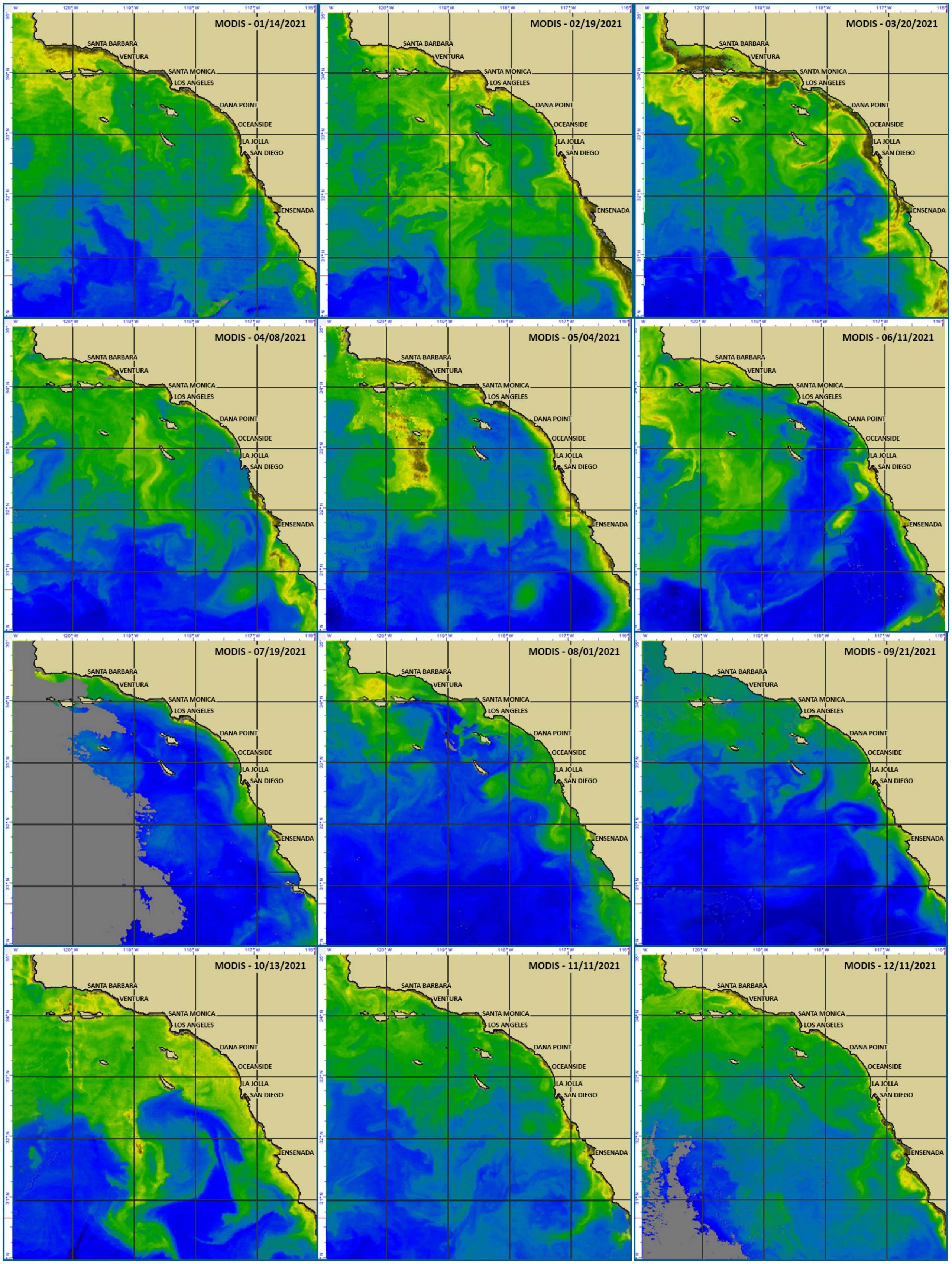

Figure 31. Representative MODS-derived chlorophyll images for each month of 2021 showing strong California Current southward push and significant phytoplankton blooms during nine months of the twelve months.

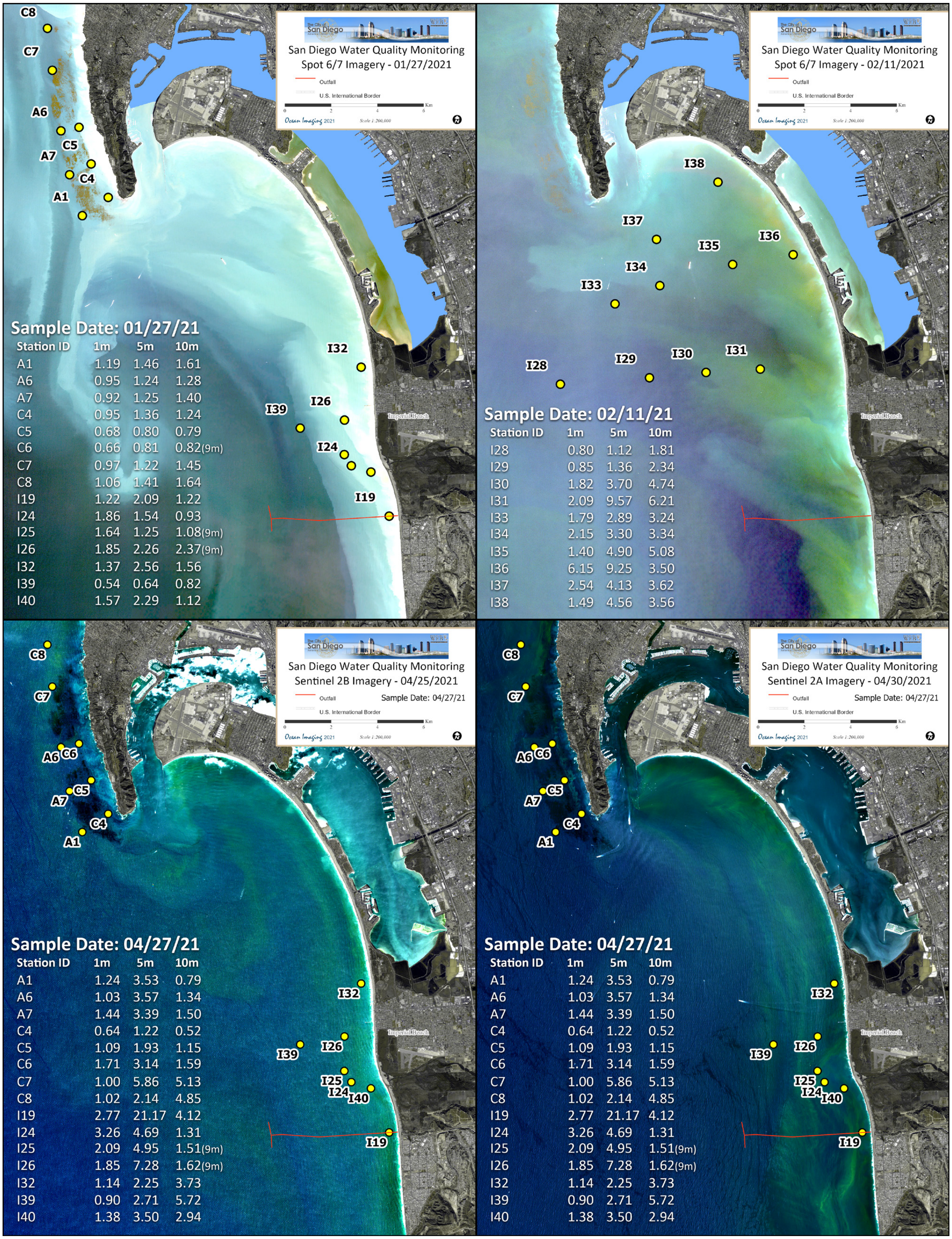

Figure 32. CTD fluorometry data plotted over Sentinel 2 and SPOT satellite imagery showing chlorophyll levels at sampling stations in correlation with the image data.

high-resolution satellite imagery on or near the same date as the field samples. While the remotely sensed data do not depict quantitative chlorophyll levels, the plankton blooms are self-evident in the imagery and correlate well with the CTD data – especially those taken on 02/11/21 and 04/27/21. One interesting day to note is the SPOT image from 01/27/2021. While the image shows very heavy coastal turbidity there is a relative lack of chlorophyll in the turbid water which is reflected in the CTD data. The image color appropriately represents the turbidity as being primarily suspended sediment as opposed to organics.

5.6.2 The South Bay Ocean Outfall Region in 2021

There were 19 instances during which the SBOO effluent plume was observed in 2021 out of the 134 high resolution satellite scenes acquired and processed (Appendix A). Of the 19, three were instances of the plume observed by different satellites on the same day. This equates to 16 days when the plume was visible in the high-resolution imagery. This is 11 fewer than observed in 2020 and below the average percentage when compared to the past 10 years. Accounting for the duplicate observations, the percentage of SBOO plume surface observations per days imaged in 2021 was 14.3% which is about five percentage points under the 10-year mean (19.4%).

The period between 11/11/20 and 01/30/21 exhibited the highest frequency of SBOO effluent plume observations in the satellite data within a period of less than three months. As noted above there were several instances during this time when the SBIWTP took on excess sewage from Tijuana exceeding the maximum allowed capacity of 25 MGD, but the EFF flow is not considered to be the primary factor linked to the high number of SBOO detections. Also discussed previously, the numerous effluent surface manifestations occurring during this time period were likely the result of two primary factors: the lack of strong vertical stratification during the winter months and relatively weak subsurface currents over the SBOO which allowed the undispersed effluent to reach the surface.

In 2021, the shoreline area of the SBOO/Tijuana River outflow region experienced 90 days on which the field sampling showed elevated bacteria levels as defined by the California Ocean Plan. The offshore SBOO region, which includes the stations over the SBOO wye experienced only three days of elevated bacteria levels at depths of six meters or shallower and the nearshore region (referred to as the "kelp" region in previous reports) experienced 20 days on which the bacteria levels were deemed elevated. There were 81 sampling days when at least one shore station showed elevated levels. The total number of sampling days for all three SBOO areas (either along the shoreline or offshore, but at six meters or shallower) totaled 122 in 2021 and 162 in 2020. Therefore, in 2021 for the three sampling regions combined, 73.8% of the sampling days resulted in elevated bacteria levels at one station or more which is close to 77.8% from 2020. However, as noted above, it should be emphasized that the vast majority of samples showing elevated levels were recorded at the shore stations and high levels offshore, near the SBOO wye, are rare. As with 2020, 2021 continued to experience a higher-than-normal number (86) of reports citing the transboundary flow of sewage, solid waste and sediment across the U.S.-Mexico border into the canyon collectors such as Stewart's Drain, the TJR main channel and thus into the Tijuana Estuary and U.S. coastal waters waters (San Diego Regional Water Quality Control Board, 2022). The satellite imagery showing substantial discharge from the TJR region compare well visually with times when the shoreline and kelp area sampling showed elevated bacteria levels (**Figure 33**). Heavy and/or persistent rainfall along with excess untreated flow into the TJR are the most plausible causes for the majority of the elevated bacteria samples and turbid waters seen in the remote sensing data. As is typical, the best water quality and clarity in the South Bay region in 2021 was observed from June through August.

5.6.3 The Point Loma Ocean Outfall Region in 2021

In 2021 the Pt. Loma region was affected by conditions already described for general San Diego County: significant seasonal rainfall during the months of January through mid-March and December with almost no rainfall from of April through November. Similar to past years, this compromised water clarity in the shoreline areas in January

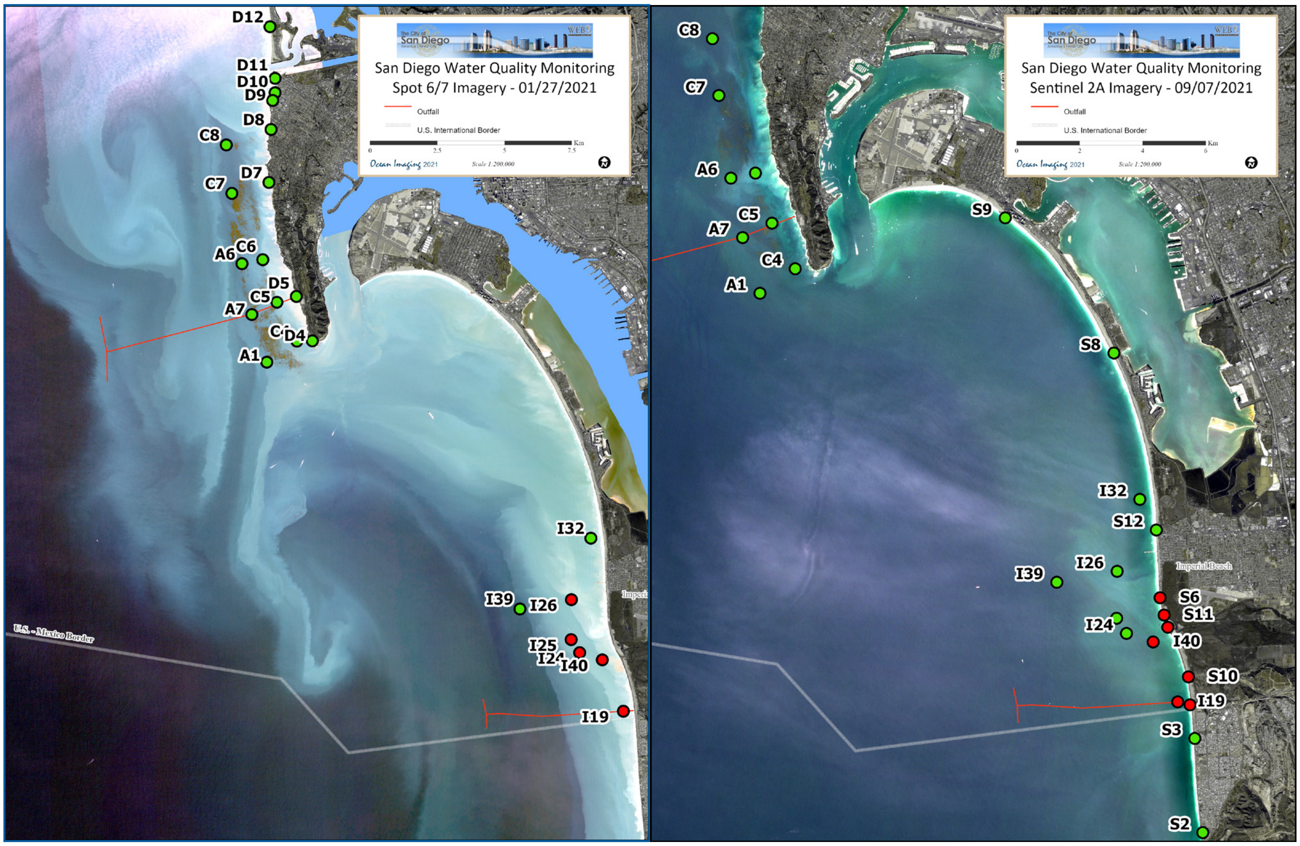

Station	Depth (M)	Entero	Fecal	Total
I19	11	140	220	800
	2	320	860	12000
	6	680	1000	12000
I24	2	400	880	8400
	6	62	82	540
	11	8	20	200
I25	2	360	560	4400
	6	28	62	200
	9	14	42	200
I26	2	340	840	3600
	6	200	860	2200
	9	100	280	2000
I40	2	200	580	5800
	6	440	920	8800
	9	72	88	600

Station	Depth (M)	Entero	Fecal	Total
I19	2	920	300	5200
	11	460	500	4000
	6	2400	160	11000
I40	2	160	220	800
	6	140	74	600
	9	140	100	1000
S5	NA	5200	1600	16000
S6	NA	720	420	6400
S10	NA	4600	880	16000
S11	NA	1800	1100	16000

Figure 33. Sentinel 2 and SPOT data with near-surface bacterial sampling data overlaid from the same day of image acquisition. Stations showing FIB measurements exceeding the single sample maximum as defined by the California Ocean Plan are shown as red dots. Green dots identify stations at which the FIB levels were in compliance. The tables below each image show the measurement values by depth for each station with elevated bacteria levels.

through March and in December as runoff from the San Diego River and Mission Bay brought sediment-laden water inside and outside the Pt. Loma kelp bed after the rain events described above.

The shoreline, kelp and offshore bacterial sampling resulted in a similar number of elevated bacteria measurements as in 2020. Shoreline field sampling yielded 3 days on which one or more stations experienced high bacteria counts. Offshore and kelp station sampling resulted in 8 days and 1 day respectively when stations recorded excessive FIBs. As expected, most of the high bacteria measurements were seen in winter months and attributed to rain events, however the offshore region did see a few days with elevated numbers in May and August on days prior to which there was no precipitation. **Figure 34** displays samples taken on 11/12/21 plotted over a SPOT image from 11/13/21. No obvious visual correlation to the slightly elevated bacteria data exists in the satellite data, yet it should be noted that all the elevated bacteria levels existed

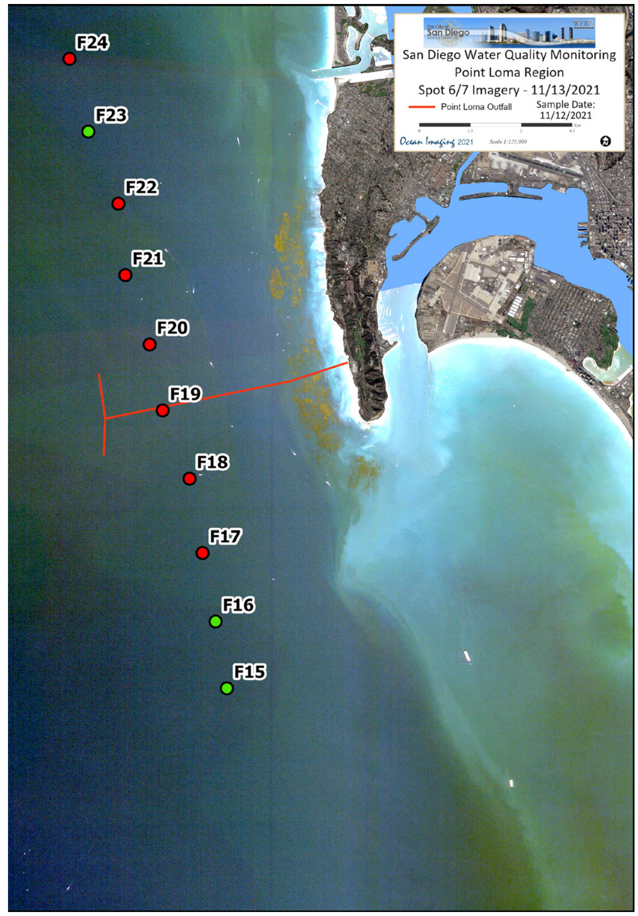

Station	Depth (M)	Entero	Fecal	Total	Station	Depth (M)	Entero	Fecal	Total
F17	1	2	NA	NA	F21	1	2	NA	NA
	25	2	NA	NA		25	2	NA	NA
	60	10	NA	NA		60	260	NA	NA
	80	280	NA	NA		80	220	NA	NA
F18	1	2	NA	NA	F22	1	2	NA	NA
	25	2	NA	NA		25	2	NA	NA
	60	52	NA	NA		60	16	NA	NA
	80	300	NA	NA		80	120	NA	NA
F19	1	2	NA	NA	F24	1	2	NA	NA
	25	2	NA	NA		25	2	NA	NA
	60	54	NA	NA		60	300	NA	NA
	80	260	NA	NA		80	110	NA	NA
F20	1	2	NA	NA					
	25	2	NA	NA					
	60	220	NA	NA					
	80	**180**	**NA**	**NA**					

Figure 34. SPOT image with bacterial sampling data overlaid from the day before image acquisition. Stations showing FIB measurements exceeding the maximum allowed as defined by the California Ocean Plan are shown as red dots. Green dots identify stations at which the FIB levels were in compliance. The tables below each image show the measurement values by depth for each station with elevated bacteria levels.

only at depths of 60 meters or deeper, which is beyond the depth reached with multispectral and thermal infrared remote sensing data.

5.7 Kelp Variability

One observation provided by the satellite image archive is the continuing variability in the size of the Pt. Loma kelp bed over time (**Figure 35**). **Table 5** shows the area in km2 of three notable kelp beds in the San Diego region over the past 14 years. The September and October dates were chosen to represent the kelp bed canopy coverage for each year since spring and fall are considered to be the time periods when the canopy size is thought to be at or near its peak. The size of the Pt. Loma bed

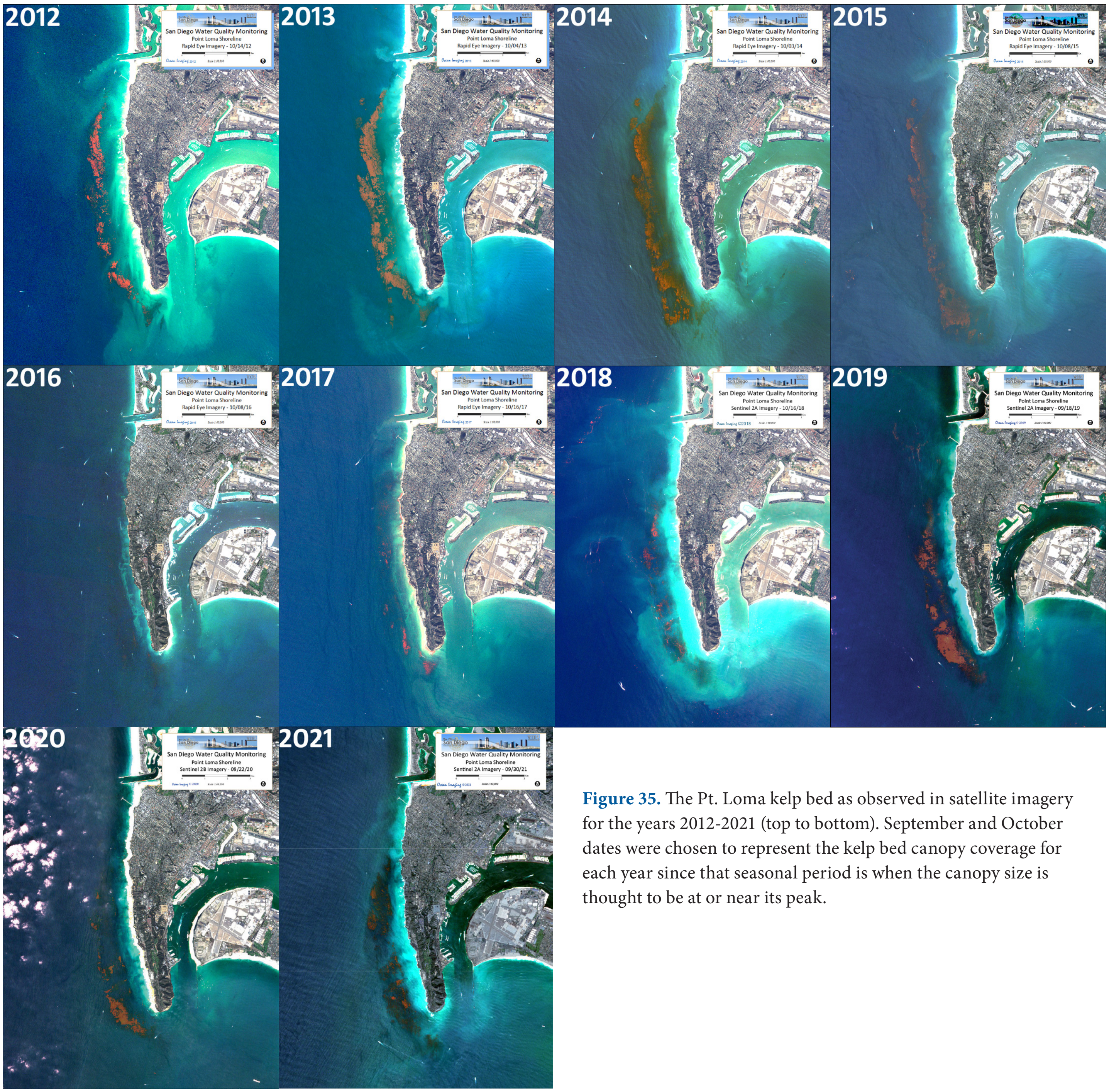

Figure 35. The Pt. Loma kelp bed as observed in satellite imagery for the years 2012-2021 (top to bottom). September and October dates were chosen to represent the kelp bed canopy coverage for each year since that seasonal period is when the canopy size is thought to be at or near its peak.

in the fall of 2021 (3.82 km2) was very close to the average canopy coverage for the 14-year period (4.04 km2). As has been reported in previous years, the satellite data show the bed begin to decrease in size during February of 2016, perhaps due to the storm events taking place during early to mid-January, effects from the 2014-2016 strong El Niño event and/or the Northeast Pacific marine heat wave (Di Lorenzo, 2016). Noted in the 2017 and 2018 annual reports, the kelp bed appeared to be coming back in January of 2017, but then decreased in size as the year progressed resulting in much smaller than average canopy coverage by the end of that year. As was also the case in 2018 and 2020, the relative high frequency of the satellite data of Pt. Loma available through this project revealed significant month-to-month variability in canopy coverage likely due to a combination of factors. In the beginning of 2021, the bed roughly held the same canopy size observed at the end of 2020, however the coverage of the exposed canopy decreased during the latter part of February through late March. Between April and October, the bed experienced several fluctuations in size showing a dramatic reduction for a few weeks in late October to early November. The bed then peaked in size in the November 28th imagery and held close to that coverage for the remainder of the year. While there were significant differences in tidal heights at the time of each satellite image acquisition, tides cannot be flagged as the primary reason for the difference in canopy coverage observed in the satellite data. There were days when the areal coverage was high, but the tide level was also high and vice versa when the imagery revealed smaller bed size, but the tides were relatively low. Additionally, passing storms that result in kelp bed damage can be considered factors, though not the sole cause of smaller kelp bed observations. The intra-annual variation as captured in the Near-IR, 6-meter SPOT imagery is visually documented in a year-long time series video in which the bed is imaged multiple times per month (https://oceani.com/SDWQ/2021_PointLomaKelpTimelapse.mp4).

It is important to point out that the canopy coverages shown in Table 5 may differ slightly from those provided in the Southern California Bight

Table 5. Kelp canopy areas of three San Diego kelp beds measured from satellite imagery collected for this project.

			Kelp (km²)		
Year	Date	Satellite	Point Loma	Imperial Beach	Tijuana
2021	09/30/21	Sentinel-2B	3.82	0.00	0.00
2020	09/22/20	Sentinel-2A	2.93	0.00	0.00
2019	09/18/19	Sentinel-2A	5.17	0.00	0.00
2018	10/16/2018	Sentinel-2A	2.44	0.00	0.00
2017	10/04/2017	RapidEye	1.05	0.00	0.00
2016	09/08/2016	RapidEye	0.22	0.00	0.00
2015	09/17/2015	Landsat 7	4.11	0.39	0.29
2014	09/14/2014	Landsat 8	5.42	0.59	0.30
2013	09/23/2013	RapidEye	5.89	0.19	0.05
2012	09/15/2012	RapidEye	2.91	0.00	0.00
2011	09/01/2011	RapidEye	1.99	0.00	0.00
2010	09/27/2010	Landsat 7	6.01	0.00	0.00
2009	09/16/2009	Landsat 5	5.96	1.01	0.21
2008	09/05/2008	Landsat 7	8.66	0.82	0.01

* Average surface canopy coverage 2008-2021 = 4.04 km2

Regional Arial Kelp Survey reports. This is because the canopy areas for the Pt. Loma bed computed for those reports are averages of four surveys performed throughout the year; while the coverage estimates shown in this report are taken from single satellite images acquired during the fall time period chosen to represent the maximum coverage seen during that time of year. Tide levels were not a factor in the inter-year comparison as there was little variability in tide level between the years (often approximately two feet or less). However, due to the overflight times of these satellites, the canopy areas could be under-represented compared to the kelp survey reports because the tide levels at the time of satellite data acquisition could vary significantly from the tides during the aerial surveys. The Imperial Beach and Tijuana beds have not been visible in the satellite data since 2015. It is being documented that kelp forests along the West Coast have been experiencing noteworthy variability in canopy size for the past several years, and thus warrants keeping a close watch on the health of the kelp beds in the San Diego region (Bell, et al., 2020; Schroeder, 2019).

6. RECENT AND FUTURE DEVELOPMENTS AND ADDITIONS TO THE PROJECT

During the period covered in this summary report OI has added several data products and capabilities to the daily offerings provided as part of the project. As discussed above, in 2016, OI began to generate ocean currents, subsurface temperature and salinity analyses along with other HYCOM-derived products in a WMS REST service format which is directly compatible with any WMS the City might be working to implement. It was intended that all the OI-delivered data products, including all the satellite imagery would be delivered via OI's ArcGIS Server for easy ingestion into the City's WMS by fall of 2017. OI is in discussion with the City about further developing the project web server into a WMS-driven dashboard style site that will facilitate the delivery of all of the existing data products, the HYCOM oceanographic products and any other data sets that the City choose to incorporate into an interactive platform. Not only will the server give the user the capability to overlay different data types on top of each other (i.e., ocean currents on top of satellite imagery) it will significantly enhance the information experience providing easy, near real-time access to the many data products delivered as part of this project.
As part of this process, the historical imagery, data and reports will remain accessible via the existing web portal. If a more capable web server comes online, OI will progressively work backwards in time to make all historical data available via the City's online WMS, including the archived HYCOM data products.

In the meantime, OI has begun the process to update the project's existing web site in order to better present the various data products and hopefully increase end user interaction. **Figure 36** provides an example of what the data access page will look like. The upgrades to the site are intended to give the visitor quick, "at a glance" access to thumbnail images for a particular monitoring region from the most recent 15 days in an interactive carousel-style gallery. Clicking on a thumbnail image will open a page with access to the matching month and imaging region. The new site will also reduce excessive text links for the older data sets but provide one-click access to the data archive pages.

As discussed above, beginning in 2017, OI also began processing and posting imagery from the Sentinel-2A, 2B, 3A and 3B satellites. In 2020 OI transitioned from the now-decommissioned RapidEye Satellite constellation to the SPOT 6 and 7 satellites. Also mentioned above, in late 2021 SAR data from the Sentinel 1A and 1B satellites were added to the suite of products. SAR can detect surfactant films associated with natural processes (Svejkovsky and Shandley 2001) and plumes containing anthropogenic substances (Svejkovsky and Jones 2001, Gierach et al. 2016, Holt et al. 2017) when optical sensors might be limited by cloud cover or heavy atmospheric haze. The primary purpose of these satellites for this project will be to provide another look at the TJR discharge plume to assess its extent and direction of flow. The runoff often contains the natural and anthropogenic surfactants that dampen the SAR signal and therefore make it detectable in the data. **Figure 37** shows a sample SAR image from 02/01/22 highlighting a potential surfactant signature from the TJR discharge. Note that the potentially contaminated water is moving northward.

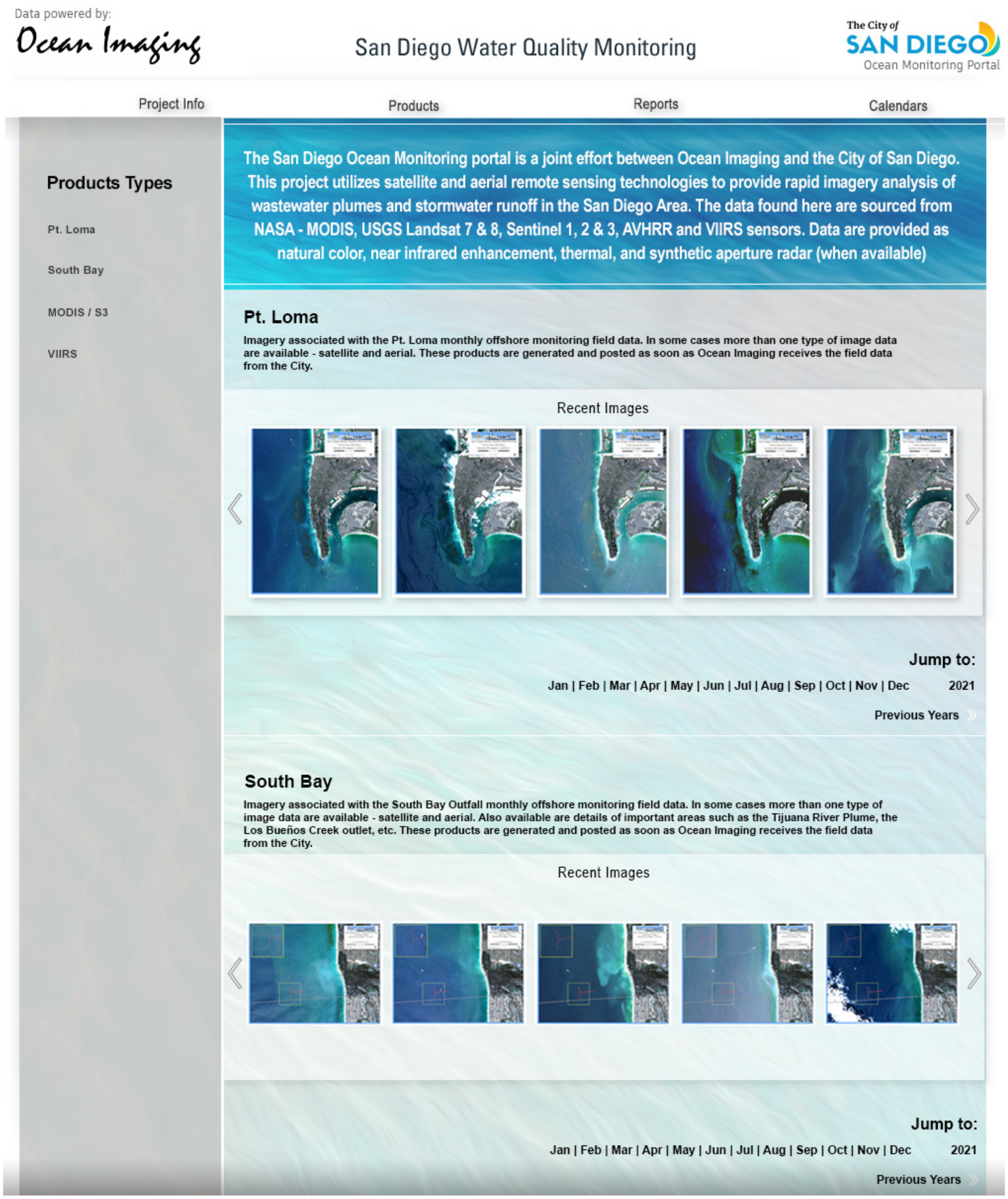

Figure 36. Sample front page of updated SDWQ web site providing near-real time access to the remote sensing data acquired and processed for this project. The new site is expected to be live in the summer of 2022.

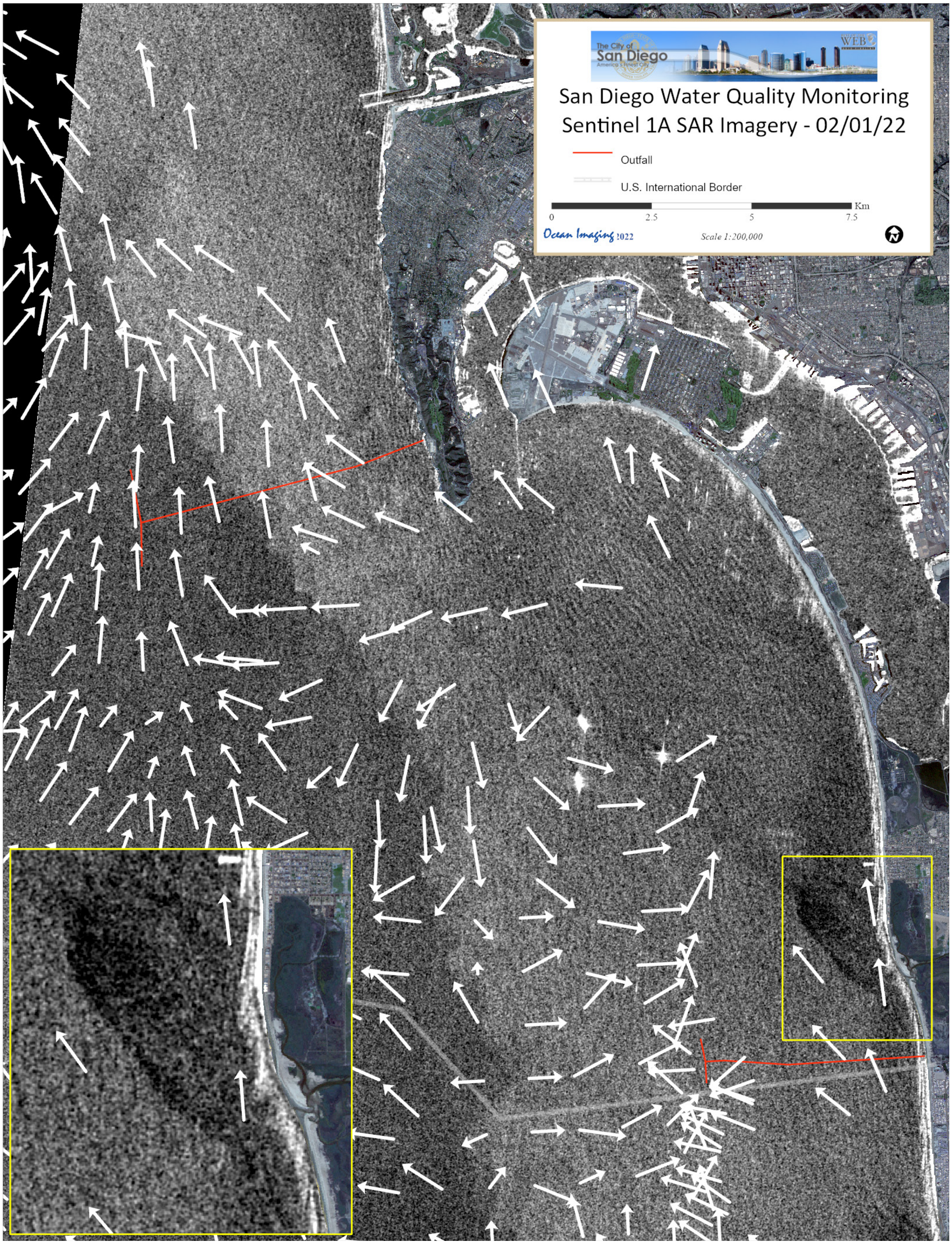

Figure 37 Sentinel 1A SAR image showing possibly contaminated TJR discharge plume moving north farther into San Diego Waters. The image was acquired on 02/01/21 at 13:45 UTC. The 25-hour averaged HF Radar currents from 14:00 UTC are overlaid to further document the northward surface flow. No other high resolution remote sensing data were available on this day, so this SAR dataset offers an additional observation of the core of the TJR plume's extent and direction.

7. REFERENCES

Amaya, Dillon J., et al. "Physical Drivers of the Summer 2019 North Pacific Marine Heatwave." Nature Communications, vol. 11, no. 1, 2020, https://doi.org/10.1038/s41467-020-15820-w.

[APHA] American Public Health Association. (2012). Standard Methods for the Examination of Water and Wastewater, 22nd edition. American Public Health Association, American Water Works Association, and Water Environment Federation.

Axiak, V., Pavlakis, P., Sieber, A. J., Tarchi, D., 2000. Re-assessing the extent of impact of Malta's (Central Mediterranean) major sewage outfall using ERS SAR. Marine Pollution Bulletin, 40(9), 734 – 738.

Bell, Tom W., et al. "Three Decades of Variability in California's Giant Kelp Forests from the Landsat Satellites." Remote Sensing of Environment, vol. 238, 2020, p. 110811., https://doi.org/10.1016/j.rse.2018.06.039.

Bertrand-Krajewski, J.-L., Chebbo, G., Saget, A., 1998. Distribution of pollutant mass vs volume in stormwater discharges and the first flush phenomenon. WaterResearch 32, 2341–2356.

Bird, E., Lewis, N., 2015. Beach Renourishment, Springer Briefs in Earth Sciences, pp. 135, DOI 10.1007/978-3-319-09728-2_2.

Bordner, R., Winter, J., Scarpino, P., eds., 1978. Microbiological Methods for Monitoring the Environment: Water and Wastes, EPA Research and Development, EPA-600/8-78-017.

California State Water Quality Control Board. "Search Beach Monitoring Data." SWRCB.gov, https://www.waterboards.ca.gov/water_issues/programs/beaches/search_beach_advisory.html.

[CDPH] California State Department of Public Health website. (2019). Regulations for Public Beaches and Ocean Water-Contact Sports Areas. Appendix A: Assembly Bill 411, Statutes of 1997, Chapter765. https://www.cdph.ca.gov/Programs/CEH/DRSEM/Pages/EMB/RecreationalHealth/Beaches-and-Recreational-Waters.aspx

City of San Diego. (2020). Biennial Receiving Waters Monitoring and Assessment Report for the Point Loma and South Bay Ocean Outfalls, 2018-2019. City of San Diego, Public Utilities Department, Environmental Monitoring and Technical Services Division, San Diego, CA.

Cristina, C.M., Sansalone, J.J., 2003. First flush, power law and particle separation diagrams for urban storm-water suspended particulates. Journal of Environmental Engineering-ASCE 129, 298–307.

Di Lorenzo, Emanuele, and Nathan Mantua. "Multi-Year Persistence of the 2014/15 North Pacific Marine Heatwave." Nature Climate Change, vol. 6, no. 11, 2016, pp. 1042–1047., https://doi.org/10.1038/nclimate3082. [ELAP] Environmental Laboratory Accreditation Program https://www.waterboards.ca.gov/drinking_water/certlic/labs/index.html

"Frequently Asked Questions About El Nino and La Nina." Climate Prediction Center - Enso FAQ, 26 Apr. 2012, https://origin.cpc.ncep.noaa.gov/products/analysis_monitoring/ensostuff/ensofaq.shtml#general.

Gersberg, R.M., Daft, D., Yorkey, D., 2004. Temporal pattern of toxicity in runoff from the Tijuana River Watershed. Water Research 38, 559–568.

Gersberg, R.M., Rose, M.A., Robles-Sikisaka, R., Dhar, A.K., 2006. Quantitative detection of hepatitis a virus and enteroviruses near the United States-Mexico border and correlation with levels of fecal indicator bacteria. Applied and Environmental Microbiology 72, 7438–7444.

Gersberg, R., Tiedge, J., Gottstein, D., Altmann, S., Watanabe, K., Luderitz, V., 2008. Effect of the South Bay Ocean Outfall (SBOO) on ocean beach water quality near the USA-Mexico border. International Journal of Environmental Health Research 18, 149–158.

Gierach, M. M., Holt, B., Trinh, R., Pan, B.J., Rains, C., 2017. Satellite detection of wastewater diversion plumes in Southern California. Estuarine, Coastal and Shelf Science, 186, 171 – 182.

Graf, C., Tinney, C., Konner, T., 2005. Water and wastewater at the international boundary. Southwest Hydrology, September/October, 16-18.

"Harmful Algal Blooms." Southern California Coastal Water Research Project, 10 May 2019, https://www.sccwrp.org/about/research-areas/eutrophication/harmful-algal-blooms/.

Holt, B., Trinh, R., Gierach, M. M., 2017. Stormwater runoff plumes in the Southern California Bight: A comparison study with SAR and MODIS imagery. Marine Pollution Bull. Vol. 118, 141-154.

Howden, M., 1995. Application of remote sensing for monitoring the Sydney deepwater ocean outfalls. Trans. on Ecology and Environment,7, 269-276.

Hyde, K. J. W., O'Reilly, J.E., Oviatt, C.A., 2007. Validation of SeaWiFS chlorophyll a in Massachusetts Bay. Continental Shelf Research, 27(12), 1677 – 1691.

Inman, Douglas L., and Scott A. Jenkins. "Climate Change and the Episodicity of Sediment Flux of Small California Rivers." The Journal of Geology, vol. 107, no. 3, 1999, pp. 251–270., https://doi.org/10.1086/314346.

Keeler, R. N., Bondur, V.G., Gibson, C. H., 2005. Optical satellite imagery detection of internal wave effects from a submerged turbulent outfall in the stratified ocean. Geophys. Research Letters, 32, L12610.

Luković, Jelena, et al. "A Later Onset of the Rainy Season in California." Geophysical Research Letters, vol. 48, no. 4, 2021, https://doi.org/10.1029/2020gl090350.

Marmorino, G. O., Smith, G. B., Miller, W.D., Bowles, J., 2010. Detection of a buoyant coastal wastewater discharge using airborne hyperspectral and infrared imagery. J. of Applied Remote Sensing, 4(1), 043502.

MBS Applied Environmental Sciences, 2017. Status of the Kelp Beds in 2016. Annual Report, http://kelp.sccwrp.org/2016/Status_of_the_Kelp_Beds_2016_Ventura_Los%20Angeles_Orange_and_San_Diego_Counties.pdf

National Weather Service Corporate Image Web Team. "NWS San Diego." National Weather Service, 24 Oct. 2005, w2.weather.gov/climate/index.php?wfo=sgx.

Nezlin, N. P., DiGiacomo, P.M., Stein, E.D., Ackerman, D., 2005. Stormwater runoff plumes observed by SeaWiFS radiometer in the Southern California Bight. Remote Sensing of Environment, 98, 494 – 510.

[NOAA] National Oceanic and Atmospheric Administration. (2022). National Climatic Data Center. http://www7.ncdc.noaa.gov/CDO/cdo.

Ocean Fact Sheet Package - United Nations. https://www.un.org/sustainabledevelopment/wp-content/uploads/2017/05/Ocean-fact-sheet-package.pdf.

Ouillon, S., Forget, P., Froidefond, J-M., Naudin, J-J., 1997. Estimating suspended matter concentrations from SPOT data and from field measurements in the Rhone River plume. Marine Tech. Society Journal, 31(2), 15-20.

Rogowski, Peter, et al. "Mapping Ocean Outfall Plumes and Their Mixing Using Autonomous Underwater Vehicles." Journal of Geophysical Research: Oceans, vol. 117, no. C7, 2012, https://doi.org/10.1029/2011jc007804.

Roughan, M., Terrill, E.J., Largier, J.L., Otero, M.P., 2005. Observations of divergence and upwelling around Point Loma, California. J. Geophys. Res., 110, C04011.

Ruddick, K. G., Lahousse, L., Donnay, E., 1994. Location of the Rhine plume front by airborne remote sensing. Continental Shelf Res., 14(4), 325 – 332.

San Diego Regional Water Quality Control Board,2022. "International Boundary and Water Commission Transboundary Flow Reports." International Boundary and Water Commission Spill Reports | San Diego Regional Water Quality Control Board, https://www.waterboards.ca.gov/sandiego/water_issues/programs/

tijuana_river_valley_strategy/spill_report.html.
San Diego Regional Water Quality Control Board, 2020. “Sewage Pollution within the Tijuana River Watershed.” Sewage Pollution within the Tijuana River Watershed | San Diego Regional Water Quality Control Board, https://www.waterboards.ca.gov/sandiego/water_issues/programs/tijuana_river_valley_strategy/sewage_issue.html.
Schiff, K. C., Allen, M.J., Zeng, E.Y., Bay, S.M., 2000. Southern California. Mar. Pollut. Bull. 41(1-6), 76-93.
Schroeder, S. B., C. Dupont, L. Boyer, F. Juanes, and M. Costa. 2019. Passive remote sensing technology for mapping bull kelp (Nereocystis luetkeana): a review of techniques and regional case study. Glob. Ecol. Conserv. 19, e00683.
SCCOOS Automated Shore Station, Institution: Scripps, University of California San Diego (Dataset ID: autoss) https://erddap.sccoos.org/erddap/tabledap/autoss.html?time,pressure,pressure_flagPrimary,temperature,temperature_flagPrimary,chlorophyll,chlorophyll_flagPrimary,salinity,salinity_flagPrimary&station=%22scripps_pier%22&time%3E=2020-12-30T08:00:00.000Z&time%3C2022-01-01T07:59:59.000Z&orderBy(%22time%22)
Svejkovsky, J., Haydock, I., 1998. Satellite remote sensing as part of an ocean outfall environmental monitoring program. In: Taking a Look at California’s Ocean Resources: An Agenda for the Future, ASCE, Reston, VA (USA), 2, 1306.
Svejkovsky, J., Jones, B., 2001. Satellite Imagery Detects Coastal Stormwater and Sewage Runoff. EOS-Trans. American Geophys. Union, 82(50).
Svejkovsky, J., Shandley, J., 2001. Detection of offshore plankton blooms with AVHRR and SAR imagery. Int. J. of Remote Sensing, 22 (2&3), 471-485.
Svejkovsky, J., Nezlin, N. P., Mustain, N.M. Kum, J. B., 2010. Tracking storm water discharge plumes and water quality of the Tijuana River with multispectral aerial imagery. Estuarine, Coastal and Shelf Science. 87(3), 387-398.
Tiefenthaler, L.L., Schiff, K.C., 2003. Effects of rainfall intensity and duration on first flush of stormwater pollutants. In: Weisberg, S.B., Elmore, D. (Eds.). Southern California Coastal Water Research Project Annual Report 2001–2002. Southern California Coastal Water Research Project Authority, Westminster, CA, pp. 209–215.
Trinh R.C., Fichot C.G., Gierach M.M., Holt B., Malakar N.K., Hulley G. Smith J., 2017. Application of Landsat 8 for Monitoring Impacts of Wastewater Discharge on Coastal Water Quality. Frontiers in Marine Science, 4:329
United Nations, 2009. Percentage of Total Population Living in Coastal Areas. http://www.un.org/esa/sustdev/natlinfo/indicators/methodology_sheets/oceans_seas_coasts/pop_coastal_areas.pdf
[USEPA] United States Environmental Protection Agency. (2014). Method 1600: Enterococci in Water by Membrane Filtration Using membrane-Enterococcus Indoxyl-β-D-Glucoside Agar (mEI). EPA Document EPA-821-R-14-011. Office of Water (4303T), Washington, DC.
Walker, N. D., Wiseman, W.J., Rouse, L.J., Babin, A., 2005. Effects of river discharge, wind stress, and slope eddies on circulation and satellite-observed structure of the Mississippi River plume. J. of Coastal Res., 21(6), 1228 – 1244.
Warrick, J.A., DiGiacomo, P.M., Weisberg, S.B., Nezlin, N.P., Mengel, M.J., Jones, B.H., Ohlmann, J.C., Washburn, L., Terrill, E.J., Farnsworth, K.L., 2007. River plume patterns and dynamics within the Southern California Bight. Continental Shelf Research 27, 2427–2448.
Werme, C., Hunt, C.D., 2000. 1998 Outfall monitoring overview. Boston: Massachusetts Water Resources Authority. Report ENQUAD 00-04. 66 pp.

APPENDIX A – 2021 HIGH RESOLUTION SATELLITE IMAGERY SHOWING SBOO-RELATED WASTEWATER PLUME

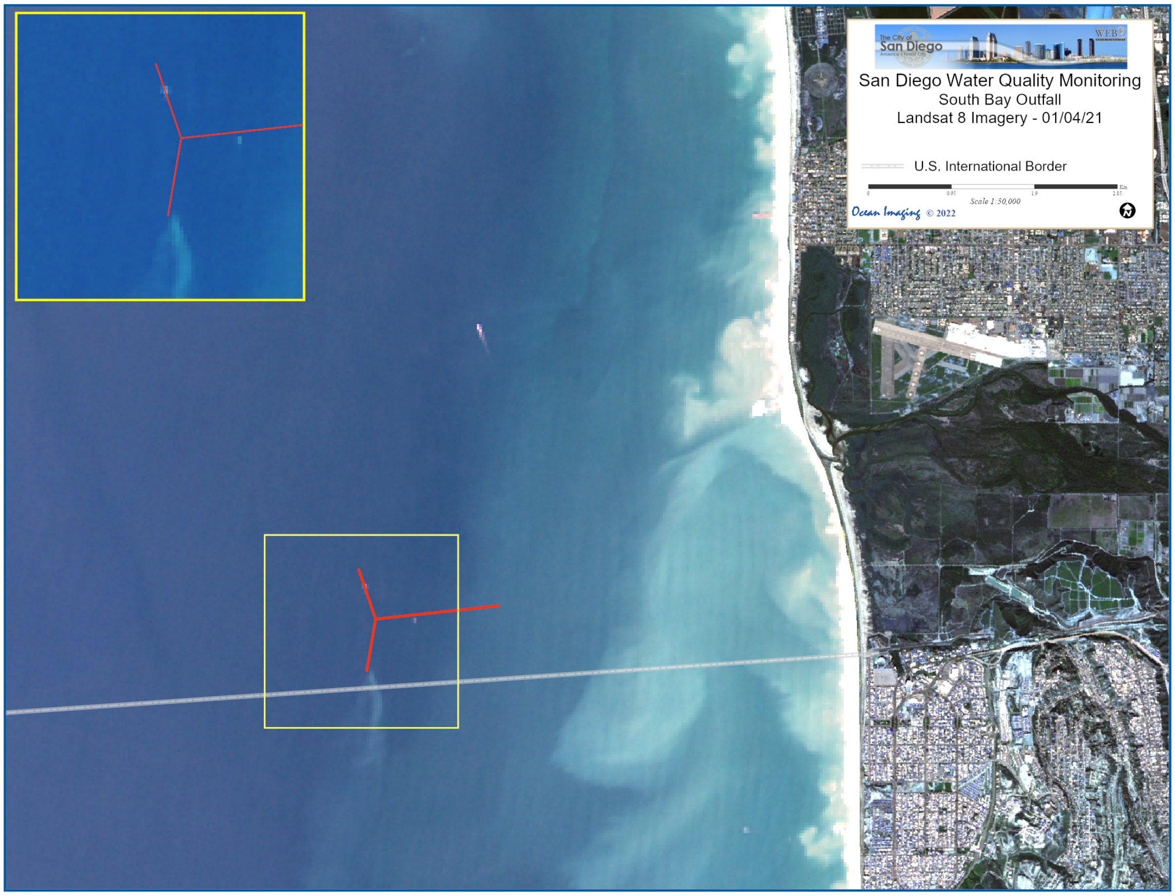

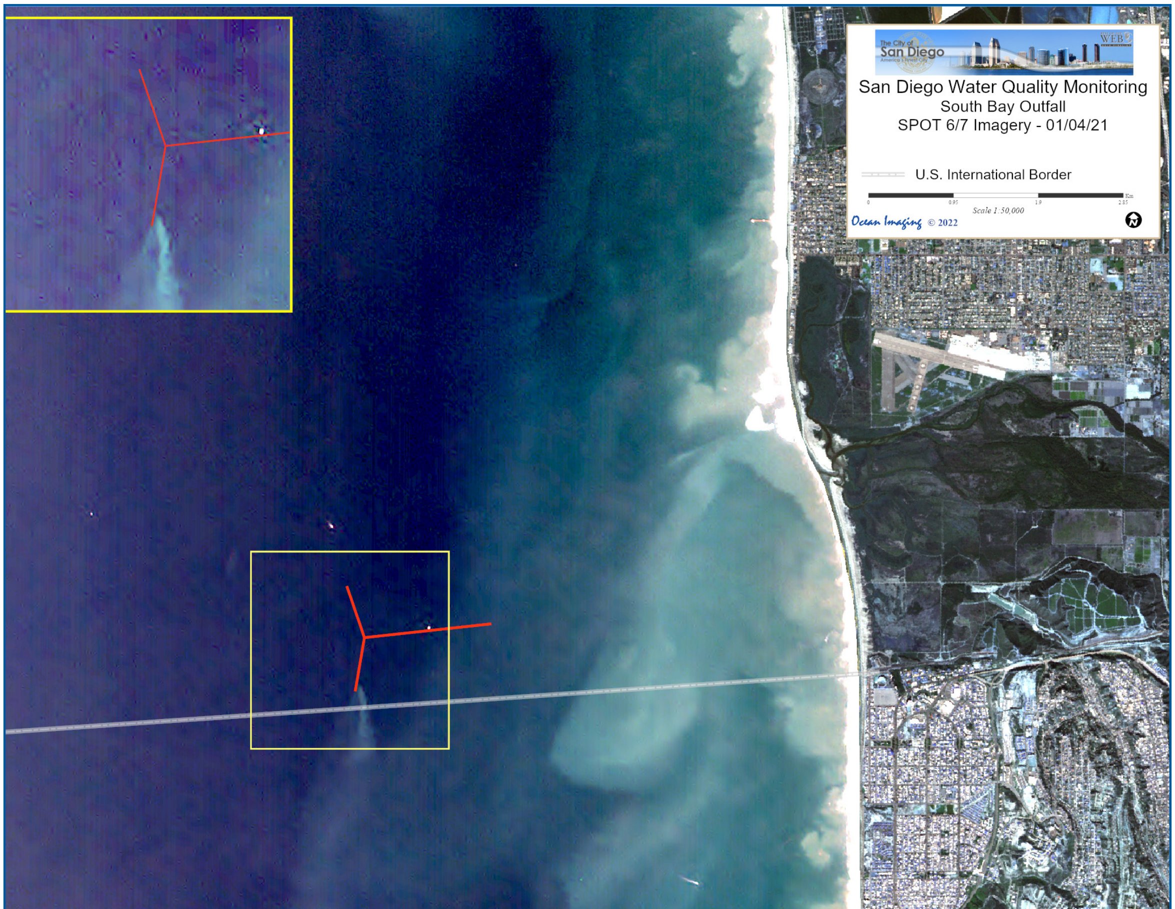
San Diego Water Quality Monitoring
South Bay Outfall
SPOT 6/7 Imagery - 01/04/21
U.S. International Border
Scale 1:50,000
Ocean Imaging © 2022

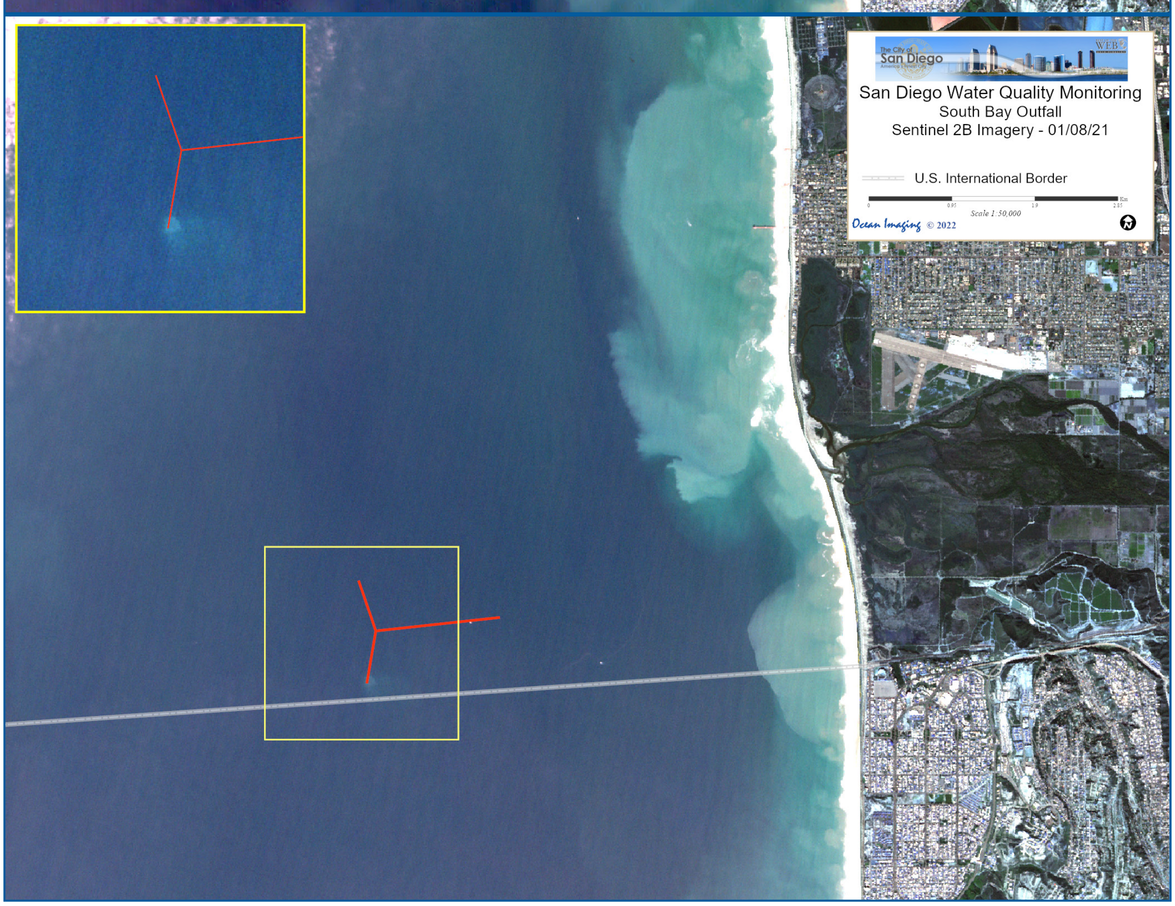
San Diego Water Quality Monitoring
South Bay Outfall
Sentinel 2B Imagery - 01/08/21
U.S. International Border
Scale 1:50,000
Ocean Imaging © 2022

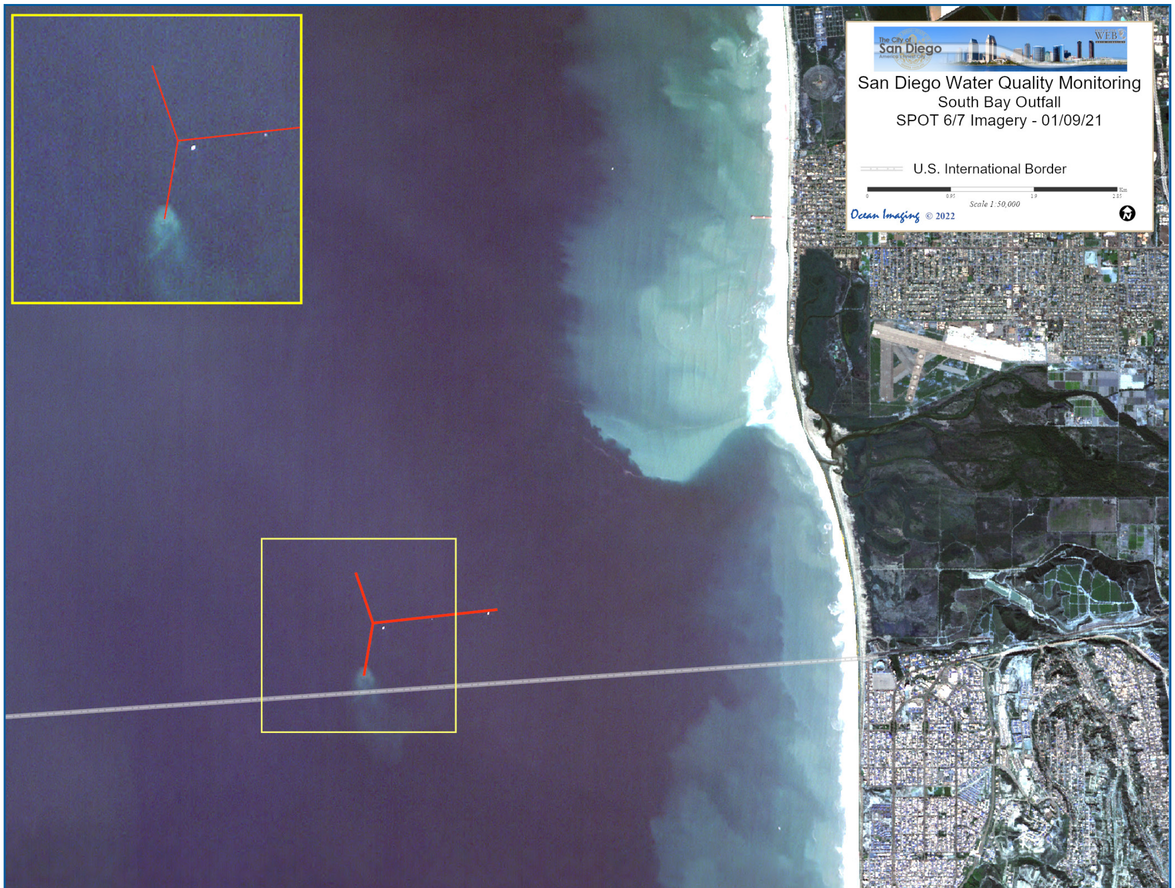
San Diego Water Quality Monitoring
South Bay Outfall
SPOT 6/7 Imagery - 01/09/21
U.S. International Border
Ocean Imaging © 2022

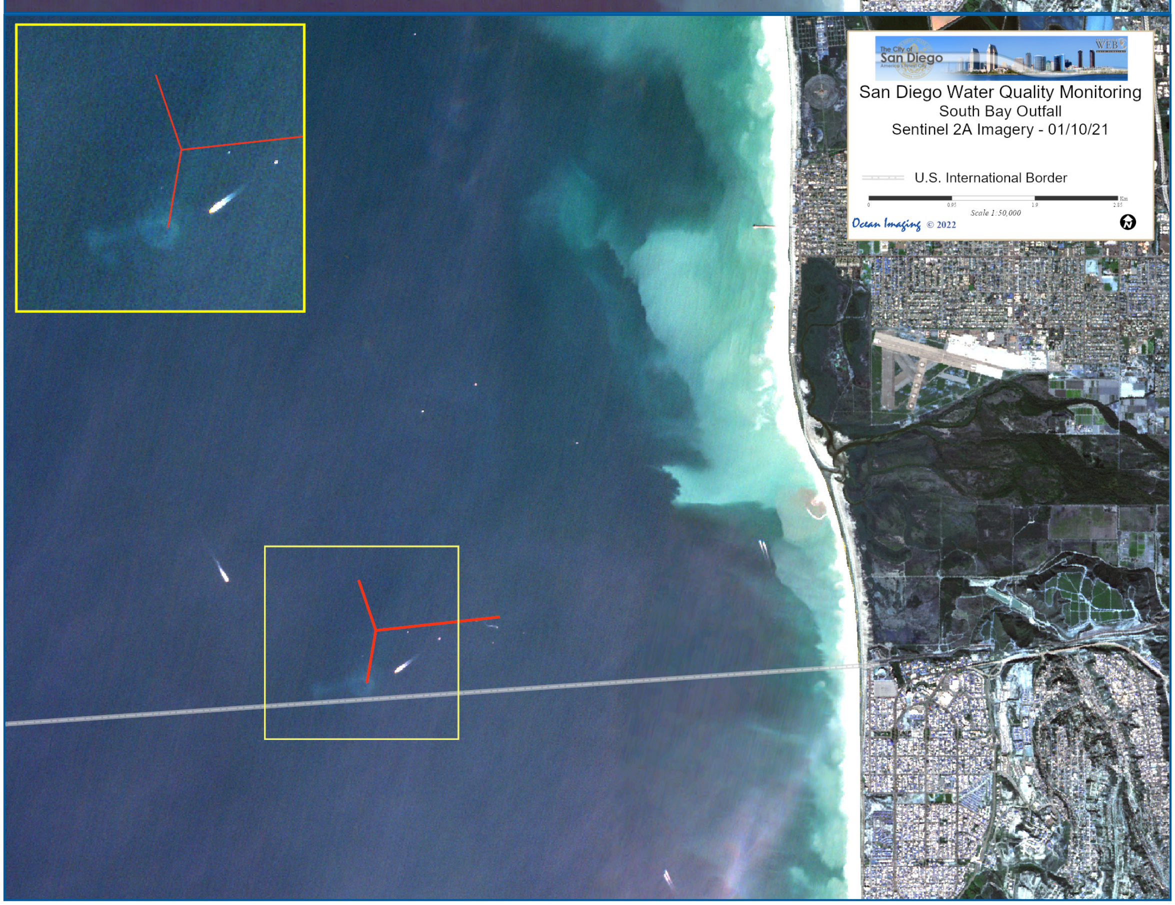
San Diego Water Quality Monitoring
South Bay Outfall
Sentinel 2A Imagery - 01/10/21
U.S. International Border
Ocean Imaging © 2022

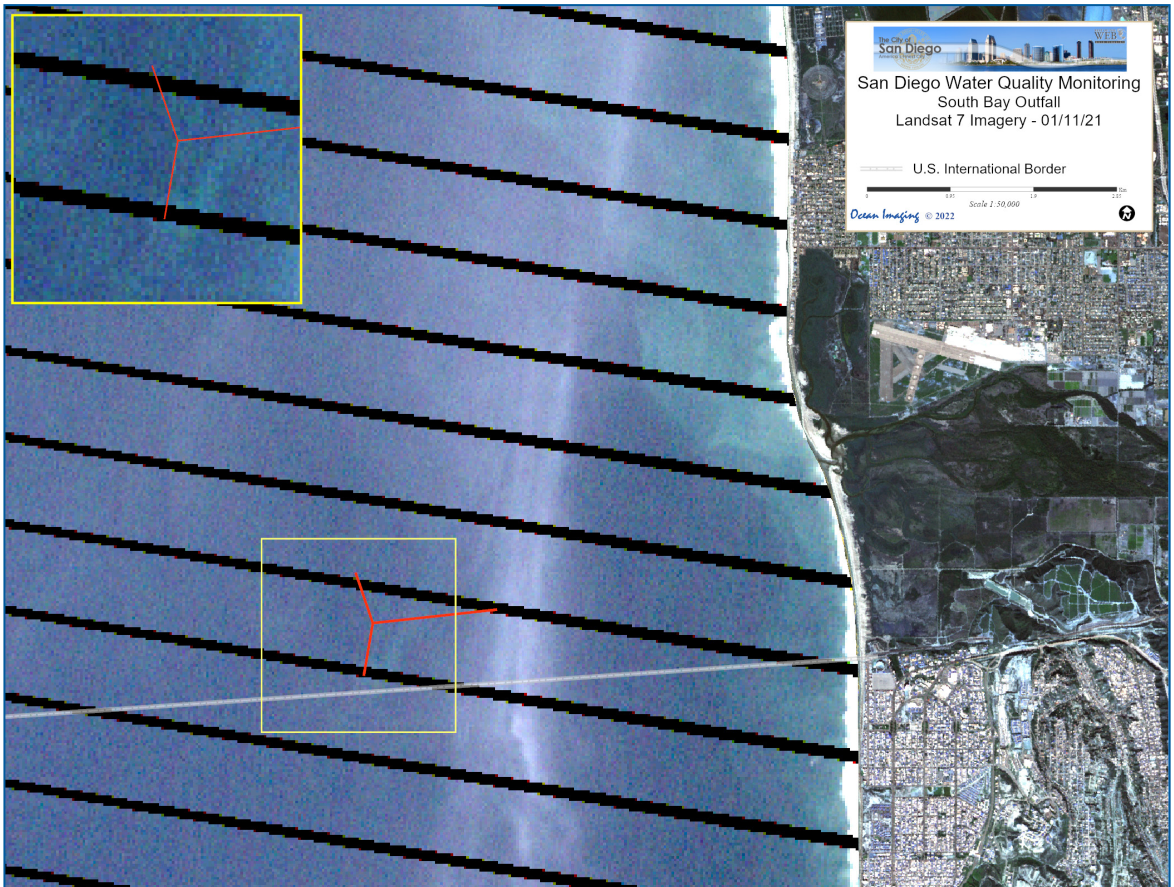
The City of San Diego
San Diego Water Quality Monitoring
South Bay Outfall
Landsat 7 Imagery - 01/11/21
U.S. International Border
Scale 1:50,000
Ocean Imaging © 2022

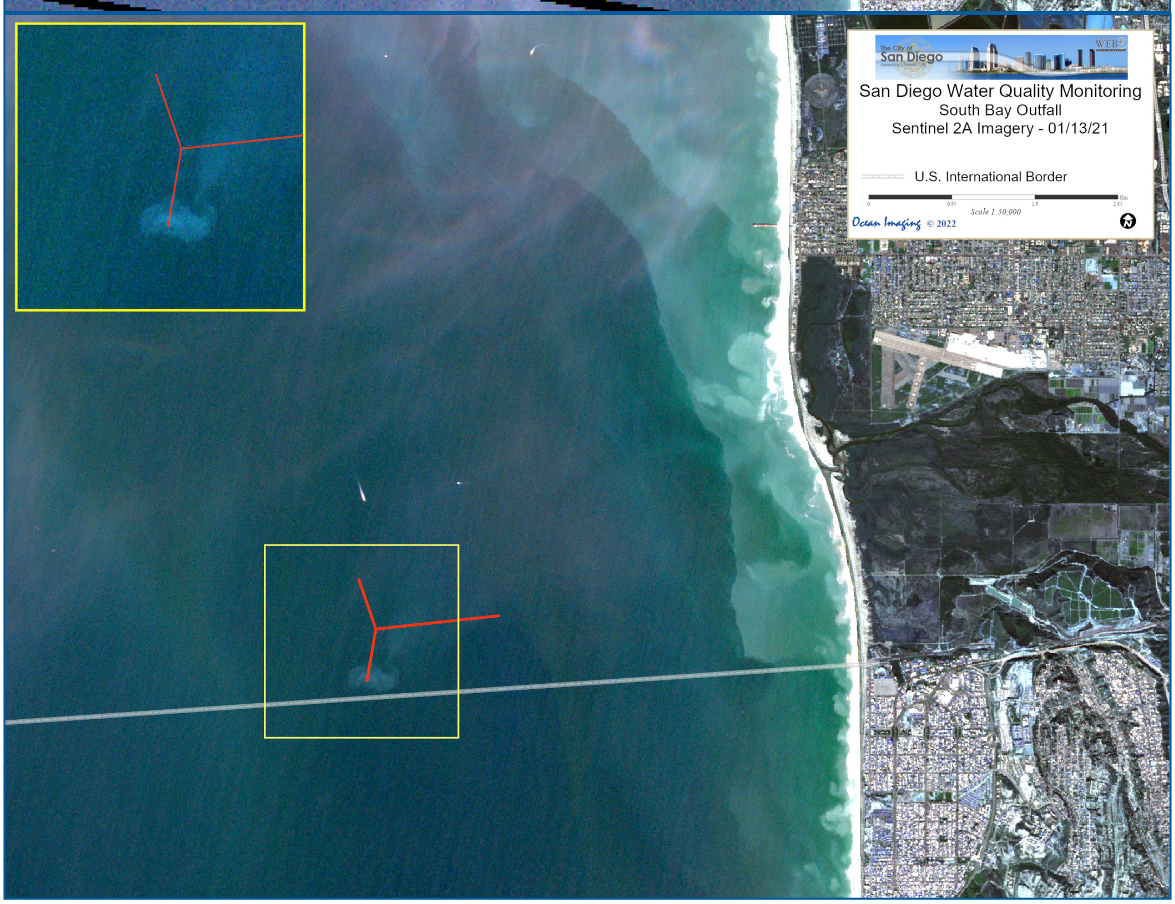
The City of San Diego
San Diego Water Quality Monitoring
South Bay Outfall
Sentinel 2A Imagery - 01/13/21
U.S. International Border
Scale 1:50,000
Ocean Imaging © 2022


San Diego
San Diego Water Quality Monitoring
South Bay Outfall
SPOT 6/7 Imagery - 01/13/21
U.S. International Border
Scale 1:50,000
Ocean Imaging © 2022

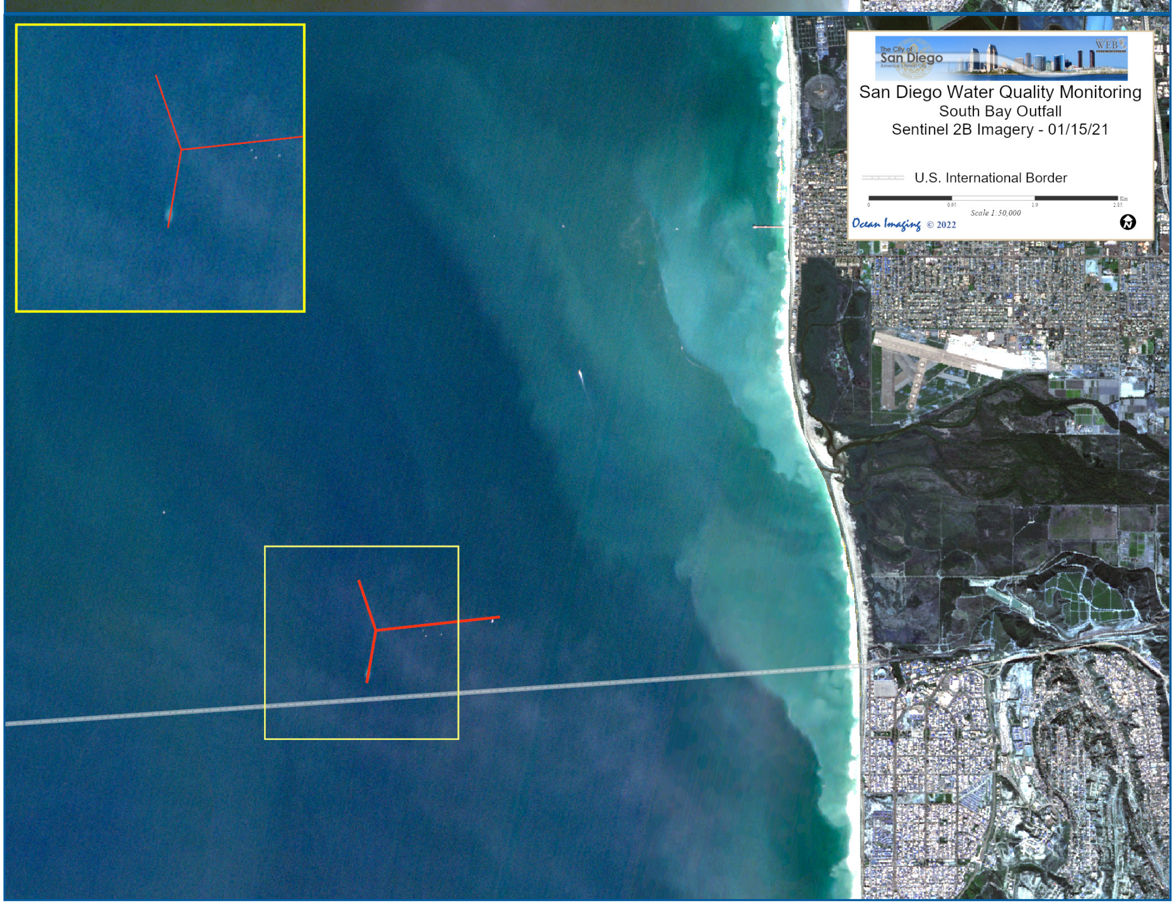
San Diego
San Diego Water Quality Monitoring
South Bay Outfall
Sentinel 2B Imagery - 01/15/21
U.S. International Border
Scale 1:50,000
Ocean Imaging © 2022


The City of San Diego
WEB
San Diego Water Quality Monitoring
South Bay Outfall
SPOT 6/7 Imagery - 01/17/21
U.S. International Border
Scale 1:50,000
Ocean Imaging © 2022

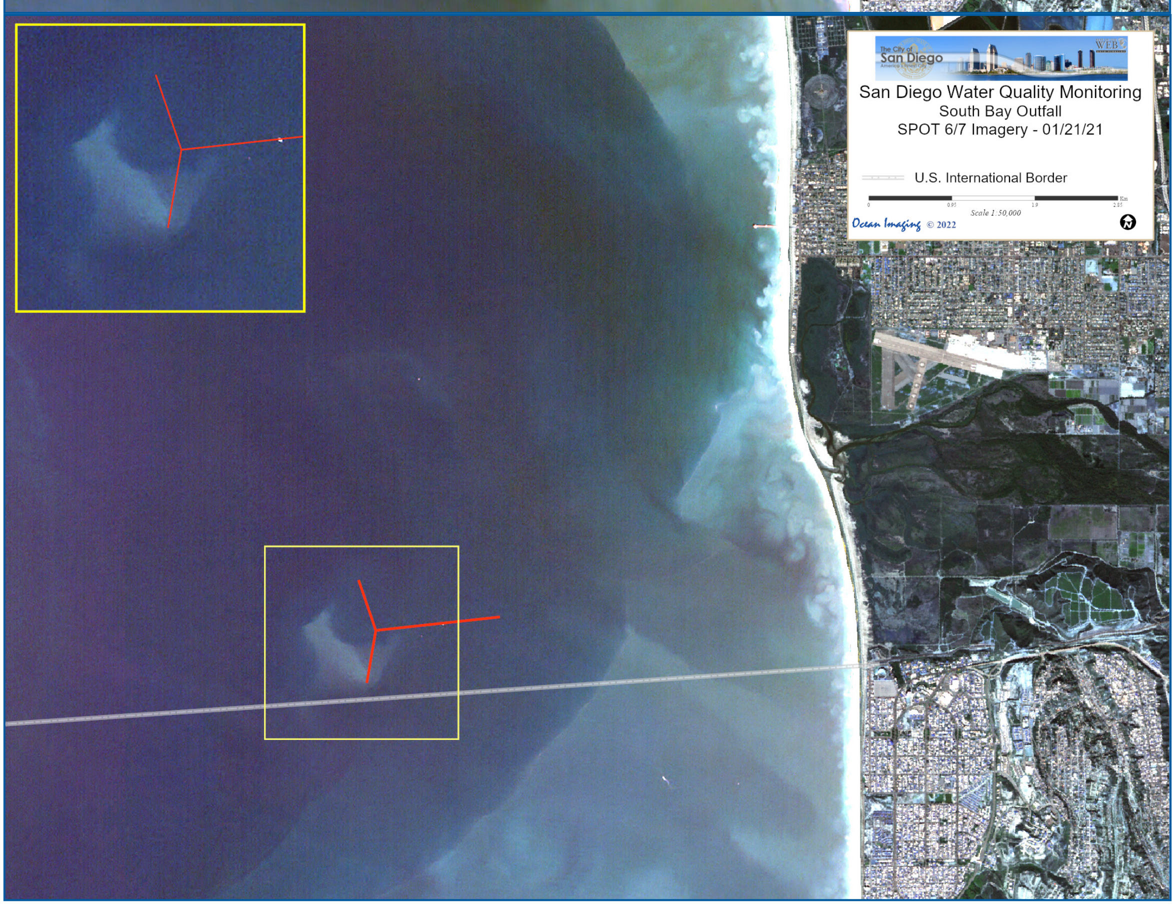
The City of San Diego
WEB
San Diego Water Quality Monitoring
South Bay Outfall
SPOT 6/7 Imagery - 01/21/21
U.S. International Border
Scale 1:50,000
Ocean Imaging © 2022

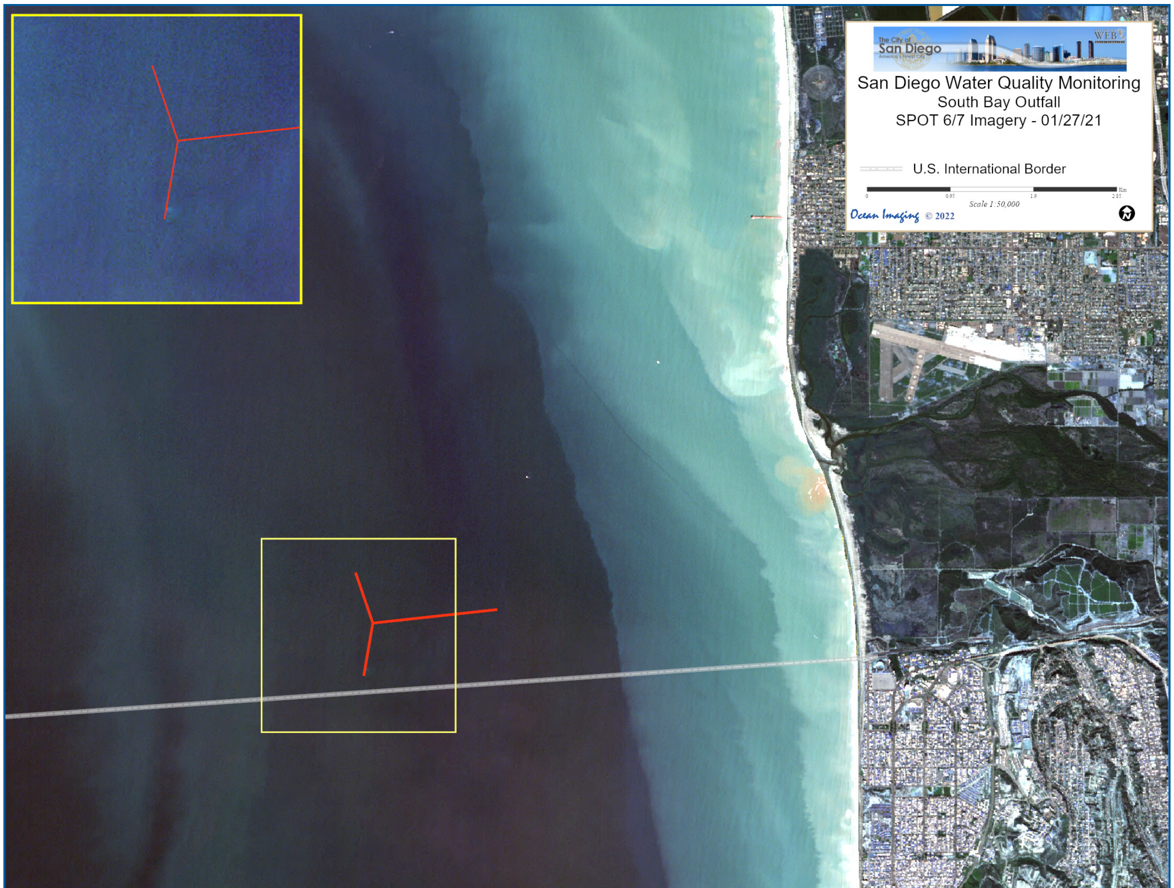
San Diego Water Quality Monitoring
South Bay Outfall
SPOT 6/7 Imagery - 01/27/21
U.S. International Border
Scale 1:50,000
Ocean Imaging © 2022

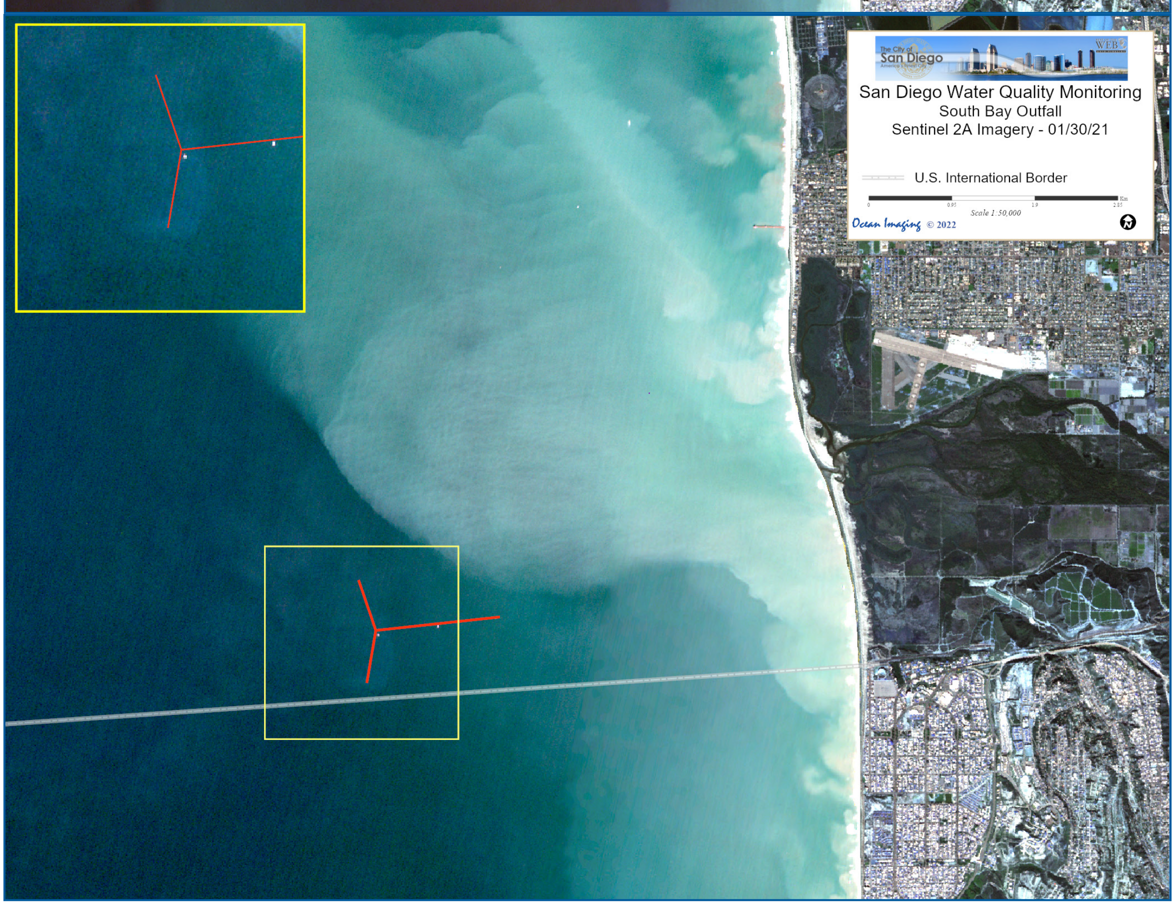
San Diego Water Quality Monitoring
South Bay Outfall
Sentinel 2A Imagery - 01/30/21
U.S. International Border
Scale 1:50,000
Ocean Imaging © 2022


San Diego
San Diego Water Quality Monitoring
South Bay Outfall
Landsat 8 Imagery - 02/05/21
U.S. International Border
Scale 1:50,000
Ocean Imaging © 2022


San Diego
San Diego Water Quality Monitoring
South Bay Outfall
SPOT 6/7 Imagery - 02/05/21
U.S. International Border
Scale 1:50,000
Ocean Imaging © 2022

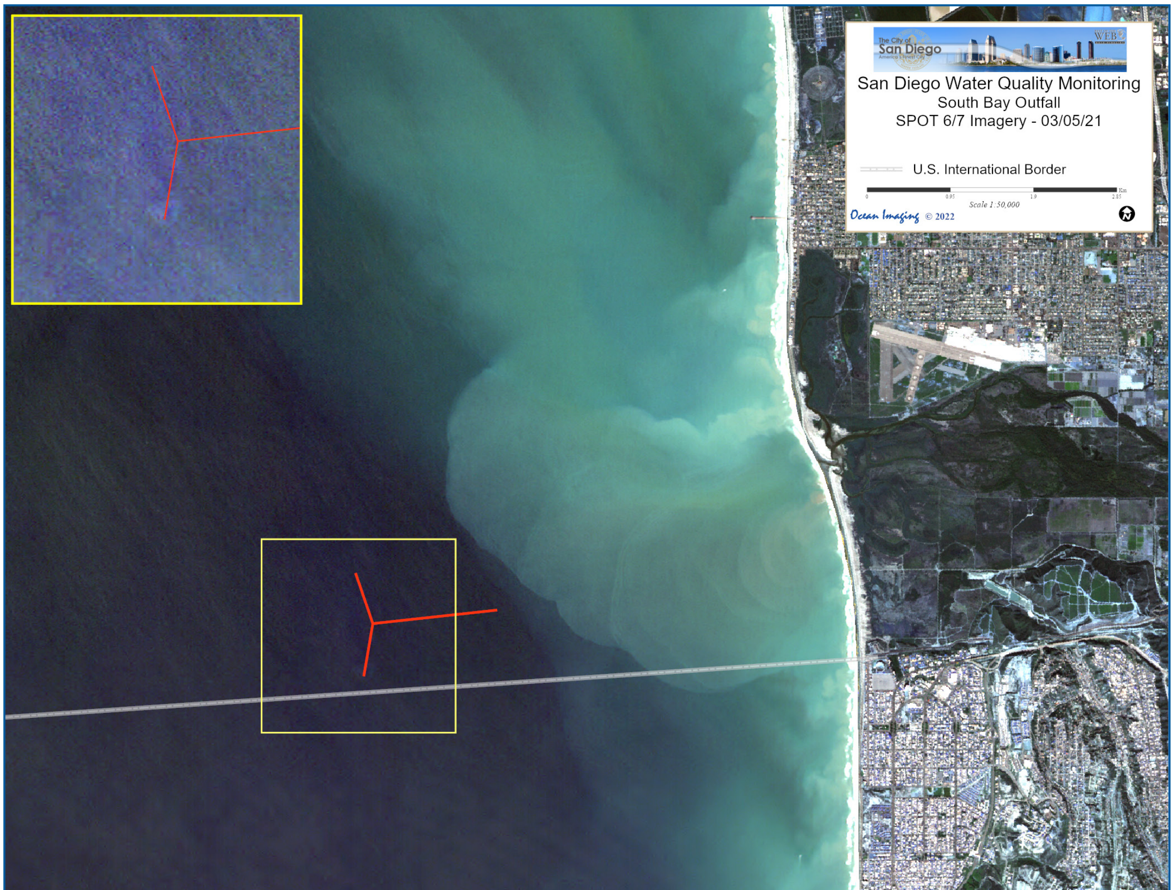
The City of San Diego
WEB
San Diego Water Quality Monitoring
South Bay Outfall
SPOT 6/7 Imagery - 03/05/21
U.S. International Border
Scale 1:50,000
Ocean Imaging © 2022

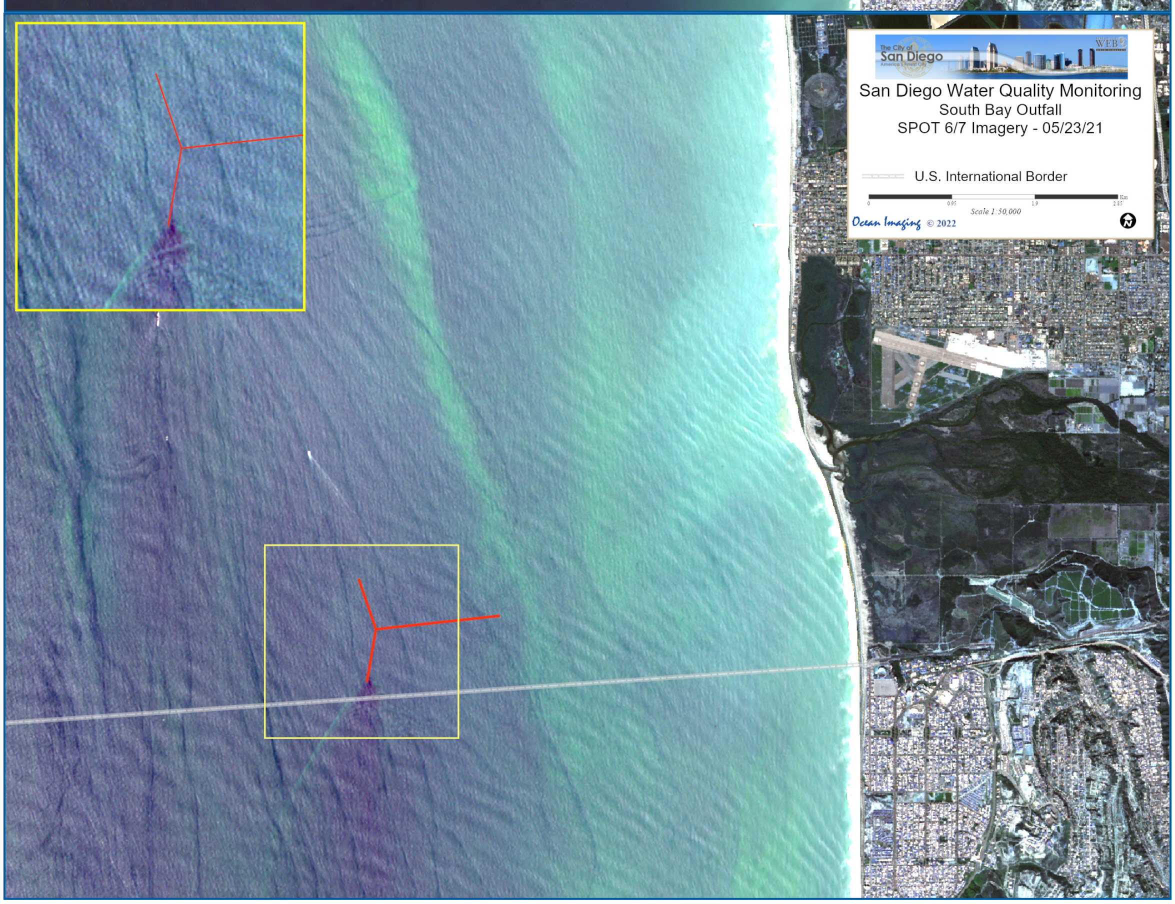
The City of San Diego
WEB
San Diego Water Quality Monitoring
South Bay Outfall
SPOT 6/7 Imagery - 05/23/21
U.S. International Border
Scale 1:50,000
Ocean Imaging © 2022

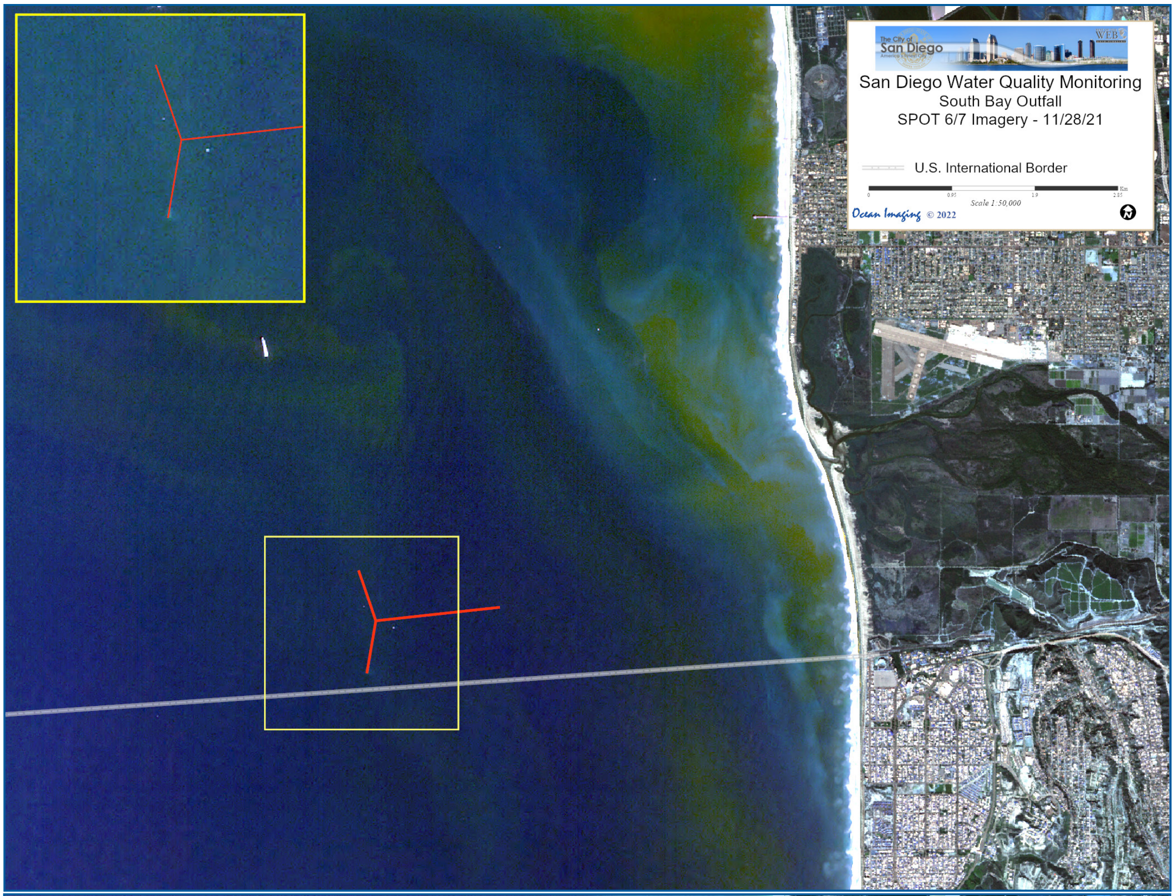
The City of San Diego
San Diego Water Quality Monitoring
South Bay Outfall
SPOT 6/7 Imagery - 11/28/21
U.S. International Border
Scale 1:50,000
Ocean Imaging © 2022

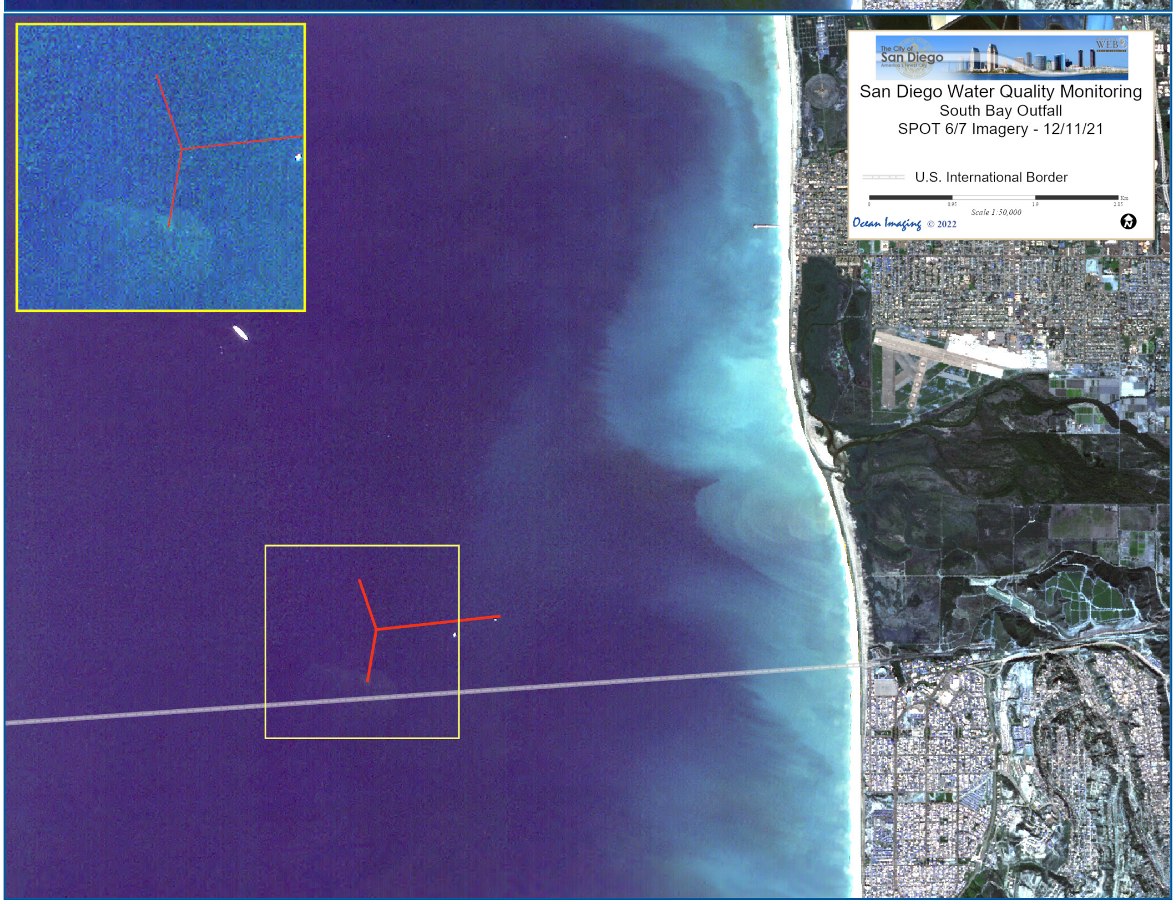
The City of San Diego
San Diego Water Quality Monitoring
South Bay Outfall
SPOT 6/7 Imagery - 12/11/21
U.S. International Border
Scale 1:50,000
Ocean Imaging © 2022